INFORMATION TO USERS

This material was produced from a microfilm copy of the original document. While the most advanced technological means to photograph and reproduce this document have been used, the quality is heavily dependent upon the quality of the original submitted.

The following explanation of techniques is provided to help you understand markings or patterns which may appear on this reproduction.

1. The sign or "target" for pages apparently lacking from the document photographed is "Missing Page(s)". If it was possible to obtain the missing page(s) or section, they are spliced into the film along with adjacent pages. This may have necessitated cutting thru an image and duplicating adjacent pages to insure you complete continuity.

2. When an image on the film is obliterated with a large round black mark, it is an indication that the photographer suspected that the copy may have moved during exposure and thus cause a blurred image. You will find a good image of the page in the adjacent frame.

3. When a map, drawing or chart, etc., was part of the material being photographed the photographer followed a definite method in "sectioning" the material. It is customary to begin photoing at the upper left hand corner of a large sheet and to continue photoing from left to right in equal sections with a small overlap. If necessary, sectioning is continued again — beginning below the first row and continuing on until complete.

4. The majority of users indicate that the textual content is of greatest value, however, a somewhat higher quality reproduction could be made from "photographs" if essential to the understanding of the dissertation. Silver prints of "photographs" may be ordered at additional charge by writing the Order Department, giving the catalog number, title, author and specific pages you wish reproduced.

5. PLEASE NOTE: Some pages may have indistinct print. Filmed as received.

University Microfilms International
300 North Zeeb Road
Ann Arbor, Michigan 48106 USA
St. John's Road, Tyler's Green
High Wycombe, Bucks, England HP10 8HR

VOLATILES, MAGMA MIXING, AND THE MECHANISM OF ERUPTION OF AUGUSTINE VOLCANO, ALASKA

by

David Alexander Johnston

A dissertation submitted in partial fulfillment
of the requirements for the degree of

Doctor of Philosophy

University of Washington

1978

Approved by /S/ McCallum
(Chairperson of Supervisory Committee)

Program Authorized
to Offer Degree Geological Sciences

Date March 9, 1978

UNIVERSITY OF WASHINGTON

Date: February 17, 1978

We have carefully read the dissertation entitled Volatiles, Magma Mixing, and the Mechanism of Eruption of Augustine Volcano, Alaska

submitted by David Alexander Johnston in partial fulfillment of the requirements of the degree of Doctor of Philosophy and recommend its acceptance. In support of this recommendation we present the following joint statement of evaluation to be filed with the dissertation.

In this dissertation, David Johnston has discussed the sequence of events which took place prior to and during the 1976 eruptions of Augustine Volcano, Alaska. He has mapped the areal extent of ash falls and ash flows resulting from the eruptions. The most prominent product of the 1976 eruption is a banded pumice consisting of a dark dacitic component irregularly interlayered with a light-colored andesitic component. The dacitic pumices appear to be "primary" whereas the adesitic pumices are hybrids formed by the mixing of dacitic magma with a mafic basaltic magma. Although the mixing event has been sufficiently thorough to remove direct evidence of the basaltic component, its prior existence can be inferred from the pervasive disequilibrium features exhibited by the phenocryst assemblage in the andesitic pumices and the presence of mafic glass inclusions within magnesian olivine phenocrysts. The calculated composition of the mafic component is that of a high-alumina basalt.

In an attempt to decipher the evolution of the magmas involved in the 1976 eruptions, Johnston has made a detailed analysis of melt inclusions trapped within phenocrysts in both the andesite and dacite, paying particular attention to those processes that affect the composition of melt inclusions. Prior to eruption the dacitic magma was vapor-saturated with ca. 6.5 wt % H_2O and 0.4 to 0.7 wt. % chlorine, indicative of an entrapment pressure between 1 and 2.5 kilobars. The volatile content of the basaltic component has also been estimated but is less well determined because of post-entrapment crystallization of melt inclusions in olivine. The basalt component appears to be H_2O-undersaturated (ca. 3-5 wt. % H_2O). The consequence of mixing and fractional crystallization on the volatile content are examined in detail. Of particular significance is the conclusion that the 1976 eruption may have been triggered by the injection of fresh basaltic magma into the water-saturated dacitic magma. This event resulted in a rapid increase in the volume of the magma chamber due to (1) addition of basalt magma, (2) boiling of the water-saturated dacitic magma, and (3) exsolution of volatiles from the mesostasis of hybrid andesitic magma.

DISSERTATION READING COMMITTEE: I. McCallum

Joseph A. Vance

[illegible]

Doctoral Dissertation

In presenting this dissertation in partial fulfillment of the requirements for the Doctoral degree at the University of Washington, I agree that the Library shall make its copies freely available for inspection. I further agree that extensive copying of this dissertation is allowable only for scholarly purposes. Requests for copying or reproduction of this dissertation may be referred to University Microfilms, 300 North Zeeb Road, Ann Arbor, Michigan 48106 to whom the author has granted "the right to reproduce and see (a) copies of the manuscript in microform and/or (b) printed copies of the manuscript made from microform."

Signature David A. Johnston

Date March 3, 1978

TABLE OF CONTENTS

	Page
List of Tables	v
List of Figures	vi
Acknowledgments	vii
CHAPTER 1: The 1976 eruption of Augustine Volcano	1
Introduction	2
The Volcano in July and August, 1975	5
Background seismicity of Augustine	10
Precursors to the 1976 eruption	12
Eruptive chronicle	14
January activity	16
February activity	26
Stratigraphy of the 1976 deposits	29
January deposits	29
February and April deposits	33
The lava dome	35
The mechanism of emplacement of the deposits	36
CHAPTER 2: Magma mixing and implications for the mechanism of the eruption	39
Introduction	40
Composition and mineralogy of the 1976 ejecta	43
Dacites	44
Plagioclase	46
Pyroxenes	48
Iron-titanium oxides	50
Other phases	50
Andesites	50
Plagioclase	53
Pyroxenes	55
Iron-titanium oxides	55
Olivine	55
Spinel	58
Hornblende	58
Aluminous clinopyroxene	60
Evidence that magma mixing has occurred	63
The composition of the magmas that were mixed	65
Volatile contents of the magmas	73
Temperature of the magmas	74
Viscosity of the magmas	75
Depth of crystallization of the magmas	77
Dacite	77
The effect of temperature	77
The effect of vapor composition	78
Other assumptions	80
The depth to the chamber	80
Basalt	81
When did magma mixing occur?	81
How did magma mixing occur ?	85

Page

Overturn of a compositionally zoned magma chamber 85
Introduction of new magma from depth 89
The physical effects of magma mixing 90
First stage: Heating and chilling 91
Second stage: Chemical homogenitization 92
Volume changes in the magma - sufficient to trigger explosive eruptions? 95
The mechanism of explosive eruptions of the volcano 98
The role of groundwater in the eruption 99
Zoning of volatiles in the magma chamber 101
Volatile loss from the chamber during the eruption 102
Summary of the eruption mechanism 103

CHAPTER 3: The abundance and evolution of volatiles in the magmas 105
Introduction 106
Determination of the pre-eruption volatile content of magmas 107
Distribution of volatiles within magmas 110
Volatile elements in crystalline phases 110
Hornblende 111
Apatite 113
Sulfides 113
Volatile elements in the melt 116
The occurrence of glass inclusions in phenocrysts in the 1976 ejecta 116
Glass inclusions in plagioclase 116
Glass inclusions in pyroxene 118
Glass inclusions in olivine and hornblende 119
Analytical methods 119
Composition of glass inclusions 122
Hazards for the interpretation of glass inclusion compositions 130
1. Post-entrapment crystallization of the inclusion 130
2. The effect of crystal-liquid interface diffusion gradients 132
3. Contamination of the interface melt by resorption prior to melt entrapment . . 135
The abundance of volatile elements in the melt phase of the basalt 137
Water 138
Chlorine 139
Sulfur 139
Fluorine 140

Page

The abundance of volatile elements in the melt phase of the dacite 140
Water 141
Chlorine 143
Sulfur 143
Fluorine 144
Evolution of volatiles within the magma 147
Water 148
Chlorine 149
Sulfur 150
Other petrologic implications 155
1. The rate of magma supply 155
2. Origin of the dacites by fractional crystallization of basalt 155
3. The calc-alkaline Fe-enrichment trend is due to magnetite, not hornblende crystallization 156
4. Trace element evolution - obscured by magma mixing 157

REFERENCES 162

LIST OF TABLES

		Page
I.	Summary of events in historic eruptions of Augustine	6,7
II.	Whole rock analyses of 1976 ejecta	45
III.	Composition of groundmass of pumices	47
IV.	Pyroxene analyses	51
V.	Olivine analyses	57
VI.	Cr-spinel analyses	59
VII.	Hornblende analyses	61
VIII.	Aluminous-augite analyses	62
IX.	Selected analyses of glass inclusions	66
X.	Composition of basalt determined by mixing calculations from composition of andesite and dacite	70
XI.	Recalculated initial trapped melt compositions for glass inclusion in olivine	72
XII.	Viscosities of the magmas	76
XIII.	Volatile content of magmas from several tectonic environments	109
XIV.	Volatile element concentrations in apatite and hornblende	112
XV.	Glass inclusion analyses	123-127
XVI.	Diffusion aureoles and relative diffusion coefficients	134

LIST OF FIGURES

		Page
1.	Oxygen and hydrogen isotopic composition of Augustine fumarole condensates	9
2.	Microseismic activity preceeding the 1976 eruption	13
3.	Plot of infrasonic events, earthquakes, and ocean tides during January eruptions	18
4.	Summit of Augustine in July 1975 and January 1976	20,21
5.	Distribution of January ash fall	22,23,24
6.	Map of 1976 deposits on Augustine Island	31
7.	Map of pyroclastic flow deposits from each eruptive episode on Augustine Island	34
8.	Composition of pyroxene phenocrysts	49
9.	Reverse zoned plagioclase phenocryst in andesite	54
10.	MgO/MgO + FeO of melts parental to olivine and opx	64
11.	Composition of olivine phenocrysts and host rocks, Central Aleutians	69
12.	Molal equivalent solubility of water in magmas at 1100° C	79
13.	Relative volumes of water dissolved in a melt and in a fluid state	93
14.	Volume increase during boiling	94
15.	Volume increase during crystallization	96
16.	X-ray intensity images of sulfide globules	115
17.	Variation of MgO/FeO*, Cl/FeO*, MgO, CaO, Na_2O and K_2O with FeO* in glass inclusions in plagioclase	128
18.	Relationship of H_2O, K_2O, and Cl in Augustine magmas	145,146
19.	FeO*- and S-contents of glass inclusions in plagioclase	152
20.	Contrasting fractional crystallization and magma mixing paths of trace element evolution	161

ACKNOWLEDGMENTS

I wish to thank the following people for their aid at various times in my graduate career: Douglas Lalla, Greg Walla, Ed Mathez, Mark Utting, The Lipman Family, and the members of my committee who patiently read this dissertation, I.S. McCallum, J.A. Vance, and J.R. Delaney. I wish also to give special thanks to Peter W. Lipman, Thomas A. Steven, and Hans-Ulrich Schmincke for sharing with me their skills, insight, enthusiasm, and commitment.

I am also grateful for the support and encouragement provided by my parents, Thomas and Alice Johnston, and close friends, C.J. Larsen, Ron Sholand, Doug Lalla, and Rick Droker.

This dissertation is respectfully dedicated to the memory of Kent Gooley and John Baird, and to all others whose opportunity to create was cut short by the war in Viet Nam.

CHAPTER 1: THE 1976 ERUPTION OF AUGUSTINE VOLCANO

INTRODUCTION

Augustine Volcano is one of approximately 40 historically active Alaskan volcanoes and one of about 70 active since the Pleistocene (Coats, 1950). It is one of the most active of these volcanoes, having erupted four times in the past century (1883, 1935, 1963-64, and 1976). This chapter deals with the 1976 eruption.

The volcano dominates Augustine Island, a small (approximately 90 km^2) unpopulated island located within Kamishak Bay on the west side of Lower Cook Inlet, 285 km southwest of Anchorage, Alaska. It lies along an active segment of the Aleutian arc which includes Mt. Wrangell (last eruption: 1929), Mt. Spurr (1953), Mt. Redoubt (1966-68), and Iliamna Peak (1947) to the north, and Mt. Douglas (no historic eruptions) and the active Katmai group farther south and west. It lies approximately 105 km above the median surface of an active Benioff zone, inclined approximately 40° to the northwest (S. Estes, University of Alaska, reported by Kienle & Forbes, 1977).

The Augustine volcanic rocks overlie Mesozoic marine and non-marine sedimentary rocks and Pleistocene glacial deposits, which are exposed on the south side of the island to nearly 1000' above sealevel (Detterman, 1973, Detterman and Jones, 1974, Buffler, 1976). The glacial deposits, which shed non-volcanic boulders onto the south flank of the island, are poorly exposed. The age of these deposits is unknown, but in view of the absence of any other evi-

dence for glaciation of Augustine, most likely corresponds to the last glacial advance in Cook Inlet, approximately 37,000 years ago (Pewe, 1975). No other evidence is yet available to establish the age of onset of Augustine volcanism.

The volcano consists of a central core of overlapping lava domes and dome marginal breccias, which are flanked by an apron of pyroclastic flow, mudflow, and debris flow deposits. A relatively recent lava flow on the northwest flank of the volcano is the only known lava flow on the island. The historically active vent at the volcano's summit appears to have been active during most, perhaps all of the volcano's history, although the existence of a strongly magnetic body beneath Point Kamishak (located at 1700' elevation on the south flank of the cone) may be due to an unexposed plug (Barrett and others, 1976), possibly filling a formerly active vent. No other evidence, however, suggests that vents have been active at any part of the mountain other than the historic vent at the summit. Dikes or other lateral intrusions are unknown.

Deposits currently exposed at Augustine appear to contain andesitic and dacitic ejecta only, closely resembling in mineralogy, texture, and composition the ejecta of the 1976 eruption (described in chapter 2). Deposits usually preserve evidence of magma mixing, in the form of banded pumices and/or disequilibrium mineral assemblages. Field observations, supported by a few chemical analyses (Becker,

1898, Detterman, 1973, Johnston, unpublished data), appear to indicate that throughout the historic and recent prehistoric activity of Augustine, there have been no significant changes in the composition, mineralogy, or mineral chemistry of the Augustine ejecta. Two interpretations discussed below, that the 1976 ejecta were the products of mixing of a basaltic and dacitic magma (chapter 2) and that the dacite was water-rich and vapor-saturated prior to eruption (chapter 3), appears to apply to the ejecta of the 1963-64 eruption of Augustine as well.

The historic and recent prehistoric deposits on the island reflect a common pattern of eruption. Pumice-rich pyroclastic flows were erupted in the violent early phase of each eruption, accompanied by ash-fall over large portions of south-central Alaska. The summit vent has usually been explosively cleared of all or part of former lava domes during this phase of the eruption. New lava domes were emplaced later, accompanied by non-pumiceous block-and-ash flows formed by dome collapse. Regional ash-fall has not occurred during this waning phase of the eruptions.

Deposits exposed on Augustine, and inferred from geophysical records obtained off-shore, do not suggest that prehistoric eruptions have been different, or significantly greater in magnitude than the historic eruptions. In particular, the 1976 eruption appears similar in style and sequence to other eruptions, although it was more voluminous

than some (e.g., 1935, 1963-64) and less voluminous than others (1883, several pre-historic eruptions). The historic eruptions of Augustine are summarized in Table 1.

THE VOLCANO IN JULY AND AUGUST, 1975

During July, August, and September, 1975, geologic, thermal, aeromagnetic, and seismic studies were performed at Augustine. While these studies were being carried out, no precursor activity was recognized. Furthermore, although thermal and aeromagnetic studies were in part repetitions of earlier studies, nothing indicated that Augustine had undergone any changes during the preceeding months to years that may have foreshadowed the eruption.

Since 1964 the summit of Augustine had been dominated by the andesitic endogenous dome that was emplaced during the 1963-64 eruption. All fumarolic activity during 1975 occurred along the margins or on the surface of this 279-meter high lava dome. The most active fumaroles were located on the west side of the dome, where vapor escaped through cavernous breccia at the base of the steep dome face, and along the northern margin of the dome, where it abruptly terminated against older rocks of the wall of the crater which this dome had filled. This contact is visible in Figure 4.

Fumarole emission temperatures and soil temperatures, measured with shallow temperature probes (less than 1 meter) and in a 24-meter hole drilled into the fumarole field west

TABLE I: Summary of events in historic eruptions of Augustine.

ERUPTION	PRECURSORS	EXPLOSIVE PHASE INITIAL	EXPLOSIVE PHASE CLIMAX	LATER PHASE	OTHER COMMENTS
1812	?	Ash deposited in Skilak Lake, Kenai Peninsula, 200 km NE of Augustine.		?	"Activity" in 1812 is reported by Doroshin, (1879).
1883	Steam visible in August, 1883; frequent earthquakes felt on island days before eruption.	Tephra eruptions one or more days prior to climax?	October 6, 1883: violent explosion, nuee ardente extends >8.6, <12.5 km down north side, impacts Inlet, creating tsunami. Nuees continue on all flanks. Summit crater formed, ash deposited in Kodiak and on Kenai Peninsula.	Active lava fountaining continues for more than 2 months, creating 400 foot summit cinder cone. Crater at end of eruption is breached to the north.	3 tsunamis struck English Bay 25 minutes after Oct. 6 eruption; first wave was 30 feet high, was followed at 5-minute intervals by waves 18 and 15 feet high.
1935	?	March 13 through April 3: ash deposited at least as far as Skilak Lake (200 km NE); ash-flows emplaced on north and west flanks of cone, reaching the shore.		Two lava domes emplaced within summit crater.	
1963-64	?	October 10, 1963: Ash eruptions with clouds to 4 km, quickly subsided; November 17, 1963, July 5, 1964, August 19, 1964: Explosions occurred. Ash deposited in Skilak Lake; ash-flows emplaced on N, S, E, and SW flanks.		Former summit crater filled by new lava dome, reaching height of 4300 feet.	

TABLE I: Summary of events in historic eruptions of Augustine. (Continued)

ERUPTION	PRECURSORS	EXPLOSIVE PHASE INITIAL	CLIMAX	LATER PHASE	OTHER COMMENTS
1976	July, 1975: no visible precursors: no change in aeromagnetic field between 1972 and August, 1975; fumarolic emissions at 95° C or less, consist of meteoric water. Steam issues from margins and flank of 1964 lava dome. October, 1975: began increased seismicity 5 km deep; late Oct., steam explosions began; ca. Dec. 20, 1975 seismic network on island ceased to operate; Jan. 21-22, 1976: seismicity increased on off-island network.	January 22, 1976: small explosions at 7:59, ca.16:30, 22:19 AST. Eruption clouds to 4-5 km; first ash-fall at Lake Iliamna, evening of January 22. Large seismic swarm from 8:00 to 22:00 AST, January 22. Summit crater formed in initial explosions?	Major eruptions: January 23: 6:58, 7:40, 16:18, Jan. 24: 8:38, Jan. 25: 4:56 AST, plus several more smaller "steam explosions"; eruption columns to 14 km. Ash-flows deposited on all flanks, especially north side, where ash-flows extend beyond the shoreline. Ash-fall on Iliamna area, Kenai Peninsula, Anchorage area, Valdez, and minor ash in Sitka. Quiescent Jan. 26 to Feb. 6; starts again with ash-fall on Kenai Peninsula plus new ash-flows on all flanks, reaching shoreline to northeast. Pyroclastic flows emplaced by collapse of vertical eruption column.	Lava dome appears in summit crater by Feb. 12; growth of dome continues through late Feb., accompanied by incandescent block-and-ash-avalanches on north flank below dome only. Pyroclastic flows emplaced by dome collapse. After 1½ months of quiescence, minor explosions occur in summit region during mid-April, accompanied by more growth of lava dome and emplacement of more block-and-ash-avalanches.	Summit crater, formed at beginning of eruption, was breached to north and controlled emplacement of subsequent block-and-ash-avalanches. Nuees ardentes in January were accompanied by devastating high temperature, high velocity shock waves that advanced more than 1½ km beyond the ash-flow basal avalanche deposits. Total volume produced in 1976 eruption: 0.17 km^3 of which 8% is ash-fall, 53% is pyroclastic flows, 39% is lava dome. 27% was emplaced in January, 59% in February, and 14% in April.

of the dome, did not exceed 95° C. Fumarole and shallow soil temperatures measured during 1974 and 1975 were essentially identical (D. Lalla, 1975, personal communication).

Fumarolic emissions during the summer of 1975 appear to have been predominantly water vapor. Some variations in the S-content of the gases are suggested by the presence of abundant S-sublimates around fumaroles on the north margin and top of the dome. A single vapor condensate collected July 24, 1975 from a fumarole on the west side of the dome yielded oxygen and hydrogen isotope ratios that fall directly upon the meteoric water line defined by Craig (1961), (Figure 1). This implies a meteoric water source and probably very limited circulation within the volcano, since no rock-water oxygen exchange appears to have occurred.

Aeromagnetic surveys of Augustine flown in 1972 and in August, 1975 showed no significant differences (D. Stone, unpub. data, reported by Kienle and Forbes, 1977). While stress or heat induced magnetic changes prior to eruptive activity have been determined by more sensitive methods at andesitic volcanoes elsewhere (e.g., Johnston and Stacey, 1969), the efficacy of magma ascent in inducing these changes appears variable, since Davis and others (1973) reported no significant magnetic changes accompanying an inflation and eruption of Kilauea Volcano. Interpretation of the apparent magnetic stability of Augustine, then, is ambiguous, but the observation establishes that no major

Figure 1: Plot of δO^{18} vs. δD for Augustine fumarole condensates. Shown also are the fresh water trend of Craig (1961), the mean isotopic composition of seawater ("O"), and the approximate composition range of juvenile magma ("M") (Taylor, 1967). Condensates from fumaroles at Lardarello ("L"), the Geysers geothermal area ("G"), and Hekla Volcano, Iceland ("H") (open circles), and surface waters at the same areas (solid boxes; from White and others, 1973) are shown to illustrate the effect of oxygen exchange between geothermal fluids and country rock. No such exchange is apparent in the July, 1976 fumarole condensate. Two samples collected February 1, 1976 from a fumarole on a pyroclastic flow and from an open fissure approximately 200 meters north of the crater margin each show a significant meteoric water component, but have apparently been modified by mixing with marine or juvenile gases, by isotopic exchange, and/or by isotopic fractionation between liquid and gaseous water. Augustine analyses were performed by N. Nehring, USGS, Menlo Park, California.

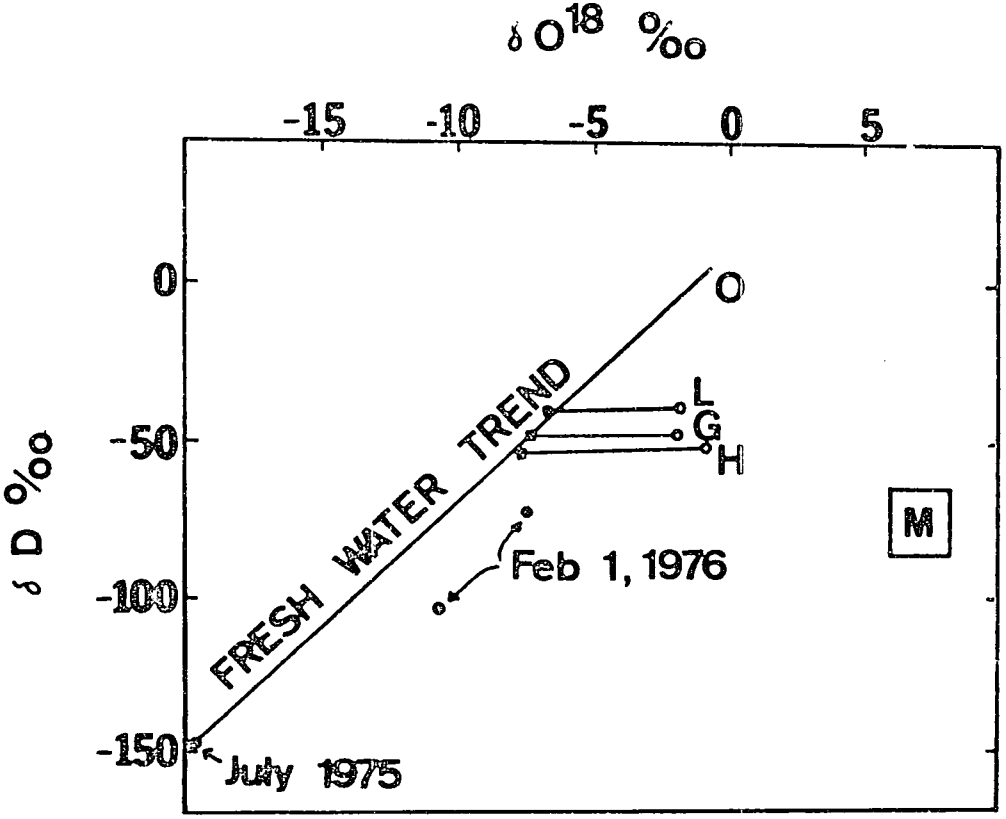
δ O18 ‰
-15
-10
-5
0
5
0
-50
-100
-150
δ D ‰
O
L
G
H
M
FRESH WATER TREND
Feb 1, 1976
July 1975

demagnetization due to ascent of magma into cold country rock had occurred between 1972 and August, 1975.

An explosion seismology experiment was undertaken August 3 and 4, 1975 by the University of Alaska and Sandia Labs to search for magma accumulations within the superstructure and shallow basement of Augustine. Ten explosions were set off on Augustine Island, and the response monitored by the permanent seismic array (six stations) supplemented by a 12-station portable array. Magma bodies larger than the resolution of the method (approximately 400 meters in diameter) were not detected at depths less than 2 km beneath the island (Pearson, 1977).

In summary, the measured thermal, magnetic, and seismic properties of Augustine Volcano, and the isotopic composition of fumarolic emissions from at least one active fumarole field, gave no indication of any changes within the volcano which might have preceeded the 1976 eruption. This may indicate either: (1) that no changes had occurred before that time; (2) that whatever changes that may have occurred did not produce any detectable differences in the measured properties; or (3) that the response to processes recently active at depth was not yet detectable at the surface.

BACKGROUND SEISMICITY OF AUGUSTINE

Seismic activity has been monitored continuously by a seismic array established by the University of Alaska on

Augustine Island in 1970. During the time that it has been monitored, Augustine's seismicity has varied from a few small events per day to intense microearthquake swarming activity. During swarms, which have occurred most frequently during the months of December to February, the number of events can increase by 2 or 3 orders of magnitude over the background level. Most of this microseismic activity occurs within the cone itself or at very shallow depths below the island, and is limited to events of very small magnitude. Two swarms, one during August-September, 1971, the other during the four months preceeding the 1976 eruption, appear to have originated deeper and attained greater magnitudes than the more common swarms that occurred each winter (Lalla and Kienle, 1978).

Plots of the hourly frequency of microearthquakes during swarms often show a diurnal peak in activity. Mauk and Kienle (1973) related this cyclicity to earth and ocean tides, suggesting that compression and dilation of the earth's crust and ocean loading can trigger seismic strain release at Augustine. Lalla (Lalla and Kienle, 1978) has recently recognized a correlation between increasing seismicity and decreasing atmospheric temperature, and has suggested triggering by formation of ice near the surface, producing seisms either by water expansion, or by decreasing surface permeability and outgassing.

The seismicity of Augustine, particularly during the

four-five months before the 1976 eruption, is being studied by D. Lalla (PhD dissertation, University of Alaska, Fairbanks, in progress) and Reeder, Lahr, and Kienle (cf., Reeder and others, 1976, ms).

PRECURSORS TO THE 1976 ERUPTION

Microseismic activity increased abruptly in early October, 1975, approximately 115 days before the eruption began (see Figure 2). This swarm contrasted with those of preceeding years, in that the microseisms reached greater magnitudes and occurred at slightly greater depths, to a maximum of 2 $\pm$ 1 km below sealevel (Lalla and Kienle, 1978), and activity remained at an elevated level for a much longer time (earlier swarms generally did not continue for more than a few days).

In further contrast to earlier swarms, the swarming that occurred after October 27, 1975 was accompanied by many unusual seismic signals characterized by long duration (up to 15 minutes), emergent arrivals, moderate amplitudes, and irregular high frequency pulses, and which appear to have been propagated at acoustic velocity from a source near the volcano's summit (J. Kienle, 1976, personal communication). Similar events have been recorded on seismometers at Ruapehu Volcano, New Zealand while steam explosions were observed at the volcano's vent (Dibble, 1974, p. 58, Fig. 10). Signals of this type were extremely rare in the seismic records of preceeding years (approximately one per year).

Figure 2: Plot of the number of local microseisms recorded on one Augustine seismic station during the last part of 1975, averaged over 5 or 6 day intervals. Gaps in the plot represent periods during which the seismic stations were not operational. Data have been provided by D. Lalla (personal communication, 1977).

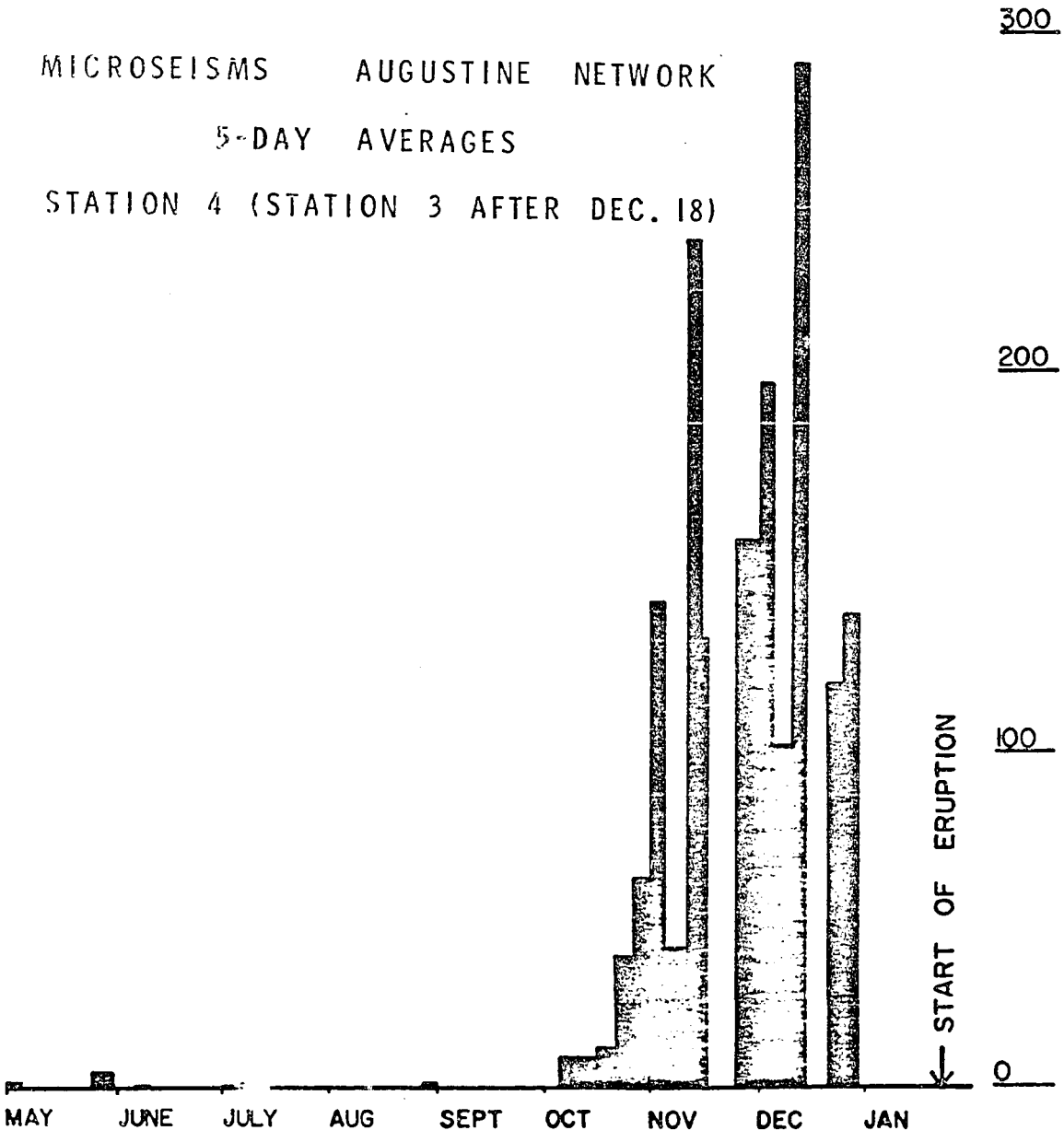
MICROSEISMS AUGUSTINE NETWORK
5-DAY AVERAGES
STATION 4 (STATION 3 AFTER DEC. 18)
300
200
100
0
START OF ERUPTION
MAY
JUNE
JULY
AUG
SEPT
OCT
NOV
DEC
JAN

Unfortunately, the 6-station seismic network operating on Augustine failed during late December, 1975. Kienle and Forbes (1977) implied that preliminary mudflow and rockfall activity caused the failure, but several observations suggest that electronic malfunctions were responsible.

1. Signals from several stations faded and reappeared during two weeks of bad weather in late December, before they finally terminated.

2. While the Augustine network was failing, nearly the entire lower Cook Inlet network was suffering similar malfunctions. Each of the three stations located closest to Augustine on the mainland were also out of operation prior to the 1976 eruption.

3. Although aerial searches were periodically undertaken, there was no visible evidence of mudflow or debris flow activity during the period that the seismometers malfunctioned.

ERUPTION CHRONICLE

The chronology of the 1976 eruption, which follows, has been established from: newspaper accounts; Surface Weather Observations of the U.S. Weather Service stations at Anchorage, Homer, Kenai, Iliamna, and King Salmon; infrasonic and seismic records maintained by the University of Alaska (Kienle and Forbes, 1977) and the USGS (Reeder and others, ms, 1976); observations of myself and W. Feetham, G. Gunkel, J. Kienle, B. Kopplin, D. Lalla, R. Motyka, and J. Stith;

and radar and other observations recorded in Smithsonian event cards 2367, 2368, and 2397, compiled, in addition to persons already mentioned, by P. Sventek. The observations recorded in these sources have been evaluated in light of deposits found on Augustine island, during investigations carried out by myself and H.-U. Schmincke.

Some contradictions exist between these sources of information, in particular, with regard to the thickness of ash deposits. There is very little reliable information concerning the distribution and thickness of ash deposits, hence volume estimates have large uncertainties.

The approximate time of individual eruptions has been established by: (1) their infrasonic and air pressure records (Kienle and Forbes, 1977; Reeder and others, 1976, ms); (2) eyewitness accounts, primarily recorded in newspapers; (3) radar observations of eruption columns; and (4) inference from times of recorded ash fall, obtained from the Surface Weather Observations and newspaper reports.

Some explanation of infrasonic records are required, because many more infrasonic "events" were recorded than were eruptions observed. Furthermore, at least one eruption apparently occurred which was not detected on the infrasonic array. Infrasonic signals were recorded on a quadrilateral array located in Fairbanks, 688 km north of Augustine. Infrasonic waves are apparently generated by air displacement during rapid ejection of volcanic ash and/or gases, and are

transmitted via sound channels in the upper atmosphere. The strength of a signal is generally proportional to the height or volume of the erupted cloud, but comparisons are extremely unreliable, and even exact eruption times cannot be determined from the records, because atmospheric conditions influence the propagation of signals (Wilson and others, 1966). Unfavorable atmospheric conditions or excessive infrasonic noise at the receiving station may obscure some signals.

Air pressure waves, also generated by air displacement during eruptions, were registered at USGS seismometers located 80 to 318 km from the volcano. The seismometers recorded all of the thirteen "events" recorded on the infrasonic array in Fairbanks, except one (January 22, 1976, 7:59 AST). Two small events (January 23, 15:59 and 16:07 AST) and a possibly large, but unverified event (January 22, 22:19) were recorded on USGS seismometers and not on the Fairbanks infrasonic array. Neither the seismometers or the infrasonic array appear to have recorded the first ash producing eruption at approximately 17:00 AST January 22, 1976.

JANUARY ACTIVITY

The earliest indication that an eruption had begun was a medium intensity infrasonic event generated at 7:59 AST, Thursday, January 22. Activity was confirmed at 10:25 when a commercial pilot observed clouds billowing from the sum-

mit. Height finding radar at King Salmon and Sparrevohn reported eruption clouds at 4000-5000 meters that afternoon.

Seismic activity, by that time only recorded on stations located on the mainland 80 or more kilometers distant, increased sharply immediately after the initial explosion. Earthquakes detectable on mainland stations increased from a steady background level of one or two events per hour to nearly 60 per hour by 19:00 January 22, and then declined again before the second infrasonic signal was generated at 3:53 January 23 (Reeder and others, 1976, ms). During this time seismic activity increased and decreased in harmony with increasing and decreasing ocean tidal loading (Figure 3).

Approximately 2 to 6 mm of ash fell in Iliamna Lodge around 17:00 Thursday, January 22, apparently following an eruption whose infrasonic signal was not felt on either USGS seismometers or the Fairbanks infrasonic array.

After several small and very small infrasonic events at 22:19, January 22 (reported by USGS only), 3:53, 5:01, and 6:16 January 23, all without reported ash-fall on the mainland, two large magnitude events occurred in rapid succession at 6:58 and 7:40. Ash from one or both of these eruptions fell heavily on Iliamna, 90 km west of Augustine, reducing visibility there to less than 30 meters during the peak of the ash-fall. Minor ash-fall following these explosions was also reported in Seldovia and Homer, located

Figure 3: Plot of the relative time of infrasonic events generated during the January phase of activity (from Kienle and Forbes, 1977), seismic events recorded on USGS seismometers located 80 km or more from the island (Reeder and others, 1976), and the magnitude of ocean tidal loading (from Kienle and Forbes, 1977). Microseisms are shown in number of events per hour (scale on right side of figure).

Major ash-producing eruptions occurred at approximately 16:30 AST January 22, 6:58, 7:40, and 16:20 January 23, 8:38 January 24, and 4:56 January 25. L and M refer to large- and medium-intensity infrasonic signals, all others are smaller.

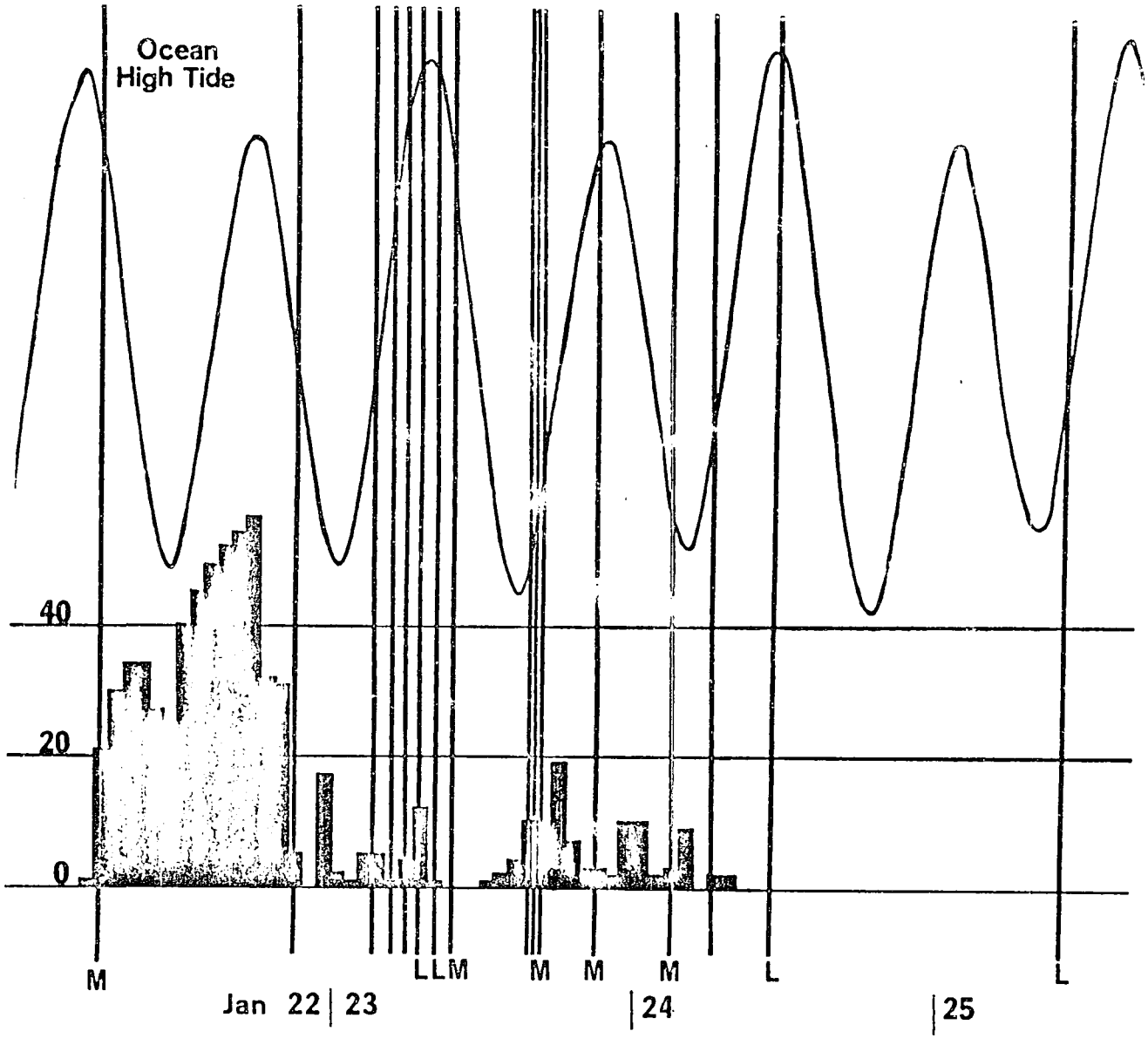
Ocean
High Tide
40
20
0
M
LLM
M
M
M
L
L
Jan 22
23
24
25

110 km east of the volcano. Radar at Sparrevohn measured the top of the clouds generated in these explosions at 10700 meters, well above the tropopause (base of the stratosphere), which at that time was at approximately 9800 meters. Spectacular lightning displays were visible within the eruption cloud during this and subsequent eruptions.

Another moderate explosion produced an infrasonic event at 10:08, January 23, which was also not accompanied by ashfall in populated areas.

Wind directions changed rapidly during the course of the eruptions, as the center of a regional high pressure weather system passed through lower Cook Inlet Friday, January 23, bringing rain and snow. East and southeasterly directed winds prevailed at high altitudes during the late hours of January 22 and early hours of January 23, and carried ash towards Seldovia, Homer, Valdez, and as far away as Sitka, where very fine ash (less than 0.05 mm diameter) fell during the evening of January 23. Ash injected into the stratosphere, apparently during the large eruptions of Friday, January 23, 6:58 and 7:40, continued to drift eastward, and on January 28, 1976, a Lidar laser system detected ash from these eruptions drifting at 14 km altitude over Hampton, Virginia (Meinel and others, 1976). More northeasterly directed winds developed later Friday and Saturday, January 24, and subsequent ash falls were directed towards Anchorage (see Figure 5).

Figure 4: The summit of Augustine Volcano in late July, 1975 (A) and on January 29, 1976 (B). Both photographs were taken from roughly the same position. The contact between the 1963-64 lava dome and older rocks that formed the crater rim before it was filled is visible as a light colored area that follows downslope from the saddle between the 1963-64 dome, which comprises the summit of the volcano, and the 1935 dome, which is the first bump on the skyline ridge below the summit on the right side of the photograph. The 1976 crater margin nearly matches this contact.

The summit spine of the 1963-64 dome is also visible in (A).

Figure 4 is carried over onto page 21.

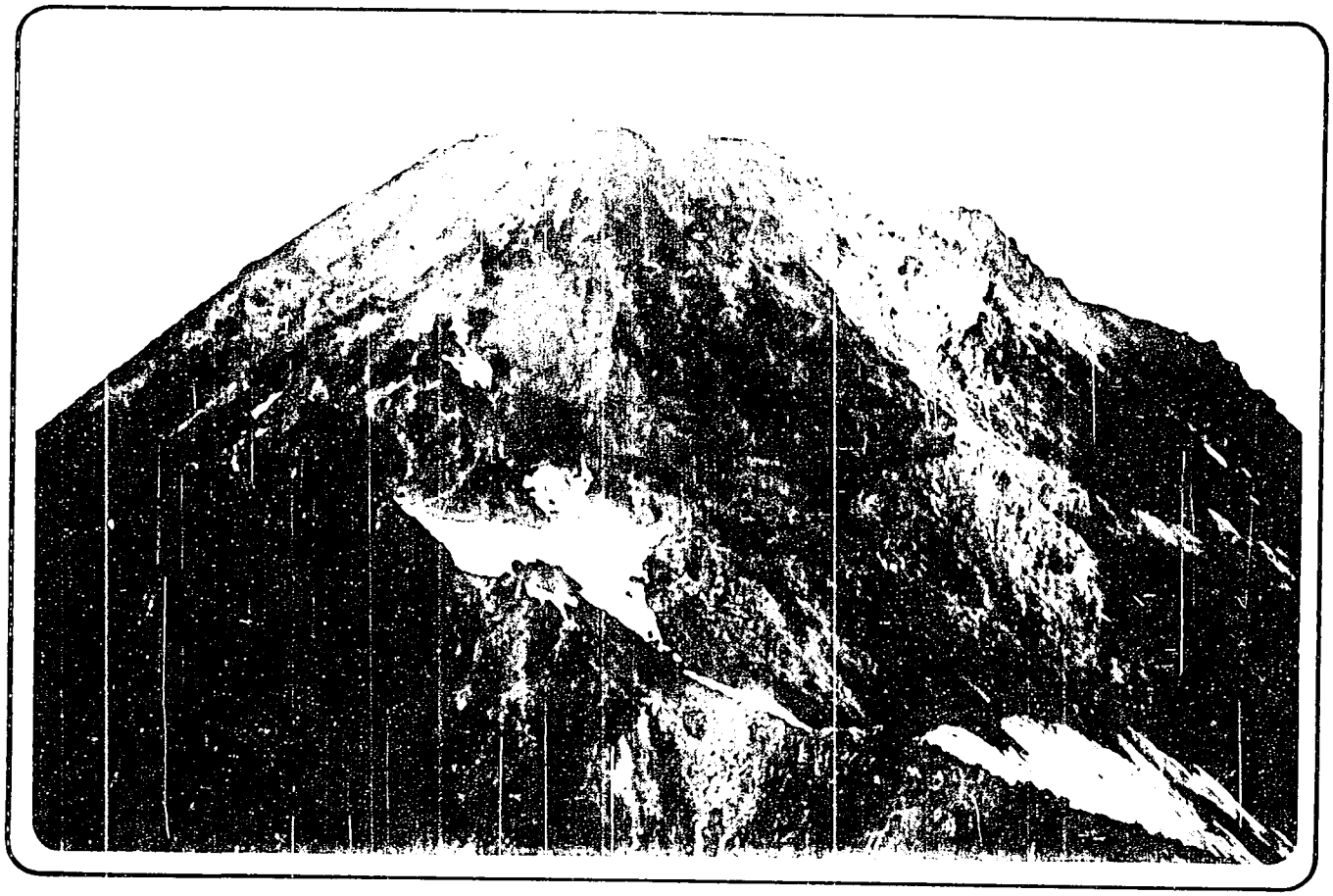

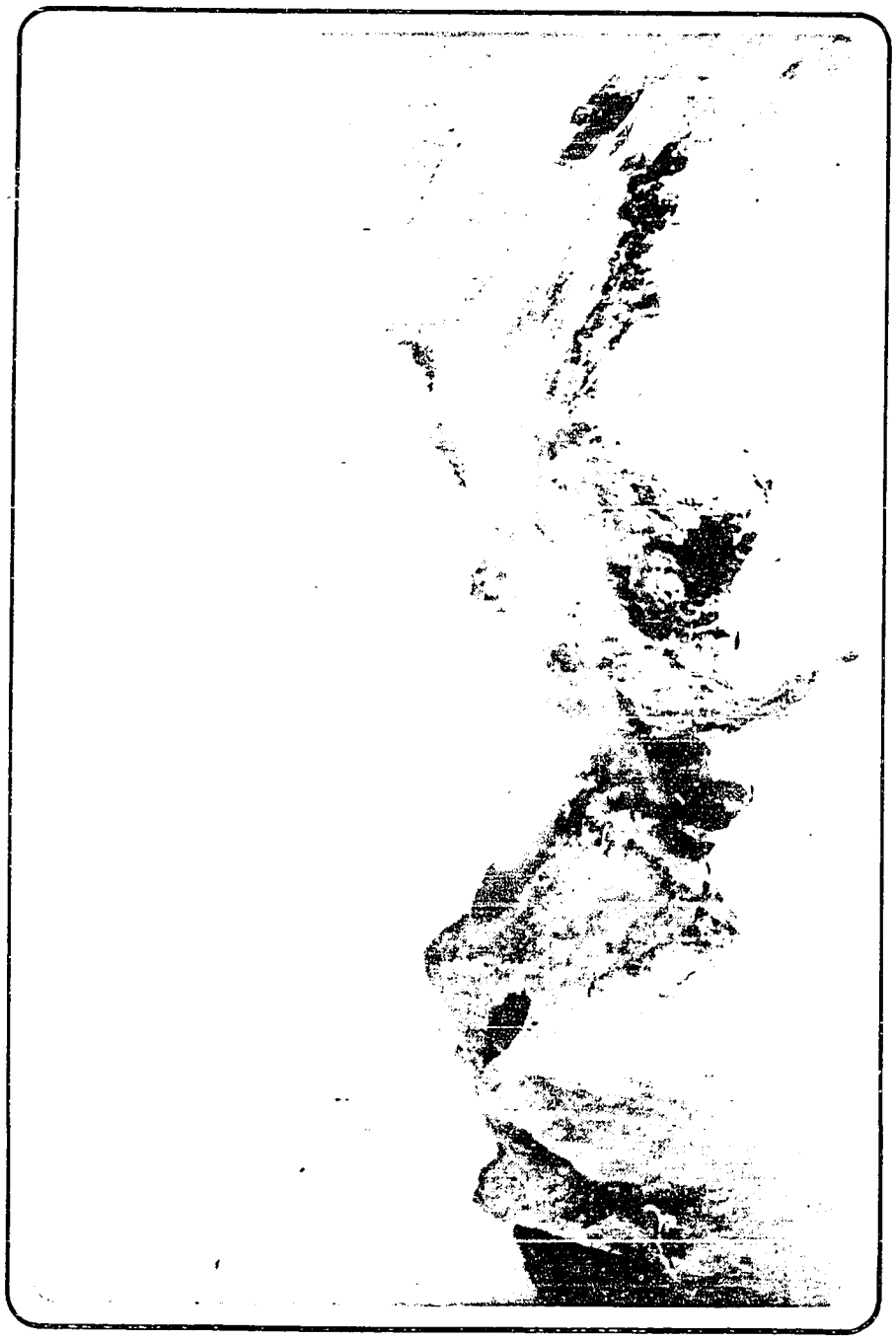

Figure 5: Areas receiving ash-fall at various times during the January phase of the 1976 eruption. Distribution has been compiled by reference to sources cited in the text, and is least reliable towards the west.

Abbreviations are: KS, King Salmon; Sp, Sparrevohn Air Force Base; I, Iliamna; H, Homer; K, Kodiak; A, Anchorage; T, Talkeetna; and V, Valdez. The distance from Augustine Island to Anchorage is approximately 285 km.

Figure 5 is carried over onto pages 23 and 24.

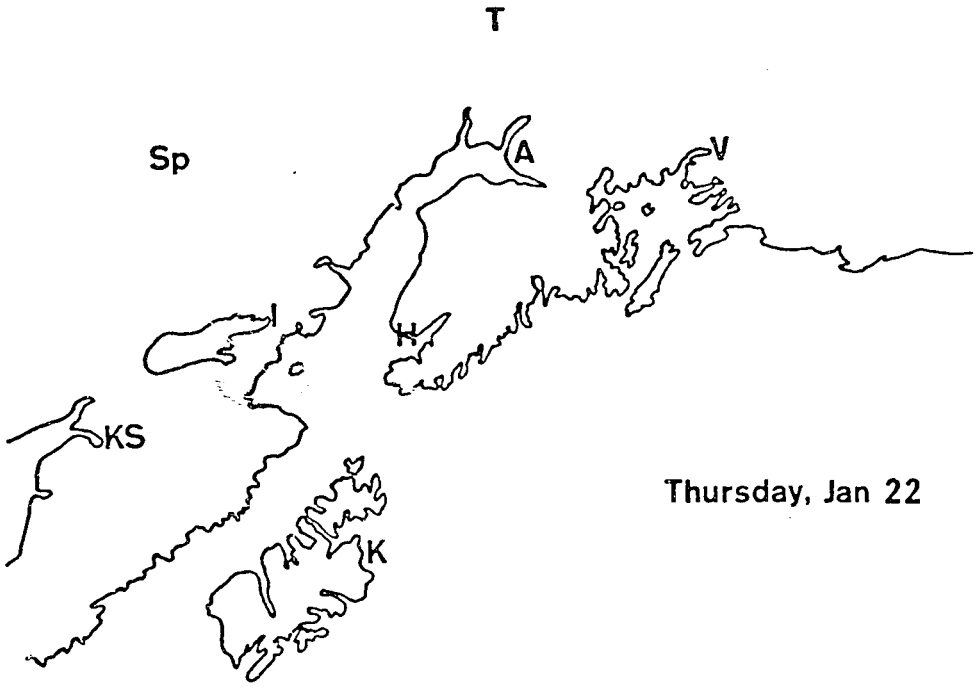
T
Sp
A
V
KS
K
Thursday, Jan 22

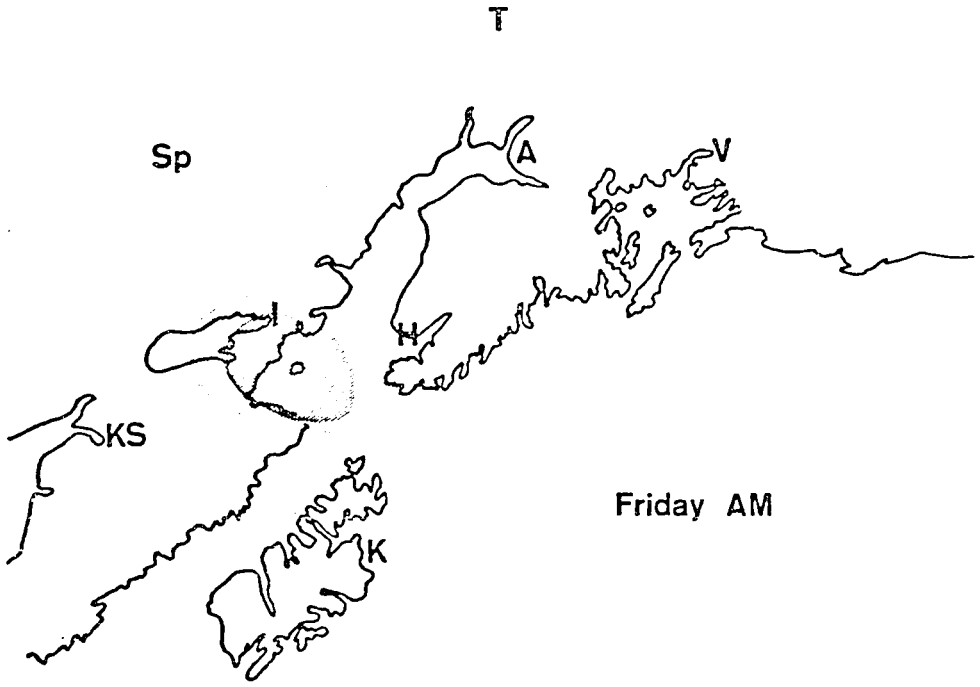
T
Sp
A
V
KS
K
Friday AM

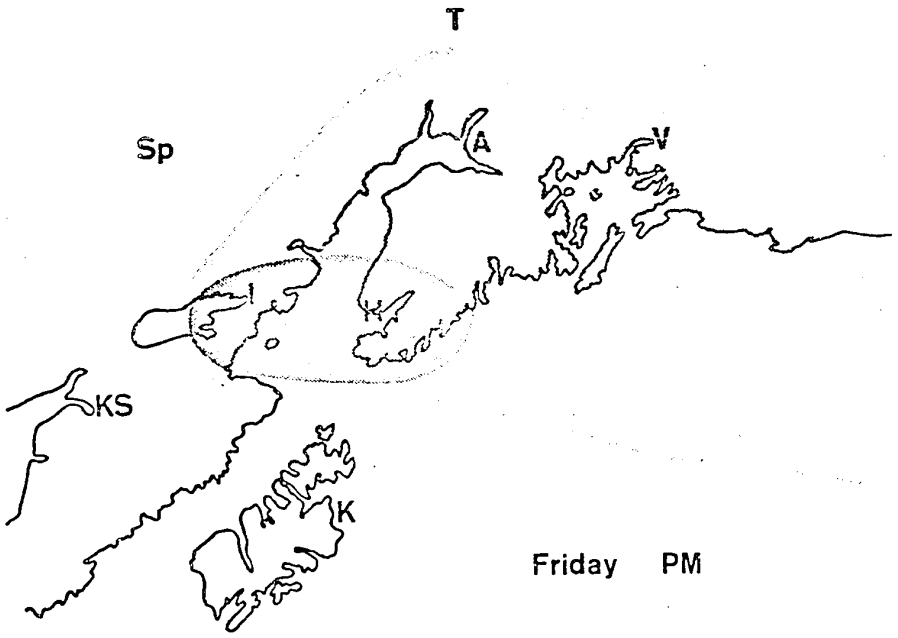
T
Sp
A
V
H
KS
K
Friday PM

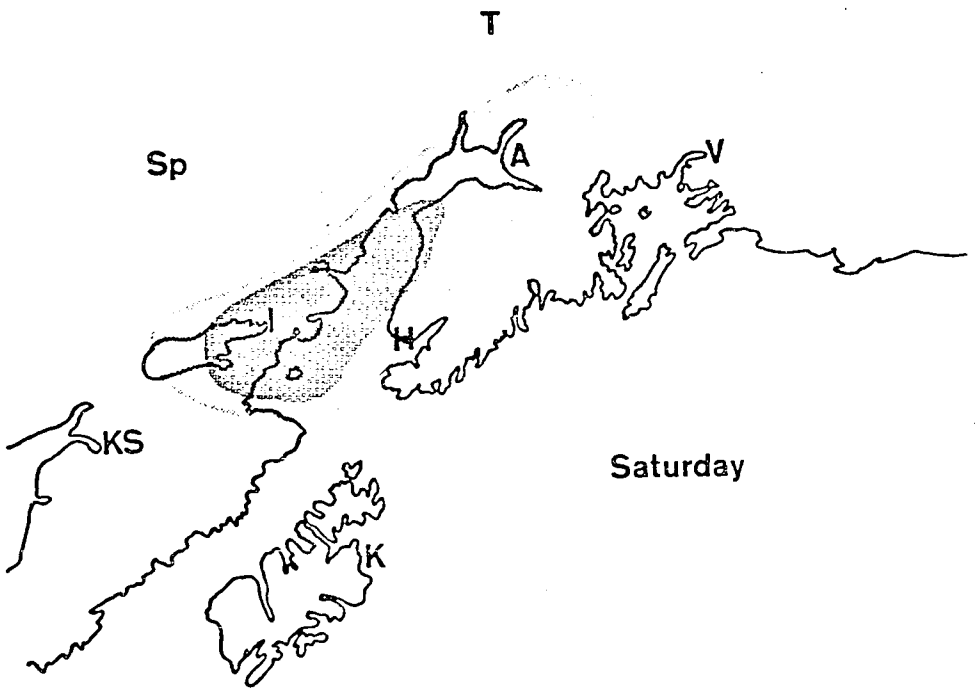
T
Sp
A
V
H
KS
K
Saturday

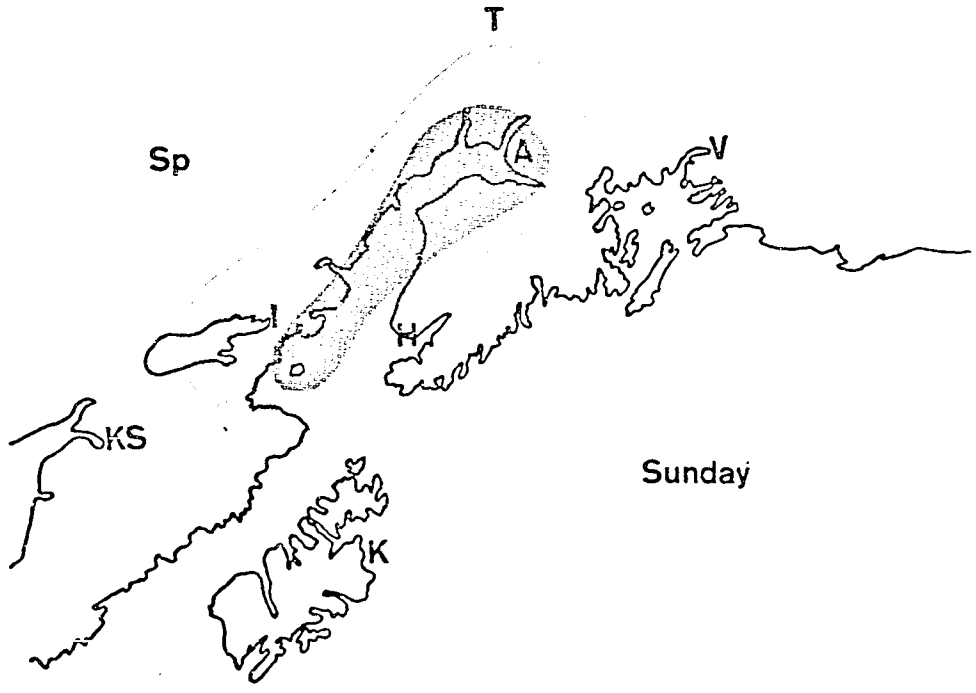
T
Sp
A
V
H
KS
K
Sunday

Photographs taken of the volcano at approximately 13:00 Friday, January 23, show the existence of a summit crater approximately 650 meters in diameter, in the place that had been occupied by an andesite dome emplaced in 1964. By that time also, ash-flow and mudflow deposits were present in drainages on all sides of the volcano.

Another large eruption occurred at 16:18 Friday, January 23, producing a cloud that reached 11 km altitude. By 17:00 the cloud had drifted over Seldovia and Homer, and the most intense ash-fall began approximately 45 minutes later, depositing fine sand-sized ash. In one hour, from 18:30 to 19:30, 186 grams of ash fell per square meter in Seldovia (R. Motyka, University of Alaska, written communication, 1976).

After several more small infrasonic events during the night of January 23 and the morning of January 24, a large explosion, described by witnesses as the largest of the three major explosions of the January episode, occurred at 8:38 AST. Radar at Sparrevohn and King Salmon traced the development of the eruption cloud as it grew 12,200 meters in three-four minutes, and spread laterally to cover an area 80 km wide. Heavy ash-fall at Iliamna again reduced visibility to less than 30 meters for almost 25 minutes, and ash-fall continued there for nearly four hours.

The final eruption of the January episode occurred at 4:56 AST, Sunday, January 25. Ash from this eruption fell

during the morning hours in Iliamna, Kenai, and Anchorage, where approximately 1.5 mm of fine ash was deposited between 9:20 and 10:55, for a while reducing visibility there from 20 to 2½ miles. For another day afterwards, noticeable ashfall occurred in the Anchorage area, reaching as far north as Curry, 420 km northeast of Augustine.

For 12 days after January 25, activity was limited to non-explosive gas emission from the summit crater. Side scanning radar and temperature measurements obtained February 1 by members of an NCAR team examining atmospheric emissions of the volcano indicated that the summit crater was approximately 200 meters deep and had a bottom temperature in excess of 350° C., the limit of measurement of the probe used.

FEBRUARY ACTIVITY

At 4:43 AST, February 6, Augustine burst into eruption again. This eruption showered fine ash that fell with rain on Kenai and Soldotna on the Kenai Peninsula, and produced new pyroclastic flows that spread down each flank of the volcano. The most extensive of these flows travelled approximately 100 meters beyond the shoreline on the northeast flank of the volcano, in the same area where pyroclastic flows had extended beyond the shoreline in January. This eruption produced a small infrasonic signal which was recorded on the array in Fairbanks.

The second major eruption of the February episode occurred at approximately 12:30 AST, February 6. The account

and photographs of an eyewitness to this eruption provide evidence that one or more large pyroclastic flows travelled down the northeast side of the volcano, and that small pyroclastic flows may have extended a few hundred meters down the northeast side of the volcano, and that small pyroclastic flows may have extended a few hundred meters down the southeast and southwest sides. This, or the earlier eruption, was the last to produce pyroclastic flows anywhere on the volcano except on the northeast flank.

Minor ash-fall was noted as far away as the Kenai Peninsula on February 6 and 7. By February 8, when the cloud physics group from the University of Washington began observing the volcano (Hobbs and others, 1976), vertical eruption columns reached only 15-20,000 feet (4½ to 6 km), and ash no longer fell on populated areas.

Over 50 air pressure waves were recorded on USGS seismometers during the following two weeks, gradually declining in frequency from a maximum of 10 on February 8 (Reeder and others, 1976, ms). Observations by various witnesses suggest that the height of vertical eruption columns and the distance that pyroclastic flows extended irregularly decreased during this period.

Unfortunately, the early history of the lava dome is not well known, because observation was generally restricted by gases issuing from its surface and margins. During February 11 and 12, long period (approximately 1 second)

oscillations were recorded on several seismometers located 50 to 80 km from the island on the west side of Cook Inlet. Kienle and Forbes (1977) have interpreted these signals as harmonic tremor, possibly related to the emplacement of the lava dome. Eyewitnesses saw the dome no later than February 12. It may have been emplaced before that date, but was almost certainly not present on February 1, when a 200-meter deep crater was seen on side-scanning radar.

A University of Alaska party returned to the island February 18-28 to reestablish seismic stations on the island. Very small bursts of ash-laden vapor were produced infrequently during the early part of this period.

Seismic stations reestablished in late February recorded very little microseismic activity until April. In early April microseismic activity began to increase dramatically, accompanied by steam explosions (detected on seismic stations as air pressure waves, D. Lalla and J. Kienle, 1977, personal communication). From April 13 to 18 ash flows were seen to fall directly from a stationary point of origin on the north face of the dome, approximately every 10-15 minutes. The debris flows were not accompanied by significant superjacent or vertical ash clouds, although vapor emission apparently increased during each flow.

Photographs taken in late February and August, 1976, illustrate that the lava dome grew perhaps as much as 100 meters during the April activity.

STRATIGRAPHY OF THE 1976 DEPOSITS

JANUARY DEPOSITS

The earliest ash layer deposited during the 1976 eruption is a thin (less than 3 mm) discontinuous tan ash, consisting of fine glass shards, crystal fragments, and lithic fragments. The ash is well-sorted, extremely fine (maximum particle size - 0.1 mm), and in thin section appears to be size-graded with the coarsest particles at the base. The ash layer is locally reworked and does not anywhere contain vesicles. The individual glass shards are blocky and angular, and bubble wall textures are not common on phenocrysts.

The overlying grey ash is present nearly everywhere on the island, where it varies from 0 to 6 cm thick. It appears to contain a greater portion of lithic fragments than the earlier tan ash, and is somewhat coarser-grained (maximum particle size - 2 mm). Both in the field and in thin section a subtle break is visible between the lower part of the ash (lighter colored) and the upper part (marked in thin section by a separate size graded layer), suggesting that the grey ash may be the product of two separate explosions. The grey ash has locally been reworked prior to emplacement of the overlying olive ash layer, but where it is not reworked, vesicles are preserved within the ash layer, indicating that the particles were still degassing after emplacement.

In the northeastern quadrant of the island, the lower ash layers are overlain by a distinctive olive ash layer,

which varies in thickness from 1 to 17 cm or more. The deposit is thickest uphill (towards the volcano) from small hills: near Burr Point, 5 km north of the vent, the deposit is 17 cm thick on the uphill side of a 10-meter high ridge, but is only 4 to 6 cm thick in the flat plain 25 meters from the ridge. The debris is somewhat coarser than the underlying ash layers (maximum particle size - 5 mm), is moderately well sorted, non-graded, and contains vesicles and lapilli (degassing) pipes that imply vigorous degassing after emplacement. Emplacement temperatures of the olive ash were high enough to slightly char wood (in contrast to the cooler underlying layers).

Laborious excavations have demonstrated that the olive ash is beneath the stratigraphically lowest of three pumiceous nuée ardente deposits emplaced during January. However, it is not possible to preclude that one or more unrecognized buried nuée ardente deposits might be present farther upslope beneath the olive and also earlier grey and tan ash layers. Pyroclastic flow deposits emplaced during the eruptions of January 23-25, 1976 are present on all flanks of the volcano, but are most extensive and thickest on the northeast flank. These deposits thin to 30-50 cm at their distal edges, and are much thicker upslope, but probably do not exceed 5-7 meters maximum. The deposits (see Figure 6) extend 4-5 km to the shoreline and a few hundred meters beyond on the northeast flank of the cone. They contain

Figure 6: Reconnaissance and air photo map of the deposits of the 1976 eruption of Augustine as of August, 1976. Pyroclastic flow deposits are shown in red, and where buried in the vicinity of Burr Point, are outlined by a dashed line. Mudflow, flood, debris fall, and alluvial deposits are shown in yellow, and the 1976 lava dome is shown in blue. Air-fall tephra deposits are not shown.

abundant pumices and expanded breadcrust bombs, more than 20% fine ash (less than 0.125 mm), and abundant coarse (to several meters maximum diameter) and fine lithic fragments derived from older Augustine deposits. Sorting is poor. Vesicles, coarse lapilli pipes, and small phreatic craters on the surface of the deposits attest to their vigorous degassing, possibly explosive, soon after emplacement. The deposits were emplaced at very high temperatures as evidenced by extensive melting and charring that occurred up to 1½ km beyond the terminus of the deposits (Johnston and others, 1977), and high temperature fumaroles (to at least 400° C) that existed on their surface days and weeks after emplacement. Glass shards in the matrix of the pyroclastic flow deposits are extremely vesicular, and crystals exhibit bubble wall envelopes.

The uppermost January ash deposit is a coarse pumice, block, and ash layer, possibly composite, which was emplaced nearly everywhere on the island. On the north side of the island, the deposit increases in thickness from approximately 1 cm 5 km from the vent to 3 cm 3½ km from the vent. Pumices, over the same distance, increase from approximately 15 to 30 cm maximum diameter; dense andesitic and dacitic bombs and lithic fragments increase from 7 to 10 cm (Schmincke and Johnston, unpublished data). The ash layer is poorly sorted, and not megascopically graded. Shards and crystal envelopes, as in the pyroclastic flow deposits, are extremely vesicular.

FEBRUARY AND APRIL DEPOSITS

Recognizable ash layers, other than pyroclastic flow basal avalanche deposits, were not emplaced during the February and April eruptions. Pyroclastic flow deposits of the first two eruptions in February, like those erupted in January, were emplaced onto all flanks of the volcano (see Figure 7), and extend to a few hundred meters beyond the former shoreline on the northeast flank of the volcano. Subsequent deposits are less extensive, and are confined to the northeast flank of the cone, where they were emplaced through a breach in the crater rim. This breach formed during the first two days of eruptions in February, apparently by erosion during passage of pyroclastic flows.

The total thickness of February and April deposits is difficult to estimate. Individual flow deposits terminate with steep flow fronts, up to 1-2 cm high, and must increase in thickness upslope. As many as 70-100 separate flows may have been emplaced, but do not entirely overlap, and appear to have partly eroded the surface on which they were emplaced. The total thickness of February and April deposits probably does not exceed 20-30 meters maximum.

In contrast to the deposits emplaced in January and the first few eruptions in February, the deposits of later February and April eruptions contain little or no pumice, less than 5% fine ash (less than 0.125 mm), more large expanded blocks (up to 10 m diameter), and a much smaller component

Figure 7: Pyroclastic flow deposits of the 1976 eruption, divided to show those emplaced during the earliest activity (January 22-25, February 5-8) in green, during later February in red, and during April in blue.

Pyroclastic Deposits

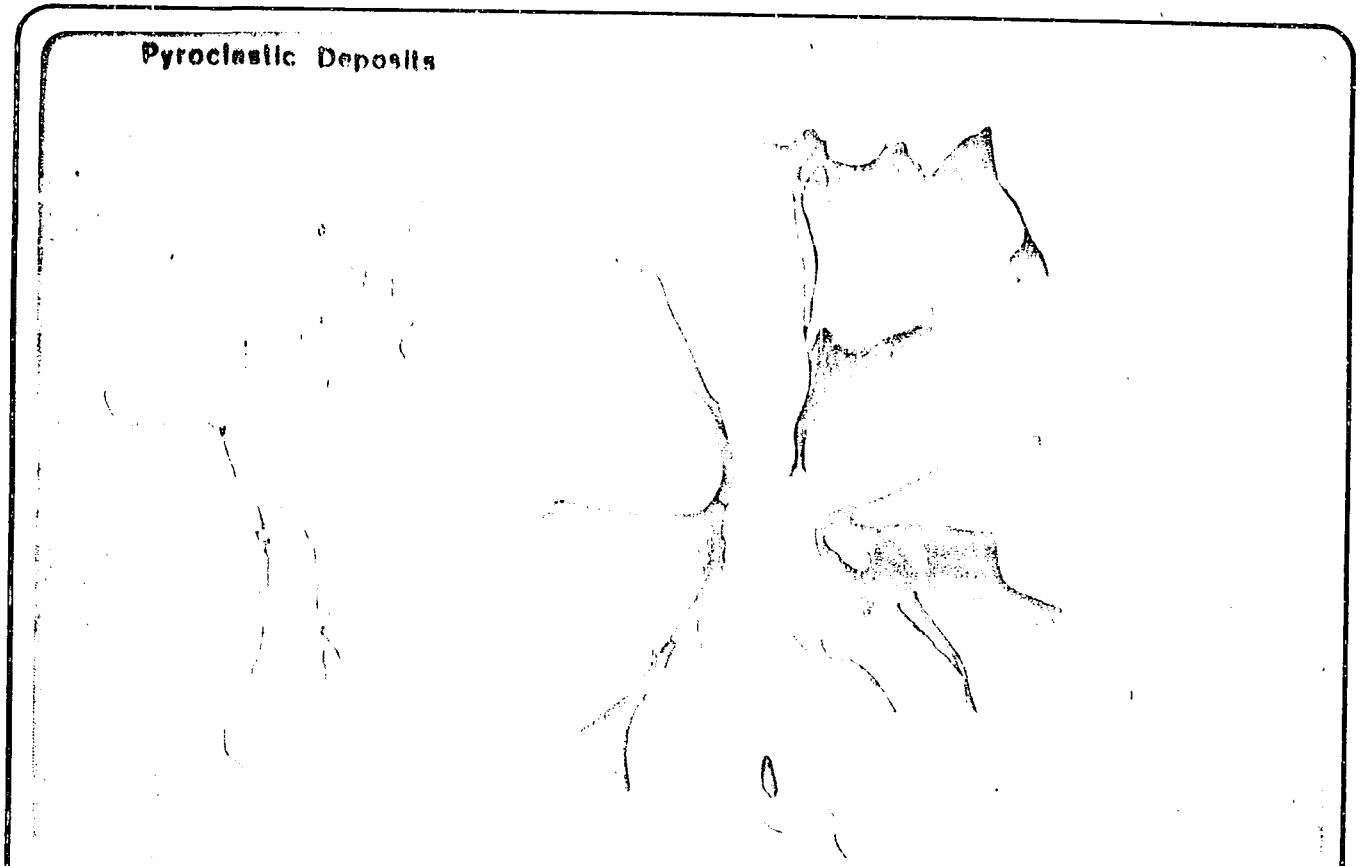

of lithic debris derived from older deposits (Schmincke and Johnston, 1977). Blocks in the late February and April deposits are primarily scoriaceous to dense andesite and dacite, similar to the material comprising the new lava dome. Glass shards and glass envelopes around crystals are less vesicular than those of the January eruptions.

High temperature emplacement of February deposits is implied by the temperature of their fumarolic emissions (greater than 600° C) measured several days after emplacement. The high temperature of emplacement of April deposits is indicated by eyewitness descriptions that the blocks in the flows were incandescent when tumbling down the volcano's slopes.

THE LAVA DOME

The new lava dome was emplaced within the summit crater formed at the beginning of the 1976 eruption, and hence, occupied approximately the same position as the lava domes emplaced at the conclusion of each historic eruption of Augustine. The new dome does not quite fill the crater, and the summit of the volcano (formerly the crest of the 1963-64 lava dome, 4,304 feet high) is now roughly 100-200 feet lower, and may be the summit of the new dome or the highest point on the south rim of the crater.

The morphology of the new dome resembles that of the 1963-64 dome. It is an endogenous dome, partially sheathed by an autoclastic breccia carapace and punctured at its

summit by a massive spine, approximately 5-10 meters high. On its north flank, the breccia carapace is absent, apparently having slid off the growing dome in February and April through the breach which is immediately below this flank. A small crater, approximately 60 m across, is present within the crater moat on the northeast flank of the dome, at the site where small steam explosions in March, 1977 were observed to originate.

Unfortunately, hazardous access has prevented close observation of most of the surface of the new dome. The massive interior, exposed on the north face, consists of uniform-appearing only slightly vesicular andesite or dacite. The blocks in the breccia carapace on the northeast flank are moderately to slightly vesicular, and appear also to be uniform grey or red (oxidized) andesite or dacite.

THE MECHANISM OF EMPLACEMENT OF THE DEPOSITS

The wide distribution, relatively uniform thickness, and graded bedding of the tan and grey ash layers reflect their deposition as air fall ash deposits, erupted, apparently, in the first two or three ash-producing explosions January 22 and 23 (ca. 16:30 AST January 22, 6:58 and 7:40 January 23). The limited distribution, variable thickness (controlled in part by topographic barriers), lack of grading, and evidence of moderately high temperature emplacement (slightly charred wood and lapilli degassing pipes) argue against an air fall origin for the overlying olive ash.

This layer appears, instead, to have been emplaced by a ground-hugging flow, and resembles deposits called elsewhere "ground surge" or "pyroclastic surge" deposits (Sparks and Walker, 1973). In light of the ambiguity of the evidence reflecting on the origin of the olive ash, and the general uncertainty of the origin of surge deposits elsewhere, several possible mechanisms may be proposed to explain this deposit, including emplacement as:

(1) an "ash-cloud" (termed "ash hurricane" by Taylor, 1958) that has separated from the basal avalanche portion of a nuée ardente,

(2) an unusually fine-grained nuée ardente,

(3) a "base-surge" (Moore, 1967).

The contrasting texture and distribution of the pyroclastic flow deposits erupted during January and February 5 and 6, and after February 6 reflect a change in the mechanism of their emplacement. Early deposits were emplaced onto all flanks of the volcano by collapse of vertical eruption columns (e.g., Sparks and Wilson, 1976), and were accompanied by regional ash-fall. Later deposits formed by collapse of the lava dome and were not accompanied by major vertical eruption columns or significant ash-fall. These were emplaced only directly downslope of the dome (Schmincke and Johnston, 1977).

The coarse pumice, lapilli, and ash layer above the January pyroclastic flow deposits, because of its wide extent

and relatively uniform thickness, also appears to have been emplaced as ash-fall out. Damage done by the impact of this ejecta upon the University of Alaska Research station at Burr Point supports this interpretation, and provides evidence, discussed elsewhere (Johnston and others, 1977) that this deposit was emplaced in the eruption of Sunday, January 25, 1976, which eventually deposited approximately 1½ mm of ash on Anchorage, 280 km distant.

CHAPTER 2: MAGMA MIXING AND IMPLICATIONS FOR THE MECHANISM OF THE ERUPTION

INTRODUCTION

Evidence for magma mixing or coeruption of two or more magmas in volcanic rocks appears to be widespread. It has been recognized in numerous calc-alkaline volcanoes of continental margins (Eichelberger and Gooley, 1976; Anderson, 1976), island arcs (Kuno, 1936; Eichelberger and Gooley, 1976), and continental interiors (Wilcox, 1944; Lipman, 1976); in basaltic and differentiated lavas of oceanic islands (Wright, 1973; Anderson and Wright, 1972; Schmincke, 1967); and at mid-ocean ridges (Sparks and others, 1977; Dungan and others, 1977).

The evidence has taken several forms: The most obvious are "mix-lavas" and banded pumices (Wilcox, 1944; Lipman, 1976; Schmincke, 1967; Fenner, 1926; Macdonald and Katsura, 1965). The former are rare, and the latter are volumetrically minor, but probably quite common in the early deposits of explosive eruptions (e.g., Roobol and Smith, 1976). Kuno (1936), Eichelberger (1975), and Eichelberger and Gooley (1976) recognized that reverse zoning of phenocrysts and disequilibrium or incompatible mineral assemblages are indicative of "contamination" by solid or molten contaminants. They found that such features are extremely common in intermediate calc-alkaline rocks. Anderson (1976) found that glass inclusions in different phenocrysts of a single rock commonly preserve evidence of distinctly different parental melts, which were mixed before eruption.

Geochemical evidence, in the form of linear variation

diagrams, has also been presented (e.g., Bowman and others, 1973), but must be viewed with caution: Such evidence is consistent with, but does not prove magma mixing. This evidence is also subject to a number of uncertainties:

1. Fractional crystallization ordinarily produces differentiation trends that do not deviate significantly from linearity over intervals of as much as 50-70% crystallization;

2. Crystallization and crystal movement which occurs after magma mixing may obscure the linear trends produced by mixing;

3. Scatter on most variation diagrams is sufficient to preclude recognition of linear vs. slightly curved differentiation trends.

Magma mixing as the mechanism of producing the observed chemical trends is disproved by a non-linear trend for <u>any</u> element (e.g., Milholland, 1975). Furthermore, it should be recognized that averaging groups of analyses (e.g., Eichelberger and Gooley, 1976) artificially improves the linearity of the data, and is, therefore, inappropriate for demonstrating magma mixing.

The petrologic implications of magma mixing are profound. Eichelberger (1975) suggested that magma mixing is the primary mechanism by which intermediate magmas of the calc-alkaline suite are generated. Magma mixing also has profound effects on the crystallization history of a magma:

Irvine (1977) described how mixing of more and less primitive magmas can lead to precipitation of particular phases at stages of differentiation when they would not ordinarily form by fractional crystallization. He suggested this as a possible mechanism for formation of chromitite layers in stratiform mafic intrustions. Magma mixing must be an important process active during the formation of many ophiolite suites (e.g., Hopson and others, 1977) and layered cumulates (e.g., McCallum and others, 1977), whose large size and relatively uniform composition preclude crystallization from a single, once entirely molten, magma body. Many of the cyclic variations that characterize the mode and mineral composition of these layered ultramafic intrusions may reflect the periodic introduction of new magma from deep sources.

Magma mixing must also affect the manner in which we study magma genesis. Clearly, the composition of the magmas involved in mixing will be obscured by the mixing process. Whole rock analyses may not reflect the original variability or the manner(s) in which that variability developed. Phenocryst zoning and glass inclusions within phenocrysts may record a more complete petrogenetic history of each magma.

Methods of modelling the trace element evolution of magmas must also be reconsidered in light of magma mixing and periodic magma resupply. O'Hara (1977) showed that changes in the relative proportions of magmas mixed within a periodically refilled differentiating chamber could lead to

variations in the trace element composition of the magmas that have been attributed previously to variations in the mineralogy or composition of mantle source rocks.

In this chapter I will present evidence that the andesitic to dacitic ejecta erupted during the 1976 Augustine eruption was the product of mixing of a basalt with a dacite. I will also examine the problem of when the magmas were mixed, by considering the size and the growth rate of plagioclase crystals formed after magma mixing began. I will examine the manner by which the magmas were mixed, whether by overturn of a zoned magma chamber or by supply of new magma from depth. And finally, I will show how water may have been rapidly exsolved from the magma during and soon after mixing, possibly triggering the 1976 eruption. In chapter 3, I will discuss some of the petrologic implications of magma mixing, the high water content of the magmas, and the implied presence of basalt.

COMPOSITION AND MINERALOGY OF THE 1976 EJECTA

Roughly 0.17 km^3 (not corrected for density contrasts) of rock was erupted during the 1976 eruption of Augustine Volcano. The pyroclastic flows constitute roughly 53% of that volume, the lava dome 38%, and the ash-fall and pyroclastic surge deposits 8%. Of the total volume, roughly 27%, or 0.047 km^3, was emplaced during the January eruptions, 59% or 0.102 km^3 was emplaced in February, and the remainder, 14% or 0.025 km^3, was emplaced during April.

Ejecta produced during the January eruptions are compositionally diverse, and include approximately 10% black coarsely vesicular andesite scoria, approximately 50% frothy white dacite pumices, and 40% banded and hybridized pumices and breadcrust bombs texturally and compositionally intermediate between the extremes. The bulk composition of several samples is reported in Table II.

Blocks and scoria included in February and April pyroclastic flow deposits and the new lava dome appear much more uniform than the January ejecta. Some variability in mode and phenocryst abundance is apparent from rock to rock, but hand specimen-scale banding is not visible. Although the new dome has not been examined except on its north and northeast side, it appears that the amount of mafic rock is less in the February and April ejecta, than it is in the January ejecta.

In this paper, dacites are broadly defined as having more than 60 wt.% SiO_2, andesites 52-60 wt.% and basalts less than 52 wt.%. This method is convenient because it facilitates discussion of unmixed "dacites" and hybrid "andecites". The distinction is arbitrary, however, and many of the "dacites" may actually be andesites if the distinction is established on other criteria, such as SiO_2 less than 62 wt.%.

DACITES

Dacite pumices contain approximately 20-50% phenocrysts

TABLE II: Whole rock chemical analyses of pumices and blocks ejected during the 1976 eruption (from Kienle & Forbes, 1977). Samples are described by Kienle & Forbes as follows: P1-1 Pumice (cream); P1-7 Scoria (grey); P1-9 Layered Scoria; P2-1 Andesite block; P3-1A Dacite block (core); P3-1B Dacite block (rim); P3-2 Dacite. Sample numbers given correspond to some of the samples for which individual mineral analyses are reported below. Analyses were performed by rapid rock techniques by Skyline Labs, Denver, Colorado.

	JANUARY				FEBRUARY		
Sample no.:	P1-1	P1-7	P1-9	P2-1	P3-1A	P3-1B	P3-2
SiO_2	63.8	60.8	61.3	58.6	63.5	62.9	64.2
Al_2O_3	15.9	15.9	15.9	16.5	15.7	16.2	15.7
TiO_2	.58	.62	.66	.68	.75	.53	.50
Fe_2O_3	1.8	1.9	2.5	1.8	1.6	2.1	2.1
FeO	3.3	4.1	3.6	4.6	3.2	3.4	3.3
MnO	.13	.13	.13	.14	.12	.12	.12
MgO	3.3	4.1	3.6	4.6	3.2	3.4	3.3
CaO	6.4	7.7	7.1	8.1	5.9	6.2	6.0
Na_2O	3.6	3.4	3.4	3.4	3.8	3.5	3.6
K_2O	1.0	.81	.83	.72	1.1	1.0	1.0
P_2O_5	.07	.05	.05	.05	.07	.05	.07
H_2O^+	.2	.2	.2	.2	.6	.2	.2
H_2O^-	.2	.2	.2	.2	.2	.2	.2
TOTAL	99.9	99.8	99.7	99.2	99.3	99.2	99.7

and scarce microphenocrysts in a glassy rhyolite groundmass (Table III). The crystals include: Plagioclase (approximately 60 volume %), hypersthene (18%), augite (17%), Fe-Ti oxides (5%), and trace amounts of apatite, chalcopyrite, and pyrrhotite.

Crystal aggregates of anhedral to subhedral pyroxene, plagioclase, and Fe-Ti oxides are a common, though volumetrically minor constituent. Several of these are pseudomorphs of hornblende or olivine. With the exception of tiny anhedral hornblende crystals observed at the core of one pyroxene crystal, neither of these minerals were observed in the dacite. Rare resorbed olivine crystals, Fo_{77-76}, with symplectite rims are present in banded and hybrid pumices and may have been present in the dacite prior to magma mixing. This interpretation is favored by the similarity between the composition of hypersthene in the symplectite rims and the phenocrysts of hypersthene in the dacite.

PLAGIOCLASE:

Plagioclase grades from phenocrysts 2-4 mm long to tabular microphenocrysts 100-200 microns long. It exhibits many radically different patterns of compositional zoning, even among the phenocrysts of a single thin section. Many have a broad, relatively homogeneous labradorite to bytownite core (An_{60-80}), and a slightly narrower oscillatory and/or normally zoned rim which reaches An_{55-47}. Patchy zoning, produced by resorption followed by renewed crystal growth

TABLE III: Composition of groundmass of pumices and blocks erupted in January and February. (Wt.%).

	JANUARY ERUPTIONS				FEBRUARY ERUPTIONS
Sample no.	P2-5	J2-6	P2-5	P2-5	AUG-4
Analysis no.	(1)	(2)	(3) 2σ	(4)	(5)
SiO_2	62.59	62.57	76.45 ± 1.24	76.31	76.64
Al_2O_3	18.80	15.49	12.31 ± .64	12.61	12.66
TiO_2	.53	1.02	.37 ± .06	.34	.35
FeO*	4.68	7.21	2.00 ± .20	1.86	1.90
MgO	1.79	2.55	.39 ± .06	.37	.36
MnO	.13	n.d.	.05 ± .04	.06	.06
CaO	7.09	5.66	1.92 ± .22	2.03	2.00
Na_2O[a]	3.84	3.48	3.39 ± .38	3.57	3.25
K_2O	1.33	1.22	1.94 ± .22	2.00	1.98
P_2O_5	.17	.20	.05 ± .04	.04	.03
Cl	n.d.	.27	.26 ± .04	.28	.23
S	n.d.	.01	.003± .01	.00	.00
F	n.d.	n.d.	.02 ± .04	.00	.02
TOTAL	100.95	99.68	99.15	99.47	99.48

[a] Na_2O-analyses are unreliable due to volatilization during microprobe analysis. Each reported analysis is an average of 5-20 separate spot analyses. In separate microprobe runs no attempts were made to reoccupy earlier analysis spots. Due to the presence of microcrystals in the groundmass of andesitic pumices, analyses 1 and 2 in this table are unreliable. Standard deviation reported for analysis 3 is typical of rhyolitic glasses.

(Vance, 1965) is common at the cores of phenocrysts, and within bands in the crystal that parallel former crystal surfaces. Zoning reversals, ordinarily not exceeding 4-5 mole % An, are also common, especially at patchy zoned horizons. Microphenocrysts are uniform or normally zoned, and resemble phenocryst rims in composition. Microphenocrysts and most phenocrysts are euhedral.

Glass, pyroxene, apatite, and Fe-Ti oxide inclusions are very common within plagioclase crystals. Very rare inclusions of pyrrhotite and chalcopyrite, intergrown in spherical globules, have also been observed. Glass and sulfide inclusions are discussed in greater detail in chapter 3.

PYROXENES:

Hypersthene and augite range in size from small equant microphenocrysts to phenocrysts 1 to 3 mm long. Though both are generally euhedral, some ragged anhedral hypersthene grains are jacketed by augite. Microprobe analyses disclose no notable differences between jacketed anhedral and discrete euhedral hypersthene grains.

In contrast to plagioclase phenocrysts, the composition of pyroxene phenocrysts appears remarkably uniform (Figure 8). Analyzed hypersthene phenocrysts are in the range $Wo_{1.2-2.8}En_{63.8-68.2}Fs_{30.5-34.0}$; analyzed augite are $Wo_{43-47}En_{64-68}Fs_{13.5-15.7}$. Optical zoning is only rarely visible within crystals, but where present is in the form of hourglass-type sector zoning or concentric rims.

Figure 8: Compositions of pyroxene phenocrysts in andesitic and dacitic pumices, and the composition of a clinopyroxene microphenocryst in an andesitic pumice (shown by an "X"), which was used to calculate equilibration temperatures based upon the Wood and Banno (1973) geothermometer. Tie lines and their corresponding temperatures are shown for a co-existing microphenocryst pair and two intergrown phenocrysts.

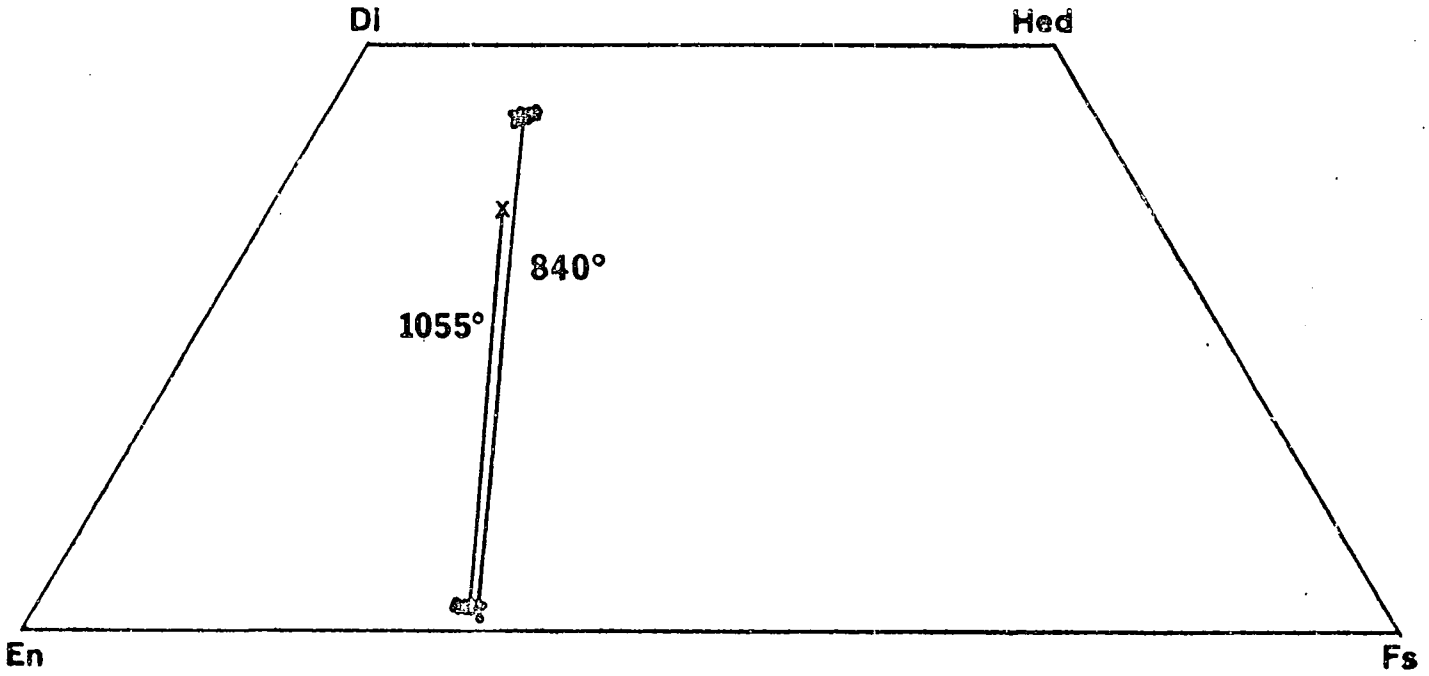
Di
Hed
X
840°
1055°
En
Fs

Pyroxene phenocrysts commonly contain inclusions of Fe-Ti oxides and glass, and less commonly apatite and plagioclase. Two tiny anhedral hornblende inclusions were seen in one augite crystal.

Representative pyroxene analyses are reported in Table IV.

Fe-Ti OXIDES

Fe-Ti oxides of the magnetite-ulvöspinel solid solution series occur as phenocrysts and as inclusions within other phenocrysts. Phenocrysts rarely exceed 1 mm in diameter, and are euhedral or anhedral and unzoned. Ti-rich ulvospinels are rare, probably less than 5% of the Fe-Ti oxides examined.

OTHER PHASES

Apatite, pyrrhotite and chalcopyrite are minor accessories in the dacite. Pyrrhotite and chalcopyrite are intergrown in tiny (less than 30-40 microns diameter) spherical globules, which have been observed only as rare inclusions in plagioclase. These sulfide globules are indicative of sulfide-saturation for the magma in which they formed, and are discussed in greater detail in chapter 3.

Apatite is present as microphenocrysts and as inclusions within each phenocryst phase in the dacite. It is relatively chlorine- and fluorine-rich (Cl=1.75-2.10 wt.%, F=1.29-1.39 wt.%), and is also discussed in chapter 3.

ANDESITES

Andesitic pumices contain approximately 10-25% pheno-

TABLE IV: Compositions of pyroxene phenocrysts and microphenocrysts in andesitic pumices (wt.%).

	PHENOCRYSTS				MICROPHENOCRYSTS		
Sample no.:	P2-5	P2-5	P2-5	P2-5	P2-5	P2-5	P2-5
Analysis no.:	(1)	(2)	(3)	(4)	(5)	(6)	(7)
Mineral:	OPX	OPX	CPX	CPX	OPX	OPX	CPX
SiO_2	53.97	53.40	52.44	52.55	52.66	53.21	51.17
Al_2O_3	.88	1.10	1.46	1.30	2.39	1.04	2.83
TiO_2	.14	.27	.36	.32	.23	.23	.72
FeO*	20.42	19.22	8.77	8.99	19.95	20.28	10.63
MgO	22.38	23.37	14.05	14.13	22.56	23.23	16.31
MnO	1.23	.61	.37	.40	.69	.70	.38
CaO	.90	1.13	22.55	21.82	1.05	1.20	17.79
Na_2O	.03	.03	.39	.36	.04	.05	.22
Cr_2O_3	.01	.02	.01	.01	.01	.02	.02
TOTAL	99.94	99.15	100.41	99.90	99.58	99.95	100.06
Wo	1.87	2.31	46.08	45.00	2.19	2.42	36.47
En	64.91	66.85	39.93	40.53	65.37	65.49	46.52
Fs	33.23	30.84	13.99	14.48	32.43	32.08	17.01

crysts within a microphenocryst-rich groundmass that is broadly andesitic in composition. The groundmass contains approximately 40-60% microphenocrysts of plagioclase, clino- and orthopyroxene, and Fe-Ti oxides, and is microvesicular.

An analysis of the interstitial glass in the groundmass of one andesite pumice is reported in Table III. An approximate analysis of the groundmass, obtained by broad beam microprobe analysis, is also reported.

Both andesite and dacite pumices contain crystals of plagioclase, hypersthene, augite, and Fe-Ti oxides. Phenocrysts of these minerals, present in the andesite pumices, resemble those in the dacite pumices in size, morphology, relative abundance, inclusion types, and, except at crystal rims, in composition. Moreover, glass inclusions within plagioclase and pyroxene phenocrysts from both rock types span the same compositional range: All are rhyolitic (see Table IX). These features imply that the phenocrysts in both rock types once grew in similar magmas.

Phenocryst rims and microphenocrysts of these mineral phases do, however, differ in the two rock types: In andesitic pumices, microphenocrysts and phenocryst rims appear to have grown in liquids distinctly more mafic than those in which phenocryst rims and microphenocrysts in dacite grew.

In further contrast to dacitic pumices, andesitic pumices contain phenocrysts of olivine (up to 2-3 volume %), and hornblende (less than 1 percent), which are absent from

dacite pumices. The olivine, in addition, contains inclusions of Cr-rich spinel (picotite), aluminous augite, hornblende, and glass which is distinctly more primitive than glass included within plagioclase or pyroxene crystals (see Table IX).

PLAGIOCLASE

Plagioclase phenocrysts in the andesite may be rimmed by a zone distinctly more calcic than the penultimate zone (An_{65-85} vs. An_{48-55}). In some grains (e.g., Figure 9) the calcic rim is separated from the inner portions of the phenocryst by a band dusted by numerous minute glass inclusions. Not all phenocrysts in andesite are rimmed by a calcic zone: in banded pumices, as few as one in three may be rimmed. In some other andesite pumices almost every phenocryst appears rimmed. Observed rims range from 0 to 100 microns wide parallel to $[\bar{0}0\bar{1}]$.

The composition of measured plagioclase microphenocrysts in the andesite groundmass ranges from approximately An_{70}-An_{80}. Many of the microphenocrysts are slightly normally zoned, most are not notably so. The microphenocrysts are euhedral, tabular, and elongate (length/width = 3-10), and range in size to a maximum of 46 microns perpendicular to (010) and 220 microns parallel to $[\bar{0}0\bar{1}]$.

In some banded pumices, the size and abundance of plagioclase microphenocrysts in the andesite increases gradually with increasing distance from the andesite-dacite

Figure 9: Plagioclase phenocryst with a calcic rim, contained in an andesitic pumice. Electron probe scan is along line shown on phenocryst. Stippled area contains numerous small glass inclusions.

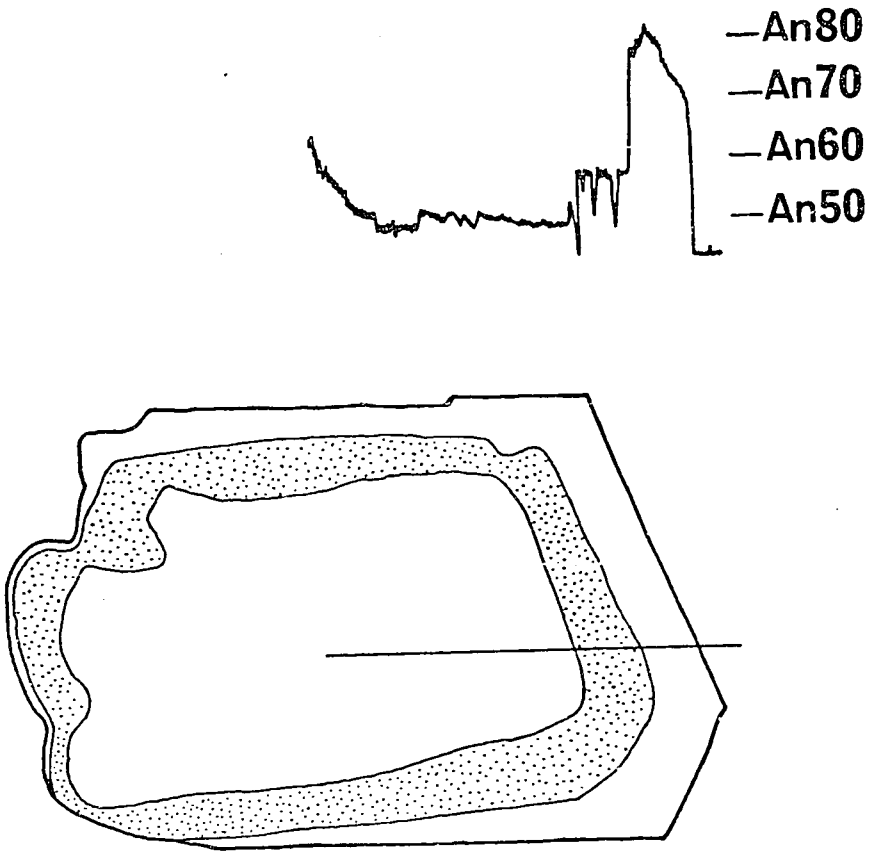
An80
An70
An60
An50
.1mm

interface.

PYROXENE

Microprobe scans disclose that many pyroxene grains in andesitic pumices are rimmed by slightly more magnesian zones, in which Mg/Mg + Fe = .67 to .68, vs. .64 to .66. The Ca-content is distinctly lower in the rim of many augite phenocrysts, and in microphenocrysts in the groundmass (see Table IV). Due possibly to their small size, zoning is not apparent in pyroxene microphenocrysts.

Pyroxene phenocrysts and microphenocrysts are generally euhedral. The later are equant to slightly elongate (length/width = 2), and generally less than 100 microns in maximum width.

Fe-Ti OXIDES

Some Fe-Ti oxides in andesitic pumices are marginally reticulate, apparently due to late resorption. Anhedral to euhedral equant Fe-Ti oxide microphenocrysts are also present within the groundmass of andesitic pumices.

OLIVINE

Two texturally and compositionally distinct types of olivine are present within andesitic pumices. The more abundant of these is slightly resorbed $Fo_{86.7}$-$Fo_{80.5}$. The other is very rare, is marginally resorbed and jacketed by orthopyroxene symplectite, and is less magnesian (Fo_{76-77}). The magnesian olivine constitutes as much as 2-3% of the volume of andesitic pumices, and is absent from dacite

pumices. The Fo_{77-76} is extremely scarce (very much less than 1%), and although it has been observed only in andesitic and other mixed pumices, because orthopyroxene in symplectite rims surrounding these olivines is compositionally similar to orthopyroxene phenocrysts in the dacite, it is likely that similar olivine is present in dacite pumices.

Both olivine types occur only as phenocrysts, which range in size to a maximum of approximately 1½ mm. The phenocrysts are generally equant to slightly elongate (length/width = 2). The faces of the $Fo_{86.7-80.5}$ phenocrysts are embayed, but not sufficiently to eradicate the formerly euhedral outlines of these crystals. Symplectite rims on the more resorbed olivine are as much as 200-400 microns wide.

Both olivines are normally zoned. The more magnesian olivine has a broad relatively homogeneous core ($Fo_{86.7-84.5}$), and decreases in Mg-content more rapidly in the outer third of the crystal. There is no optical or compositional evidence in any of the crystals examined for resorption, zoning reversals, or other composition breaks, except for moderate fluctuations (less than 400 ppm) in the Ni-content in the outer third of some phenocrysts. The less magnesian olivine appears also to be continuously zoned from Fo_{77} at the core to Fo_{76} where it intersects the symplectite rim. Representative olivine compositions are reported in Table V.

Olivine phenocrysts contain inclusions of Cr-rich

TABLE V: Composition of euhedral or slightly resorbed crystals of olivine in andesitic pumices (Wt.%).

Sample no.:	P1-8	P1-8	P1-8	P1-8	P1-8	P1-8	P1-9	P1-9
Analysis no.:	(1) CORE	(2)	(3)	(4)	(5)	(6) RIM	(7) CORE	(8) RIM
SiO_2	40.72	40.55	40.05	39.12	38.82	38.66	40.04	38.92
TiO_2	.01	.02	.02	.02	.01	.06	.06	.27
FeO*	12.55	12.75	14.62	17.91	17.79	18.14	13.05	16.90
MgO	46.03	46.13	44.91	42.21	42.48	41.90	45.51	41.75
MnO	.21	.24	.23	.30	.27	.31	.20	.57
CaO	.30	.25	.29	.26	.28	.37	.19	.74
NiO	.22	.21	.17	.11	.09	.05	.25	.06
Cr_2O_3	.04	.03	.03	.01	.01	.01	.00	.01
TOTAL	100.08	100.18	100.30	99.93	99.75	99.50	99.30	99.20
Fo	86.73	86.58	84.56	80.77	80.97	80.49	86.14	81.49
Fa	13.27	13.42	15.44	19.23	19.03	19.51	13.86	18.51

Analyses (1) to (6) are from a single normally zoned grain and represent equally spaced point analyses from the core to the rim. Analyses (7) and (8) are from another grain.

spinel, hornblende, aluminous clinopyroxene, sulfides, and partially crystalline glass. These are discussed in detail below, and in chapter 3.

SPINEL

Euhedral Cr-rich spinel (picotite) crystals are present in every olivine phenocryst observed. The tiny (10-40 microns) cubes vary in abundance within individual crystals, and may constitute as much as 1-2 volume % of some olivine crystals. Many of the spinel crystals occur in clusters, and appear to be concentrated near the center of the olivine phenocrysts.

Analyses of two separate spinel grains are reported in Table VI. Only 6 spinel grains, from a single olivine phenocryst (Fo_{86}), have been analyzed, but these appear extremely uniform.

Tiny spinel crystals are also present within aluminous augite crystals that are enclosed within or adjacent to olivine phenocrysts.

HORNBLENDE

Marginally resorbed hornblende phenocrysts are present in trace amounts in nearly all andesitic pumices, and compositionally similar tiny hornblende crystals are included inside most olivine phenocrysts. The hornblende is variable in size and shape. In hand specimen, large phenocrysts up to 5-6 mm long and 2-3 mm wide were observed; phenocrysts observed in thin section are ½ to 2 mm long and slightly to

TABLE VI: Composition of Cr-rich spinel crystals included in an olivine phenocrysts (Analysis 7, Table V), (Wt.%).

Sample no.:	P1-9	P1-9
Analysis no.:	(1)	(2)
TiO_2	.74	.76
Al_2O_3	33.47	33.30
Cr_2O_3	24.89	25.05
Fe_2O_3[a]	12.21	12.29
FeO[a]	14.92	14.81
MgO	14.80	14.91
MnO	.30	.29
NiO	.34	.30
ZnO	.47	.43
TOTAL	102.14	102.14
	Structural Formulae, O = 32	
Ti	.128	.131
Al	9.072	9.027
Cr	4.526	4.555
Fe^{3+}	2.114	2.128
Fe^{2+}	2.870	2.849
Mg	5.073	5.111
Mn	.058	.056
Ni	.063	.055
Zn	.080	.073

[a]Proportions of Fe^{2+} and Fe^{3+} were calculated from an electron probe analysis on the basis of the ideal spinel formula.

very elongate (length/width = 2-5). In thin section all phenocrysts appear slightly resorbed, and have a narrow (10-25 microns) rim of very fine-grained reaction products.

Hornblende included in olivine is anhedral and subequant, and approximately 50-200 microns wide. In contrast to hornblende phenocrysts, the inclusions are not rimmed by a fine-grained reaction rim.

Hornblende analyses are reported in Table VII. Zoning is not apparent in the phenocrysts or the included hornblendes examined. Classified according to the scheme of Leake (1968), the amphibole is a tschermakitic hornblende.

Hornblende phenocrysts contain sulfide inclusions, rare glass inclusions, and rare titaniferous magnetite.

ALUMINOUS CLINOPYROXENE

Anhedral to euhedral crystals of aluminous augite occur within and adjacent to olivine phenocrysts. These crystals range from approximately 20 to 300 microns wide and appear to be equant.

Electron probe analyses of representative aluminous augite are reported in Table VIII. These augites differ from the more common augite phenocrysts of the andesite and dacite in that they are more magnesian (Mg/Mg + Fe = 0.81-.82 vs. 0.64-.66), and more aluminous (approximately 3½ to 8 wt.% vs. 1 to 2½ wt.%). In contrast to phenocryst rims and microphenocrysts in andesite, they are also more calcic (47 mole% vs. 36-42 mole% Wo component). These appear not

TABLE VII: Composition of hornblende in andesites (Wt.%).

	PHENOCRYST		INCLUSION IN OLIVINE
Sample no.:	J-1-3B	J-1-3B	J-1-3B
Analysis no.:	(1)	(2)	(3)
	CORE	RIM	
SiO_2	41.31	41.65	41.12
Al_2O_3	14.18	14.29	15.37
TiO_2	2.04	2.20	1.47
FeO*	10.11	9.91	10.12
MgO	15.23	15.43	15.15
MnO	.10	.07	.13
Na_2O	2.50	2.47	2.09
K_2O	.21	.23	.15
P_2O_5	.02	.02	.03
Cl	.02	.02	.03
S	.01	.01	.01
F	.00	.00	n.d.
TOTAL	96.97	97.96	96.85
Number of ions on the basis of 24 oxygen			
Si	6.324	6.306	6.278
Al	2.558	2.550	2.766
Ti	.235	.251	.168
Fe	1.294	1.255	1.292
Mg	3.475	3.482	3.448
Mn	.013	.009	.017
Na	.743	.725	.618
Ca	1.844	1.891	1.827
K	.042	.045	.029
P	.003	.003	.005
Cl	.004	.006	.009
S	.002	.004	.003

TABLE VIII: Composition of aluminous clinopyroxene microcrystals included in olivine and hornblende (Wt.%)

Sample no.:	J-1-3B	J-1-3B
Analysis no.:	(1)	(2)
SiO_2	47.89	49.41
Al_2O_3	8.11	6.00
TiO_2	1.25	0.71
FeO*	6.95	6.62
MgO	13.47	14.45
MnO	0.15	0.13
CaO	22.09	22.28
Na_2O	0.27	0.26
TOTAL	100.18	99.86
HOST	hornblende	$Fo_{82.9}$
Mg/Mg + Fe (molar)	0.78	0.80
Mg/Mg + Fe of the host	0.73	0.83
Number of ions based upon 6 oxygen		
Si	1.773	1.831
Al	.354	.262
Ti	.035	.020
Fe	.215	.205
Mg	.743	.798
Mn	.005	.004
Ca	.876	.885
Na	.019	.018

Wo 46.86
En 42.28
Fs 10.86

to be significantly zoned, but vary appreciably in alumina content from grain to grain.

Cr-rich spinel inclusions were observed in several aluminous augite grains.

EVIDENCE THAT MAGMA MIXING HAS OCCURRED

Several features of the 1976 ejecta imply that two compositionally distinct magmas were mixed prior to the 1976 eruption. Banded andesitic to dacitic pumices with glassy andesitic to rhyolitic groundmasses are the most obvious evidence of coeruption of two magmas, but the following mineralogical features of andesitic pumices indicate that they are hybrids:

1. Olivine and hypersthene phenocrysts grew in melts with distinctly different Mg/Mg + Fe (Figure 10).

2. The cores of plagioclase and pyroxene phenocrysts in both andesitic and dacitic pumices span the same composition range, and enclose similar rhyolitic glass inclusions. In andesitic pumices, however, the plagioclase phenocrysts are rimmed by zones distinctly more calcic (An_{65-85}) than the penultimate zones (An_{47-55}); the latter match the composition of plagioclase rims in dacite pumices. Similarly, hypersthene phenocrysts are slightly more magnesian and less calcic. Plagioclase and pyroxene microphenocrysts in both pumice types are similar in composition to the rims of coexisting phenocrysts.

3. Olivine phenocrysts contain more primitive glass

Figure 10: MgO/MgO + FeO of melts parental to euhedral or slightly resorbed olivine (Fo86-80) and hypersthene, calculated from distribution coefficients reported by Roeder and Emslie (1970) and Weill and others (1975). The hypersthene parent ratios were calculated using the 1000° C distribution coefficient, but reasonable changes in this temperature produce only minor changes in the calculated values. This diagram illustrates the non-equivalence of the parent magmas of the minerals.

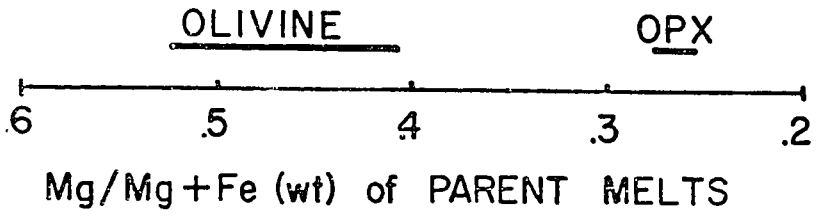
OLIVINE
OPX
.6
.5
.4
.3
.2
Mg/Mg+Fe (wt) of PARENT MELTS

(formerly melt) inclusions than do pyroxene and plagioclase crystals (see Table IX).

4. Olivine and hornblende phenocrysts are resorbed, and appear to have been unstable in their enclosing magmas. Microphenocrysts and reversely zoned rims on phenocrysts of plagioclase and pyroxene are euhedral, and appear to have been crystallizing from their enclosing melt.

The paucity of xenoliths, and in particular the lack of mafic xenoliths suited to yield olivine and hornblende crystals upon disaggregation, argues against contamination by incorporation of rock material.

THE COMPOSITION OF THE MAGMAS THAT WERE MIXED

Dacitic pumices with glassy rhyolite groundmasses do not appear to be hybrids. Phenocryst rims and microphenocrysts seem to have been in mutual equilibrium, and the euhedral shapes of most crystals imply crystal-melt equilibrium as well. Hence, it appears that the dacitic magma was one end-member involved in magma mixing. The bulk composition of this magma must have varied slightly in concert with variations in total phenocryst content (20 to 50 volume %), but the phenocryst rims and rhyolitic groundmass compositions are fairly uniform. Variations in phenocryst content may reflect crystal settling.

The pre-mixing composition of the basic component is not so readily established, since no mafic pumices or blocks have yet been found that do not contain phenocrysts inher-

TABLE IX: Selected analyses of glass inclusions (Wt.%).

Rock Type:	JANUARY Andesite	JANUARY Andesite	JANUARY Andesite	JANUARY Dacite	FEBRUARY Dacite	JANUARY Dacite
Sample no.:	P1-7-A	J-1-5	J-1-5	P2-5	AUG-4	J-1-1
Analysis no.:	(1)	(2)	(3)	(4)	(5)	(6)
SiO_2	54.83	64.00	72.09	71.36	73.23	69.76
Al_2O_3	23.60	18.23	12.17	12.65	11.82	13.11
TiO_2	.52	.03	.24	.24	.16	.37
FeO*	2.47	2.65	1.62	1.57	1.68	2.30
MgO	.63	1.51	.42	.40	.38	.32
MnO	n.d.	.08	.05	.06	.04	.06
CaO	9.30	3.81	1.44	2.20	1.35	1.93
Na_2O[a]	1.31	3.40	3.02	2.88	2.87	3.53
K_2O	.51	.60	1.76	1.59	1.91	1.72
P_2O_5	.18	.38	.05	.02	.04	.10
Cl	.34	.81	.39	.37	.38	.33
S	.24	.05	.00	.02	.01	.01
F	n.d.	.00	.01	.12	.00	.02
TOTAL	93.93	95.56	93.25	93.49	93.86	93.45
HOST	Fo_{84}	Fo_{86}	An_{52}	Plag	An_{47}	OPX

[a] Na_2O-analyses are unreliable due to possible volatilization during microprobe analysis.

ited from the dacite. From the petrography of andesitic pumices, we may infer that:

(1) The basic component was more mafic than the andesite pumices, since the andesites are the result of mixing between that basic component and the dacite.

(2) Olivine with Cr-spinel and aluminous clinopyroxene inclusions and hornblende with scarce magnetite inclusions were the only phenocrysts in the mafic magma before mixing, since these are the only phenocrysts in andesitic pumices that were not inherited from the dacite.

Since the $Fo_{86.5-80.5}$ is only slightly resorbed, it appears likely that it has relatively recently come to be out of equilibrium with its surroundings, most likely since the magma mixing event began. Hence, it follows that the melt from which the olivine crystallized is probably the mafic component involved in the mixing event. We may, then, be able to evaluate the composition of the mafic component by estimating the nature of the melt parental to the olivine.

An indirect estimate of the composition range of the magma parental to the Augustine $Fo_{86.7-80.5}$ can be made by comparing this composition to that of olivine which grew in another calc-alkaline rock suite (from Bogoslof and Umnak Islands, Central Aleutians; Byers, 1959), and whose parent magma is presumably represented by the enclosing rock. This is done in Figure 11, illustrating that olivine as magnesian as that erupted from Augustine may form in basaltic magma

that contains less than 50 wt.% SiO_2.

The composition of the melt phase mixed with the dacite may be estimated in several ways:

(1) The composition of olivine can be used to calculate, from distribution coefficients, the Mg/Mg + Fe of the basic magma parental to the olivine (shown in Figure 10), and, if an olivine-liquid equilibrium temperature can be estimated, its absolute MgO and FeO contents. For the approximate temperatures at which olivine may have crystallized in the Augustine magma (1150° C to 1055° C, discussed below), the melt parental to the olivine ranged from 6.75 (± 1.2) to 6.2 (± 1.1) wt.% MgO and 7.07 (± 1.2) to 9.15 (± 1.6) wt.% FeO as the olivine changed from $Fo_{86.7}$ to $Fo_{80.5}$ (calculated using distribution coefficients reported by Weill and others, 1975).

(2) The composition of the mesostasis of the basic component can be estimated by subtracting the contribution of the rhyolitic groundmass of the dacite (analysis 3, Table III) from the composition of the andesitic groundmass of andesitic pumices (analysis 1, Table III). This method will not yield an unique solution without knowledge of either the relative proportions of each component in the mixture, or the composition of one or more elements in the basic magma prior to mixing. The latter can be obtained from the olivine parent magma MgO- and FeO-contents estimated above. The results, presented in Table X, are hindered by the low

Figure 11: The composition of olivine phenocrysts and their host rocks for a suite of rocks from Bogoslof Island, Central Aleutians (Byers, 1955), compared to the composition of euhedral or slightly resorbed olivine ($Fo_{86.7-80.5}$) contained in the Augustine mixed pumices. One sample reported by Byers, a clear case of disequilibrium (a quartz-olivine andesite), was not plotted. This diagram suggests that the Augustine olivine crystallized in a basaltic parent with less than approximately 50 wt.% SiO_2.

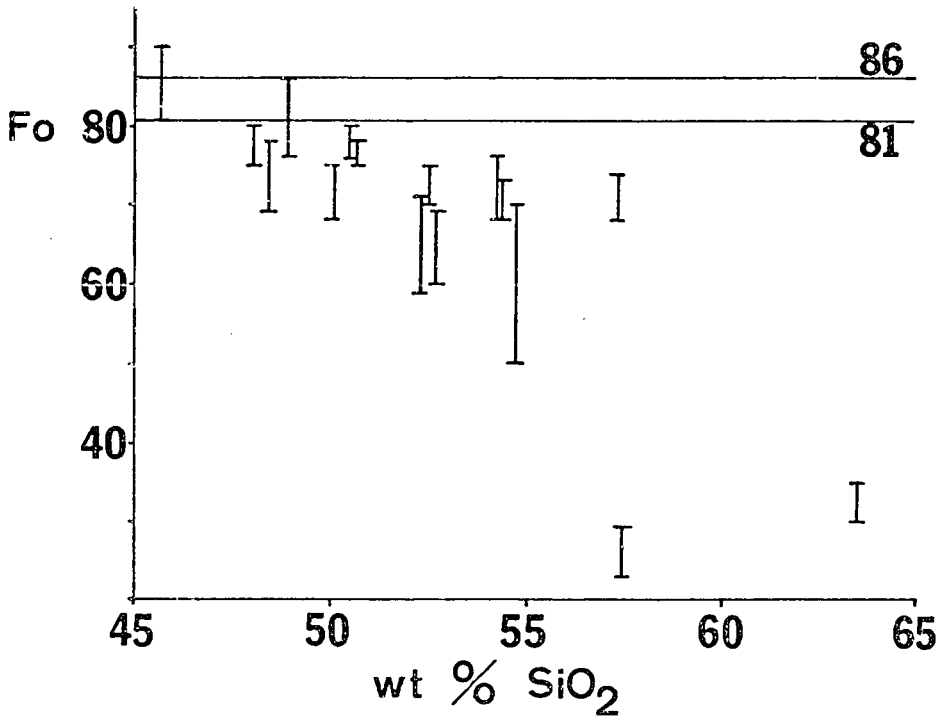
86
81
Fo
80
60
40
45
50
55
60
65
wt % SiO2

TABLE X: Composition of basaltic component which must be mixed with rhyolite (analysis 3, table III) to form andesite groundmass (analysis 2, table III), if mixed in the proportions shown.

	1 part basalt: 2 parts rhyolite	1 part basalt: 1 part rhyolite	2 parts basalt: 1 part rhyolite
SiO_2	34.81	48.69	55.63
Al_2O_3	21.85	18.67	17.08
TiO_2	2.32	1.67	1.35
FeO*	17.63	12.42	9.82
MgO	6.87	4.71	3.63
MnO	.35	.25	.20
CaO	13.14	9.40	7.53
Na_2O[a]	4.26	4.55	5.13
K_2O	-0.18	.50	.86
P_2O_5	.50	.35	.28

[a] Na_2O estimates are unreliable due to possible volatilization of Na during electron probe analysis. FeO, MgO, and TiO_2 estimates are less reliable than other elements due to their variability in the andesite analysis.

reliability of the analyses of the partly crystalline groundmass of andesitic pumices, but suggest that the mafic component is a high-alumina basalt.

(3) An indirect indication of the composition of the mafic component is also given by the composition of glass (formerly melt) inclusions within olivine phenocrysts. The use of glass inclusions, particularly to estimate the pre-eruption volatile-content of magma, is discussed in chapter 3, and will be discussed only briefly here. Analyses of several representative glass inclusions are reported in Table IX. More glass inclusion analyses appear in Table XV, in chapter 3. Extremely variable compositions of the glass inclusions in olivine reflect varying amounts of post-entrapment crystallization primarily involving silica-poor olivine, hornblende, augite, sulfides, and uncommonly spinel. At least 2/3 of the volume of some inclusions appear to have crystallized after entrapment, and consequently, the composition of the residual glass bears little resemblance to that of the initially trapped melt. The major obstacle to reconstructing the composition of the initial trapped melt is determining the mode and composition of phases formed during crystallization. In Table XI I have shown the results of adding to the measured glass inclusion compositions amounts of various crystal phases sufficient to return MgO to its calculated euilibrium concentration (assuming T=1150° C). The results agree reasonably well with the analyses shown in

TABLE XI: Results of mixing calculations to reconstruct initial trapped melt composition of glass inclusion in olivine. Components (hornblende or olivine and glass) are mixed in proportions suitable to return MgO in the initial trapped melt to 7.96 wt.%, the concentration calculated for equilibrium between Fo86 host and melt at T = 1150° C, using distribution coefficients of Weill & McKay (1975). Different mineral compositions are chosen to reflect the changing composition of the host or daughter phase, as crystallization from the trapped melt reduces the Mg/Mg + Fe of the residual melt. The composition of the initial trapped melt most likely was between analysis 3 and 6, if olivine and hornblende were the only minerals to form after entrapment.

	1 Glass Inclusion P1-7-A	2 Analysis 1 + 16% Fo_{86}	3 Analysis 1 + 17½% Fo_{81}	4 Analysis 1 + 25.7% Fo_{73}	5 Analysis 1 + 50% hbd Mg/Mg+Fe = 0.72	6 Analysis 1 + 64% hbd Mg/Mg+Fe = 0.62
SiO_2	54.83	52.40	52.10	50.05	48.24	46.40
Al_2O_3	23.60	19.72	19.46	17.53	18.95	17.65
TiO_2	.52	.44	.43	.39	1.36	1.60
FeO*	2.47	4.20	5.13	10.74	6.19	9.36
MgO	.63	8.00	7.96	7.96	8.03	7.98
CaO	9.30	7.80	7.67	6.91	10.48	10.81
Na_2O[a]	1.31	1.09	1.08	.97	1.89	2.05
K_2O	.51	.43	.42	.38	.37	.33
P_2O_5	.18	.15	.15	.13	.11	.08
Cl	.34	.28	.28	.25	.18	.13
TOTAL	93.69	94.51	94.68	95.31	95.80	96.39

[a] Na_2O-analyses are unreliable due to volatilization during microprobe analysis.

Table X and discussed in (2) above, indicating that the basic component may have been a high-alumina basalt.

VOLATILE CONTENT OF THE MAGMAS

This topic is dealt with in detail in chapter 3, but several important results of that discussion will be briefly summarized here, in order that their implications can be discussed.

The pre-eruption volatile content of the dacite can be estimated from the volatile content of glass inclusions in plagioclase and pyroxene. Electron probe examination of these inclusions indicates the following:

(1) The dacite was saturated with respect to a chlorine- and water-rich fluid phase when glass inclusions were trapped during crystallization.

(2) The rhyolitic mesostasis of the dacite contained approximately 6½ $\pm$ 1½ wt.% H_2O (determined by difference), 0.3 to 0.6 wt.% Cl, 100-500 ppm S, and less than 100 ppm F prior to eruption.

The pre-eruption volatile content of the basalt is more difficult to determine, because of the scarcity of glass inclusions in olivine and hornblende and their complex post-entrapment history, including crystallization of volatile-bearing hornblende and sulfides. The presence of hornblende and absence of plagioclase from the basalt indicates crystallization occurred under moderate to high water fugacities (Yoder and Tilley, 1962; Holloway and Burnham, 1972).

Analyses of glass inclusions further imply that the basalt was probably not water-saturated, but contained approximately 3½-4½ wt.% H_2O, 0.2-0.6 wt.% Cl, 500-2400 ppm sulfur, and probably less than 100 ppm F.

TEMPERATURES OF THE MAGMAS

Crystallization temperatures have been estimated from the composition of coexisting olivine-spinel and hypersthene-augite, using empirical geothermometers of Evans and Frost (1974) and Wood and Banno (1973). Equilibration of olivine-spinel appears to have occurred at roughtly 1100-1150° C. This temperature, which is relatively low for a basalt, is consistent with liquidus temperatures of hydrous olivine tholeiites determined in experimental runs by Holloway and Burnham (1972) and Allen and others (1975). Holloway and Burnham determined the liquidus of an olivine tholeiite, with $P_{vapor}=P_{total}$ and $a_{H_2O}=0.6$, to be 1100° C. Allen and others examined the same rock under conditions of $P_{H_2O}=P_{total}$, and found the liquidus to be at approximately 1075° C. The upper temperature stability limit of hornblende in the two studies also differed slightly. Holloway and Burnham found hornblende to be stable below the liquidus at a maximum temperature of 1060° C. Allen and others found hornblende to be a liquidus phase at approximately 20 kb and 1075° C.

These observations suggest, then, that the basalt crystallized initially in the range 1100-1150° C, and was

possibly at a somewhat lower temperature (in view of the presence of hornblende) when it was mixed with the dacite.

The crystallization temperature of dacite has been deduced from the compositions of intergrown hypersthene-augite phenocryst pairs using the empirical relation and method defined by Wood and Banno (1973). These results indicate a temperature of approximately 840° C (± 30° C, according to Wood and Banno).

Coexisting but not intergrown pyroxene microphenocrysts in andesitic pumices are somewhat variable in composition. Application of the Wood and Banno geothermometer to selected pairs yields temperatures to a maximum of 1055° C (± 30° C). The compositions of pyroxene crystals used to determine these temperatures are illustrated in Figure 8.

VISCOSITY OF THE MAGMAS

A magma's viscosity is strongly dependent upon its water content and temperature (Shaw, 1972). The pre-eruption viscosities of Augustine magmas were low because of their high water contents, and due to high temperatures produced in the dacite by addition of basalt. The viscosities of the rhyolite groundmass of a dacite pumice, the andesitic groundmass of a hybrid pumice, and of a basalt possibly similar to that introduced into the dacite (Byers, 1959, analysis 4, p. 280) have been summarized in Table XII. These values only represent the viscosity of the melt phase itself, and not the viscosity of the entire magma, which is

TABLE XII: Summary of viscosity estimates, calculated according to the method of Shaw (1972).

	TEMPERATURE ($^{\circ}$ C.)					
	1150	1100	1050	1000	900	840
Rhyolite 6.6 wt.% water	560 p.	1000 p.	1895 p.	3750 p.	17,500 p.	50,500 p.
Andesite 6.6 wt.% water	85 p.	140 p.	230 p.	430 p.	1,600 p.	3,976 p.
Basalt (Byers, 1959) 3.9 wt.% water	4 p.	5 p.	7 p.	11 p.	28 p.	53 p.
Basalt 1.0 wt.% water	50 p.	78 p.	130 p.	230 p.	715 p.	1,845 p.

somewhat greater due to the presence of crystals. The extent of the increase can be estimated using the relationship determined by Einstein (1906):

$$\eta_s = (1 + 2.5\,\phi)\,\eta_o$$

where η_s is the viscosity of melt plus crystals, ϕ is the volume fraction of crystals present, and η_o is the viscosity of the melt phase.

THE DEPTH OF CRYSTALLIZATION OF THE DACITIC MAGMAS

The water content of a water-saturated melt depends upon: Temperature, melt composition, vapor composition, and pressure. Burnham (1975) demonstrated that divergent magma compositions, when recast into quantities equivalent in their interaction with water to one mole of $NaAlSi_3O_8$, have identical equimolal water solubilities at pressures to 6 kb. The isothermal (1100° C) pressure dependence of the equimolal solubility of pure water, determined by Burnham and Jahns, (1962) and Hamilton and others (1964), is shown in Figure 12. This diagram is the basis of a geobarometer, subject to slight modification due to temperature differences, and possibly major modification due to the presence of other components in the vapor phase.

The effect of temperature:

The solubility of water in silicate melts decreases by approximately 0.1 wt.% for every 100° C temperature increase (Burnham and Davis, 1974). Geothermometry of intergrown hypersthene-augite phenocrysts yields an average temperature

of 840° C, but pyroxene microphenocrysts, formed after magma mixing, yield temperatures of up to 1055° C. Without knowledge of specific temperatures at which individual melt inclusions have been quenched, precise corrections are not possible, but they should not exceed 0.3 kb, based upon pressure estimated from Figure 12.

The effect of vapor composition:

The presence of volatile species other than water will generally reduce the solubility of water in a melt. At low relative concentrations of the other gases, the effect is minor: 30 mole percent CO_2 in a binary H_2O-CO_2 fluid at 1450° C and 20 kb only produces a 10% reduction in the solubility of water relative to that of pure water in albite melt (Mysen, 1976).

Chlorine may, in contrast, profoundly increase the solubility of water in a magma. The only study that has even peripherally dealt with this problem, however, is that of Koster van Groos and Wyllie (1969). They observed that "the presence of 0.3 [weight] percent NaCl causes an increase in the H_2O solubility comparable with an increase in pressure from 1 to 3 kb". In light of this observation, and the relatively high chlorine content of the Augustine magmas, the true entrapment pressure of the melt inclusions may be less than 1 kb. If, however, the observation of Koster van Groos and Wyllie (1969) does not bear out, the entrapment pressure may be as high as 2½ kb.

Figure 12: Molal euivalent solubility of water in magmas at 1100° C (after Burnham, 1975). The equimolal water contents recalculated by the method of Burnham (1975) of all melt inclusions analyzed fall into the area delineated by the fine lines; the mean value is near the middle of this area. Pressures read directly from this diagram may be too high due to lower quenching temperatures for the inclusions (most likely requiring a correction of less than 0.3 kb), and due to the presence of chlorine in the inclusions, which may increase water solubility by as much as a pressure increase from 1 to 3 kb (Koster van Groos and Wyllie, 1969). In light of this, the pressure of melt entrapment can only be limited to the range from approximately 1 to 3 kb.

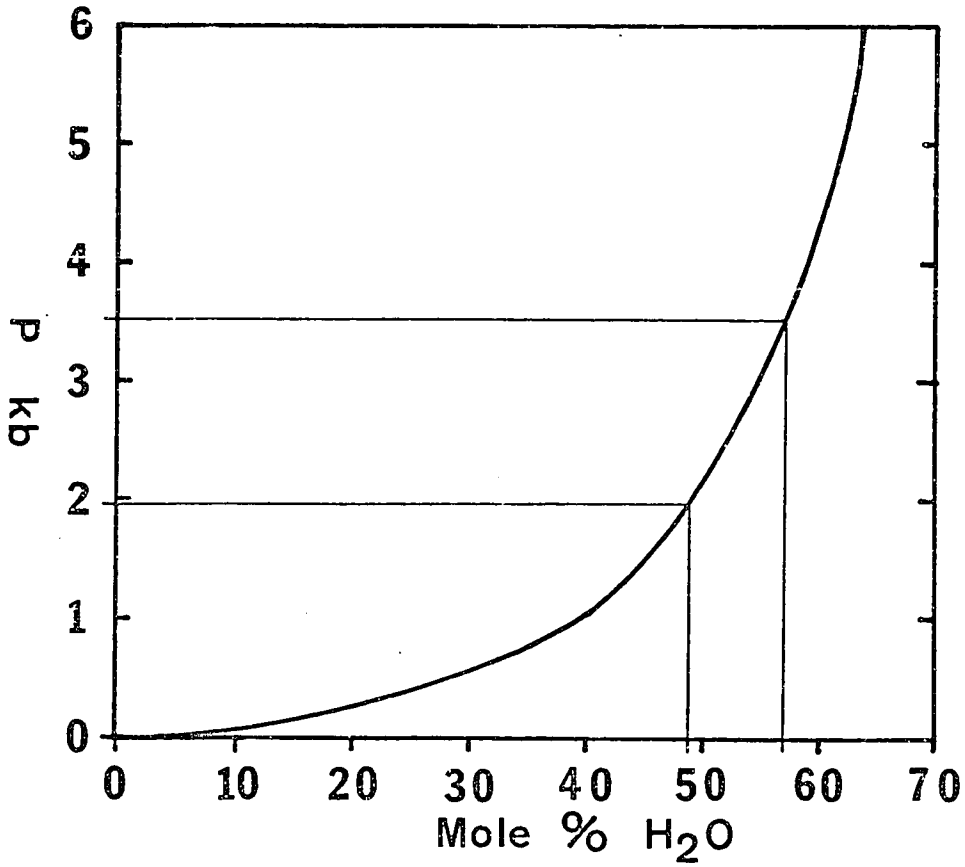
6
5
4
3
2
1
0
P kb
0
10
20
30
40
50
60
70
Mole % H_2O

Other assumptions:

It is critical for the geobarometric application of melt inclusions that vapor saturation occurred at the pressure of melt entrapment, and that this pressure did not decline during post-entrapment modifications. The host phenocryst surrounding a melt inclusion acts as a pressure vessel, maintaining the pressure of entrapment during magma ascent (Roedder, 1965, p. 1769). However, post-entrapment crystallization, which reduces the volume of the trapped glass, would reduce the pressure within the inclusion if vapor exsolution did not increase the volume of the trapped components. Slight increases or decreases in pressure might occur inside the inclusions, but increasing or decreasing limits to the solubility of volatiles in the trapped melt would moderate the pressure changes in vapor-saturated melt inclusions. Melt inclusions that enclose initially vapor-undersaturated melt will not exsolve vapor to counterbalance the volume decrease during crystallization until reaching the solubility limit (via vapor enrichment and/or pressure decline), and hence will yield minimum pressure estimates.

The depth to the chamber:

In summary, the water content of water saturated melt inclusions in dacite implies an entrapment pressure between less than 1 kb and approximately 3 kb, depending upon the effect of chlorine on the solubility of water in the melt. This corresponds to depths of approximately 2 to 10 km,

assuming $P_{magma}=P_{lithostatic}$.

Shallow seisms that occurred at Augustine during the period 1-3 months before the 1976 eruption have been located by a tripartite seismometer array located directly on Augustine Island (Douglas J. Lalla, University of Alaska, personal communication, 1977). These events locate from the surface to a maximum depth of 5 km.

DEPTH OF CRYSTALLIZATION OF THE BASALT

Experimental determinations of the stability of F and Cl-poor amphibole in olivine tholeiites (Holloway and Burnham, 1972; Allen and others, 1975) place constraints upon the pressure at which amphibole crystallized in the Augustine basalt. Amphibole is unstable at pressures greater than approximately 21 kb and at pressures less than roughly 7 kb at temperatures greater than 1050° C. These pressures correspond to depths of 75 to 25 km, if $P_{magma}=P_{lithostatic}$.

Unfortunately, the physical meaning of these pressures is difficult to evaluate, in as much as the amphibole may have grown either within a static magma chamber, or as the magma ascended.

WHEN DID MAGMA MIXING OCCUR?

Mixing may have: (1) been a continuous process in the pre-eruption chamber; (2) preceeded the eruption by an undetermined length of time; (3) occurred during the eruption.

Textural evidence suggests that magmas as diverse as

those comprising the 1976 ejecta were not continuously mixed during the growth of the plagioclase phenocrysts. Although many different compositional zoning and resorption patterns are apparent within a single thin section, major zoning breaks (e.g., Figure 9), accompanied by a composition change of more than 4 to 5 mole % An, are present only at phenocryst rims. Moderate compositional fluctuations can be explained by crystal settling or flotation in a somewhat compositionally diverse magma, but major reversals appear to require a more substantial mixing process involving much more basic magma.

It is also unlikely that mixing occurred only after the 1976 eruption began, since the earliest ash erupted from the volcano was mixed. The magma mixing event indicated by the 1976 ejecta, then, appears to have been a discrete event that preceeded the eruption by an unknown length of time.

Calcic-labradorite and bytownite microphenocrysts in the groundmass of hybrid andesitic pumices have grown since the magma mixing event began. If we knew the growth rate of these microphenocrysts, we could estimate the length of their growth period and, in turn, establish a minimum estimate for the length of the mixing-eruption interval.

Kirkpatrick (1977a) measured growth rates of 1.7 to 11.0 X 10^{-10} cm sec^{-1} perpendicular to (010) for labradorite phenocrysts that grew in the basaltic Makaopuhi and Alae lava lakes of Kilauea Volcano, Hawaii. Crystal growth rate

comparisons for lavas of different composition and cooling history are tenuous, since growth rate is a function of temperature (T), the liquidus temperature of the magma (T_ℓ), the undercooling (ΔT), and magma viscosity (η). Kirkpatrick (1977b) showed that the growth rate (Y) of a crystalline phase growing by interface-controlled growth in a melt of one composition can be compared to a known growth rate in a melt of a different composition with the expression:

$$Y = Y_o \frac{T\eta_o}{T_o\eta} \frac{[1 - \exp(-L\Delta T/RTT_\ell)]}{[1 - \exp(-L_o\Delta T/RT_oT_{\ell_o})]} \qquad \text{Eqn 1}$$

where the subscript o refers to the composition for which rates are known, R is the gas constant, and L is the latent heat of fusion.

Kirkpatrick (1977a) concluded that the tabular elongate (length:width = 5-10) plagioclase crystals that grew in the lava lakes formed by interface-controlled growth. Because plagioclase microphenocrysts in the Augustine andesite pumices are also tabular elongate (l:w = 3-10) crystals, it appears that these also grew by interface-controlled growth, and at relatively small undercooling (less than 50° C, Lofgren, 1974). Hence, equation 1 can be used to compare plagioclase growth rates in Augustine lavas and Kirkpatrick's samples, assuming that the composition difference between the calcic to sodic labradorites examined by Kirkpatrick and the An_{70-77} bytownites of Augustine do not introduce a significant difference in the growth rate.

The small differences in (RTT_ℓ) between the Augustine and Hawaiian lavas (T and T_ℓ differ by less than 200° C) can be safely ignored in equation 1, permitting the following approximation:

$$\frac{[1 - \exp(-L\Delta T/RTT_\ell)]}{[1 - \exp(-L_o\Delta T/RT_oT_{\ell_o})]} \cong \frac{L\Delta T}{L_o\Delta T} \qquad \text{Eqn 2}$$

The compositional and morphological similarity of microphenocrysts in the Augustine and Hawaiian lavas suggests that L and ΔT are similar for the two cases as well, hence the entire term in the brackets in equation 1 can be ignored. The most significant differences, then, between crystallization rates in the Augustine and Hawaiian lavas will result from differences in magma temperature and viscosity. Viscosity is, of these, the most important factor.

Viscosity is, unfortunately, difficult to evaluate, since it varies profoundly with temperature and composition, especially with water content of the melt. In-situ measurements by Shaw and others (1968) yielded viscosity estimates of 500 to 4000 poises for the melt phase in the Makaopuhi lava lake, and temperatures from 1200° C to 1130° C. The viscosity of the Augustine andesite groundmass (analysis 1, Table III) has been calculated using the method of Shaw (1974), assuming a pre-eruption water content of 6.6 wt.%. The estimated viscosity is 225 poises at 1055° C (the temperature of equilibration of pyroxene microphenocrysts) and 1585 poises at 900° C. Applying these values to equation 1,

the growth rate of Augustine plagioclase crystals may have been as much as twice the rate measured by Kirkpatrick in the lava lakes. If the viscosity of the Augustine andesite is higher than the calculated value, then the difference factor will be less than 2.

For a growth rate twice that reported by Kirkpatrick (1977a), the time required to grow the largest calcic microphenocrysts observed in Augustine 1976 andesites is 13 to 80 days. This is a minimum estimate for the interval between the beginning of the mixing event and the eruption, since: (1) larger microphenocrysts may exist that were not observed; (2) crystallization need not have started immediately after mixing.

Mixing may have coincided with the sudden onset of precursor seismicity approximately 120 days before the eruption.

HOW DID MAGMA MIXING OCCUR:

Magma mixing prior to the 1976 eruption may have resulted from: (1) turbulence or convection within a compositionally zoned magma chamber, or (2) addition of new basic magma to a differentiated dacitic chamber.

Overturn of a compositionally zoned magma chamber

The existence of compositionally zoned magma chambers has been inferred from three lines of evidence:

(1) The existence of compositionally zoned ash-flow and ash-fall tuffs (Lipman and others, 1966; Smith and Bailey, 1966; Lipman, 1967; Smith, 1976; Hildreth, 1976).

These deposits may be characterized by continuous or discontinuous changes in major and trace element composition, mineral composition and abundance, and pre-eruption oxygen fugacities and temperature (Lipman, 1971; Hildreth, 1976).

(2) Variations in composition of the ejecta of a single eruption. The historic eruptions of Mt. Hekla, for example, have begun violently with ejection of rhyolitic tephra, and within hours or days have shifted to gentle effusion of basaltic andesite lava (Thorarinsson and Sigvaldason, 1972).

(3) Simultaneous eruption of lavas of different composition from different vents on a single volcano (e.g., Baker, 1968; Vlodavetz, 1959). During the 1937-39 eruption of Kliuchevsky Volcano, Kamchatka, lavas emitted simultaneously from flank vents progressively decreased in SiO_2 content from 53.93 wt.% to 51.03 wt.% with increasing distance (8 to 15 km) from the active summit vent (Vlodavetz, 1959).

As was apparent from Figure 10, the liquids parental to olivine and hypersthene phenocrysts in the Augustine ejecta were distinctly different. The uniformity of phenocryst rim compositions (excluding those that grew after the magma mixing event began) implies that the two magmas involved were relatively uniform in composition. Furthermore, there is no evidence that intermediate magmas existed before the mixing event. These features of the Augustine ejecta

contrast with the variability and intergradation that characterizes the composition of deposits interpreted to be from zoned chambers elsewhere.

A consideration of the mechanism of convection also suggests that magma mixing at Augustine did not occur by overturn of a zoned chamber.

Convection is driven by density gradients. The downward reduction in density resulting from thermal gradients anticipated within a uniform composition magma chamber may be adequate to permit a convection cell to form (Shaw, 1965). The existence, size, and form of the convection cell is a function of the chamber size and shape, thermal gradients, crystallinity or vesicularity of the magma, and other factors (Shaw, 1965; Elder, 1977).

Compositional zoning in magma chambers may prevent or modify convection, since the density of magma increases with decreasing differentiation index more rapidly than it decreases with the concomitant temperature rise. The density of a basalt liquid, which may be similar to that involved in the 1976 eruption (Byers, 1959, analysis 4, p. 280) at 1100° C, 2 kb, with 2 and 3.85 wt.% water is 2.59 and 2.48 g/cm^3 respectively (calculated according to the methods of Bottinga and Weill, 1970). The calculated density of the rhyolite mesostasis of a dacite pumice (analysis 3, Table III), at 850° C and with 6.9 wt.% water, is 1.88 and 1.95 g/cm^3 at 1 and 3 kb respectively.

This estimated liquid density contrast does not preclude convective mixing of a zoned chamber containing these liquids, since convection may be triggered by processes that create temporary density inversions within the magma, including bubble growth and crystallization. Grout (1918) described such a process of "two-phase convection":

> "a mass of lava in which crystals have formed has a greater 'aggregate specific gravity' than it had just before, and a local development of crystals would also almost certainly start convection."

The effective density of liquid + crystals or liquid + bubbles is not equal to the weighted sum of the densities of the components, since crystals or bubbles will fall or rise within their enclosing liquid. However, this weighted sum represents a limiting approximation, which is most closely approached for magmas with small bubbles or crystals which rise or fall slowly.

A significant reduction in the density of the basalt due to the development of vapor bubbles is unlikely, since it is unlikely that the basalt is sufficiently volatile rich for a significant quantity of bubbles to grow. For the approximate ratio in which phenocrysts occur in the Augustine dacites (plag:opx:cpx:mt-il = 8:3:3:1) the weighted aggregate of crystals and liquid would not exceed 2.5 g/cm^3 (the approximate density of the basalt liquid) until 53-55% of the magma was crystallized. In view of the large size of most phenocrysts, the weighted sum undoubtedly exceeds the real effective aggregate density. Furthermore,

crystals appear to be insufficient in abundance to have created a temporary density inversion.

In summary, then, both the lack of evidence for magmas intermediate between the dacite and the basalt, and the probable inadequacy of convection for mixing a zoned chamber containing these components, imply that pre-eruption magma mixing was not the result of convective overturn within a compositionally zoned magma chamber. The most likely alternative is that new basalt entered the dacite-filled magma chamber.

Introduction of New Magma from Depth

Seismic evidence for the ascent of basalt from depth has not yet been recognized at Augustine (Lalla, 1977, personal communication). In fact, there is very little evidence at any volcano linking deep seismicity to eruptive activity (e.g., Carr and Stoiber, 1973). The most outstanding example of deep seismicity preceeding an eruption, 55 km deep swarming and harmonic tremor before the 1959 Kilauea eruption (Eaton and Murata, 1960), is itself unique: No other Hawaiian eruptions have been connected with such seismicity, although numerous eruptions have been monitored, and there is adequate evidence from ground deformation and petrologic studies that new magma is entering shallow subsurface magma chambers from below (Fiske and Kinoshita, 1969; Wright, 1959).

In part, the worldwide lack of seismic evidence un-

doubtedly reflects the limited data base. It must also reflect our inability to distinguish tectonogenic from volcanogenic earthquakes, a difficulty often circumvented by only considering shallow seisms, e.g., less than 20 km (Minakami, 1974) among volcanogenic earthquakes.

In part, also, magma ascent may be unaccompanied by seismic activity. For example, although seismometers were located as close as 600 meters from the vent, no seismic activity was detected accompanying the ascent and extrusion of magma during the 1971-72 eruption of Soufriere Volcano, West Indies (Aspinall and others, 1973).

PHYSICAL EFFECTS OF MAGMA MIXING

Introduction of basalt at 1100°-1150° C into dacite at approximately 850° C should result in chilling of the basalt and heating of the dacite, and production of hybrid magmas of intermediate composition and temperature. Mechanical mixing, promoted by the low viscosities of the participating magmas (Table XII), accelerated the rates of these processes by increasing the area of contact between the two magmas, but homogenization was ultimately dependent upon the rates of thermal and molecular diffusion across the interface. Heat diffuses several orders of magnitude faster than ions (thermal diffusion coefficient = $10^{-2} cm^2 sec^{-1}$, Jaegger, 1969; ionic diffusion coefficients = 10^{-5} to $10^{-8} cm^2 sec^{-1}$, Shaw, 1974; Magaritz and Hoffmann, 1976), hence, magma mixing may be treated as a two-stage process: In the first

stage the basalt was chilled and the dacite was heated, and in the second the two chemically homogenized to yield an intermediate magma.

FIRST STAGE: HEATING AND CHILLING

During the first stage several changes may have occurred:

1. The viscosity of the dacite decreased and of the basalt increased as one was heated and the other chilled (see Table XII).

2. Local heating may have stimulated convective mixing within the chamber (e.g., Sparks and others, 1977).

3. Crystallization may have started in the chilled basic magma. Textural evidence indicates that extensive crystallization occurred within the basic magmas following mixing, but thus far no crystals have been recognized that clearly began to grow before the magma was chemically homogenized.

4. Crystals in the heated dacite may have started to resorb. In the dacite samples examined, however, phenocrysts appear unresorbed, even very near the interface in banded pumices. This suggests that crystal dissolution was relatively insignificant.

5. Heating caused the solubility of volatile components, particularly water, to decrease in the dacite. The decrease of water solubility amounted to approximately 0.1 wt.% per 100° C increase (Burnham and Davis, 1974). Because the dacite was already vapor-saturated (see chapter 3), the

reduction in the solubility limit led to exsolution of an aqueous fluid from the melt. The rates of nucleation and growth of bubbles in magmas are quite rapid (Murase and McBirney, 1973), hence vesiculation may have occurred within hours of heating, probably before the magmas could be chemically mixed.

Exsolution of water from the dacite resulted in an increase in the volume of the magma, since water vapor (a fluid over the appropriate pressure range) occupies a substantially greater volume than the same amount of water when it is dissolved in the melt (Burnham and others, 1969; Burnham and Davis, 1974). The volume change is strongly dependent upon pressure and temperature, and is illustrated in Figure 13. The calculated volume increase experienced by the rhyolitic mesostatis of the dacite due to effervescence accompanying heating is shown in Figure 14 as a function of temperature at 3kb and 1 kb, the inferred maximum and approximate minimum pressures of crystallization of the dacite (see chapter 3). The maximum volume increase experienced by the rhyolite mesostasis due to effervescence upon heating is approximately 2-5%, but the actual volume change must have been considerably less, since most of the dacite could not have become so hot.

SECOND STAGE: CHEMICAL HOMOGENIZATION

Several changes also occurred as a consequence of chemical homogenization:

Figure 13: The relative volumes of water dissolved in a melt (calculated from Burnham and Davis, 1974) at 840° C, pure water vapor at 840° C, and pure water vapor at 1000° C, (Burnham and others, 1969), at 1 kb and 3 kb total pressure. The volume at 3 kb increases by 200% in going from a dissolved condition at 840° to a vapor at 1000° C. At 1 kb the volume increase is 450%.

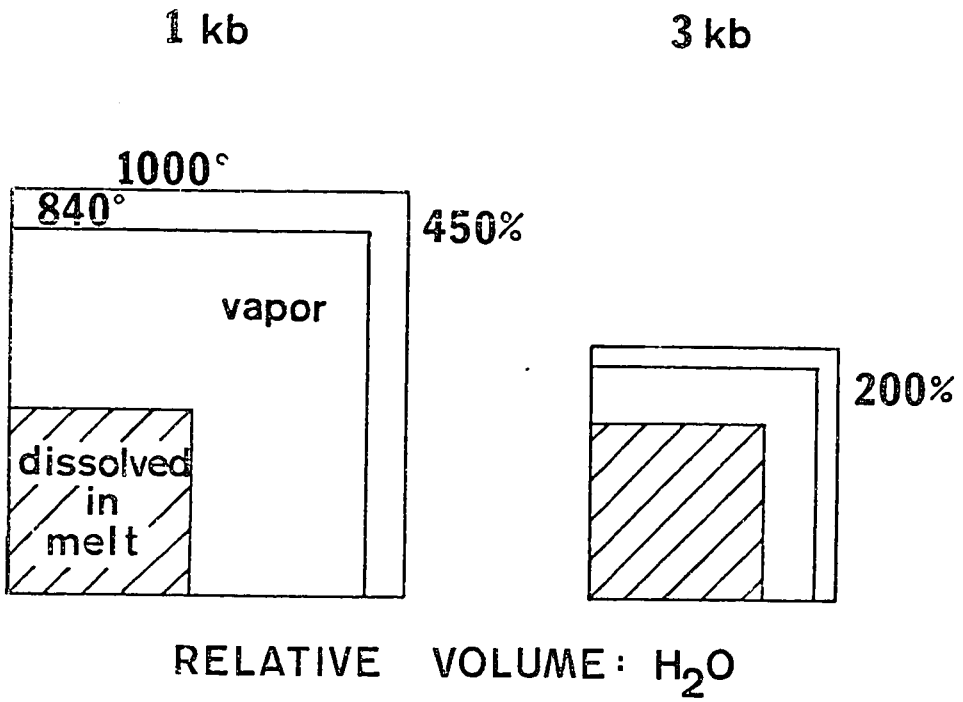

RELATIVE VOLUME: H_2O

Figure 14: The relative volume increase produced by heating the rhyolitic interstitial liquid of an Augustine dacite pumice, containing an initial water content of 6.58 wt.%, determined at 3 kb and 1 kb total pressure. This diagram was prepared by recalculating the analysis by weight (Table III) into an analysis by volume, using partial molar volumes of molecular species reported by Bottinga and Weill (1970) and Burnham and Davis (1974). The relative volume increase of the magma was then determined by assuming a 0.1 wt.% reduction in water solubility per 100° C of temperature increase, and calculating the proportion of the magma volume that would be changed from a dissolved to a vaporized state at various temperatures. The volume of dissolved water is estimated from the data of Burnham and Davis (1974) and the volume of pure H_2O vapor from Burnham and others (1969). The volume increase produced by maximum heating of the rhyolitic melt is approximately 2-5%, but the magma would increase by a smaller amount, since it contains crystals whose volume does not appreciably change during heating.

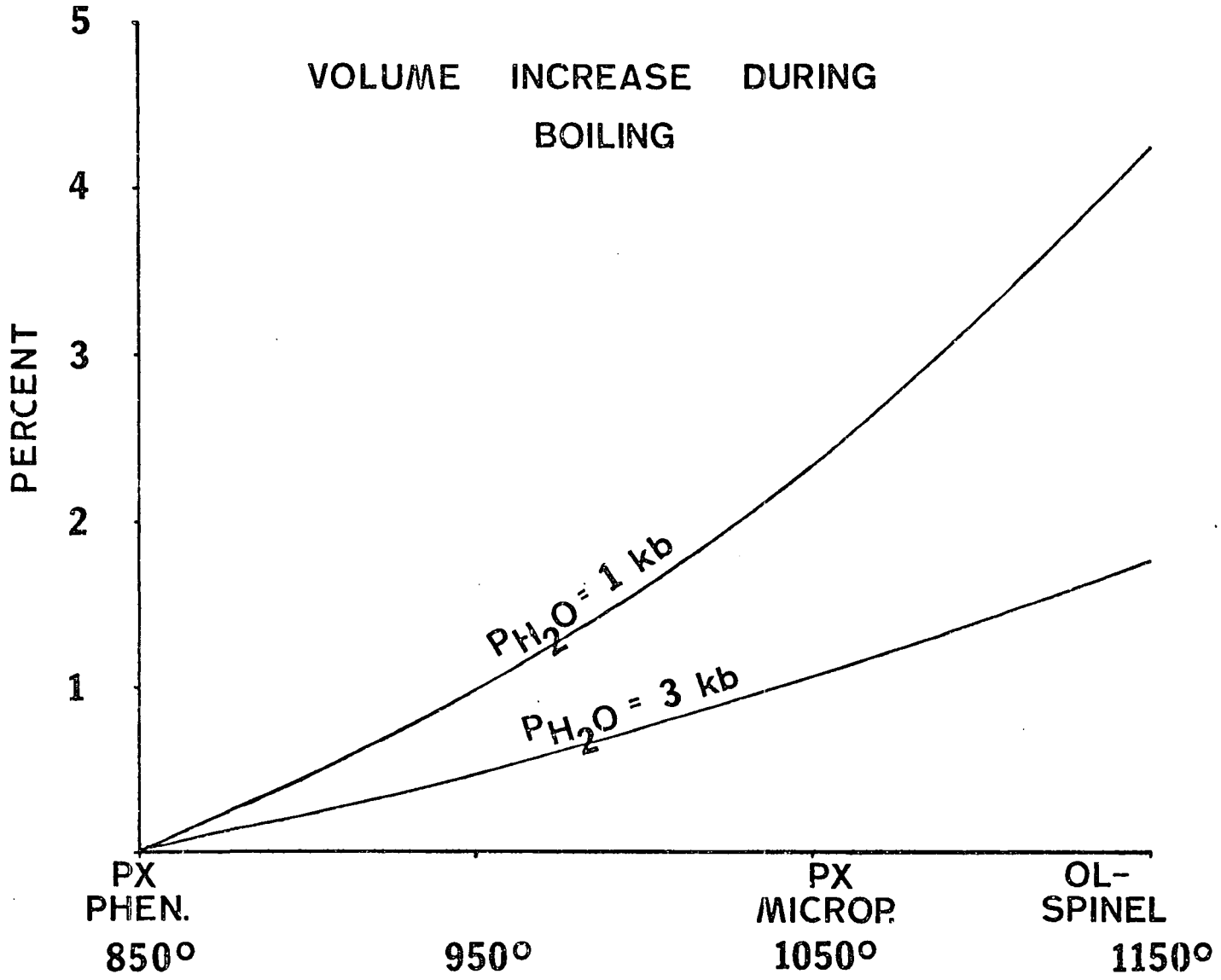
VOLUME INCREASE DURING BOILING
PERCENT
5
4
3
2
1
P_{H_2O} = 1 kb
P_{H_2O} = 3 kb
PX PHEN.
850°
950°
PX MICROP.
1050°
OL-SPINEL
1150°

1. The viscosity of the hybrids was intermediate between that of the dacite and the basalt (see Table XII).

2. New chemical equilibria resulted in minor marginal resorption of some minerals. (Some of the resorption may have occurred during heating.)

3. Chemical mixing initially resulted in formation of hybrid magmas undersaturated with respect to water, as saturated dacite was mixed with undersaturated basalt.

4. Approximately 40-60% of the molten mesostasis of the hybrid magmas crystallized after mixing. As this occurred the concentration of water increased within the residual melt, until water saturation was achieved. Subsequent crystallization was accompanied by exsolution of an aqueous fluid phase, and consequent increase in the magma volume. This is illustrated in Figure 15, prepared for a melt with an initial water content of 5 wt.%, which becomes saturated when the water concentration reaches 6½ wt.%.

VOLUME CHANGES IN THE MAGMA--SUFFICIENT TO TRIGGER EXPLOSIVE ERUPTIONS?

The volume of the magma confined within the chamber apparently increased before eruption due primarily to the following factors:

1. Addition of a volume of new basalt.

2. Effervescence accompanying heating of the vapor-saturated dacite.

3. Effervescence during partial crystallization of the

Figure 15: The relative volume increase of the mesostatis of hybrid magmas due to effervescence accompanying post-mixing crystallization. It is assumed that the hybrid magma contains 5 wt.% water before crystallization begins, and is saturated when the concentration of water reaches 6½ wt.%. It is further assumed that the saturation limit remains constant, that crystallization involves anhydrous phases only, and that the volume of the aqueous fluid phase is equal to the volume of pure water vapor, given by Burnham and others (1969). Temperature is assumed to be 1050° C.

The groundmass of Augustine hybrid pumices contains 50-60 volume % microphenocrysts.

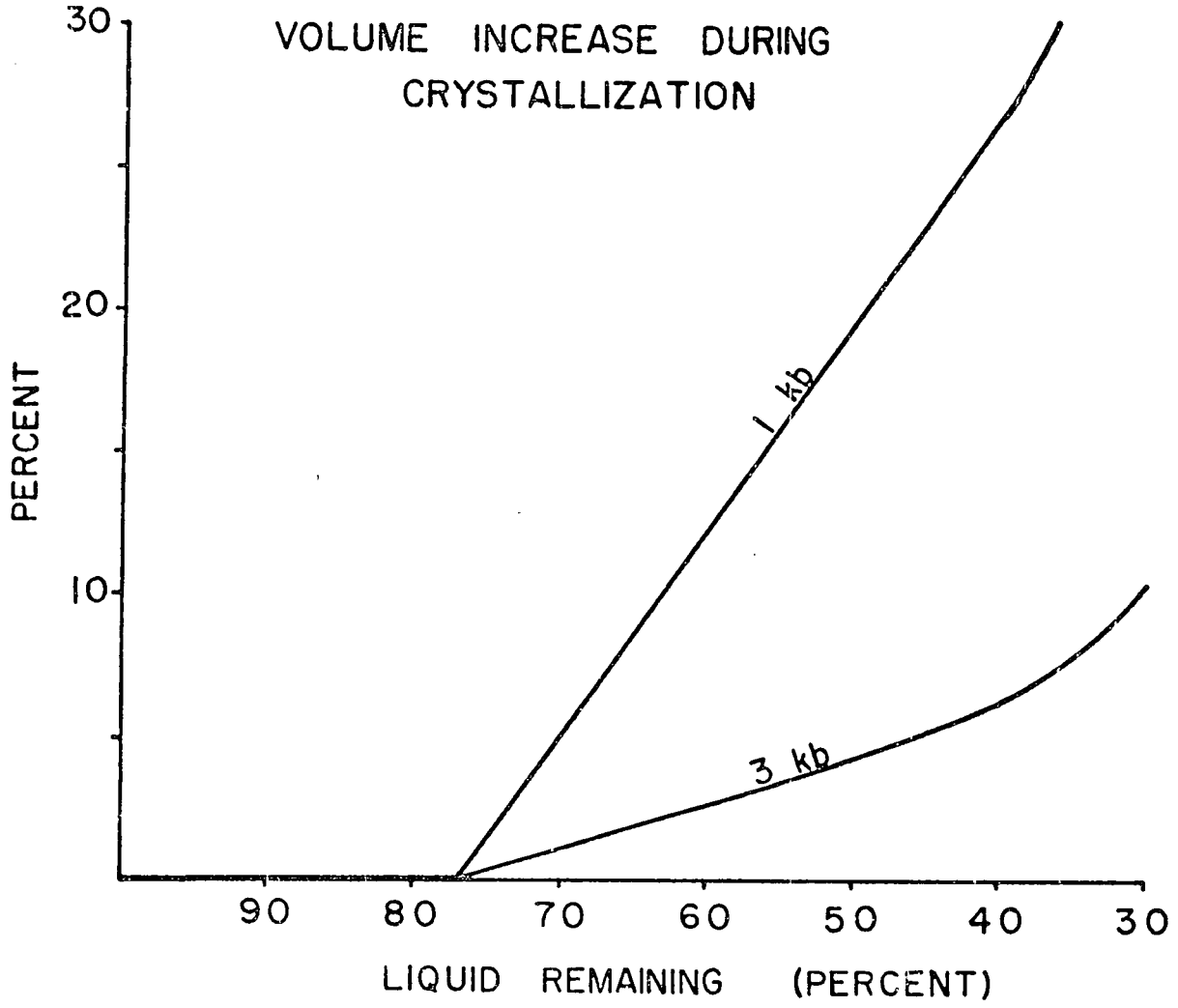
VOLUME INCREASE DURING
CRYSTALLIZATION
30
20
10
PERCENT
1 kb
3 kb
90
80
70
60
50
40
30
LIQUID REMAINING (PERCENT)

mesostasis of hybrid magmas.

The volume increase resulting from addition of a volume of basalt is impossible to ascertain, since the relative volumes of basalt and dacite in the chamber are unknown. If the relative abundance of these components within the ejecta reflect their proportions within the chamber before eruption, then the volume increase may have been as much as 15%. It is difficult as well to evaluate the rate or time of addition of all of the basalt, whether it was added within hours or months, and whether it entered entirely before eruption, or in part after the eruption began.

As noted before, the effervescence due to the reduction in water solubility resulted in a relatively small increase in magma volume, which was probably very much less than the volume increase due to addition of new magma. The volume may have increased relatively quickly, however, since heat diffuses rapidly, particularly in systems undergoing convection.

The volume increase due to effervescence accompanying partial crystallization of the mesostasis of hybrid magmas may have been more substantial, as much as 6 to 26% in magmas with initial water contents of 5 wt.%, (equal portions of basalt and dacite). Effervescence (and the volume increase) did not begin until approximately 23% of the magma volume had crystallized, but thereafter the volume increased rapidly. The rate of volume increase would have increased

with time after the mixing event began, as the degree of mixing and crystallization increased.

The effect of the following factors upon the volume of the magmas was probably much less than the three factors just mentioned:

1. Thermal expansion or contraction of heated and chilled melt and crystals.
2. Volume decrease of the melt during its conversion to crystals.
3. Volume increase during resorption of crystals.
4. Release of volatiles during the breakdown of amphibole.
5. Effervescence of CO_2-rich volatiles from the basalt during chemical homogenization.

In summary, magma mixing appears to have resulted in a sudden, rapid increase in the volume of the magma within the subsurface chamber. This expansion may have triggered the 1976 eruption.

THE MECHANISM OF EXPLOSIVE ERUPTIONS OF THE VOLCANO

Like the explosive eruptions of many andesitic volcanoes, the 1976 eruption of Augustine began with an explosion of only moderate intensity, intensified over the following several days, and then waned gradually until it ceased. Several hypotheses have been put forth to explain the initial explosive and subsequent effusive pattern of volcanic eruptions:

(1) McBirney (1973) suggested that the explosivity is

due to explosive expansion of groundwater heated by ascending magma. Groundwater is driven off in the early activity, hence subsequent eruptions decline in intensity.

(2) Kennedy (1955) argued, on theoretical grounds, that the cooler top and walls of a magma chamber should concentrate volatiles, producing a stratified magma reservoir, sequential eruption of which would lead to a gradual decline in the volatile-content of the ejecta, and, in turn, explosivity.

(3) Bennett (1971), Anderson (1975), and Heiken and others (1976) proposed that the magma remaining within a chamber is rapidly degassed during the early phases of an eruption by the reduction in confining pressure that accompanies partial draining of the chamber. Later eruptions decline in intensity due to the prior degassing.

THE ROLE OF GROUNDWATER IN THE ERUPTION

Several observations suggest that groundwater may have participated in the early phases of the 1976 eruption:

(1) The earliest ash deposit (the tan ash), in contrast to the overlying deposits, is non-vesicular, consists of blocky, angular rather than vesicular glass shards (c.f., Heiken, 1972), and was deposited by a relatively small vertical eruption cloud.

(2) A pyroclastic surge deposit (the olive ash) was emplaced early in the eruption. Similar surge deposits elsewhere have been ascribed to phreatic or phreato-magmatic

eruptions (Moore, 1967).

(3) The number of infrasonic and air pressure signals recorded January 22-25, 1976 (13 and 16, respectively) is greater than the number of separate ashfalls that were reported on the mainland (5 to 7) or the number of ash layers preserved on Augustine Island (4 to 9, but 6 most probable). Satellite observations (Kienle and Forbes, 1977) confirm that eruption clouds were produced at the same time as the "extra" infrasonic signals, although these clouds were apparently too small to be recorded on King Salmon or Sparrevohn radar. Because these clouds did not produce significant ash deposits or fall-out, it is possible that they consisted predominantly of vapors, probably groundwater explosively flashed within the disrupted crater or magma conduit.

(4) Steam emitted February 1, 1976 from a fissure 200 meters north of the crater margin appears, from its isotopic character to consist primarily of meteoric groundwater, although it had been modified by other processes (see Figure 1).

Unfortunately, none of these observations are conclusive, since (1) our ability to recognize phreatic or phreatomagmatic eruption deposits is rudimentary, and other processes may be responsible for the features described in (1) and (2) above; (2) there need not be a relationship between eruption events and the between-eruption fumarole

emissions, mentioned in point (4) above; and (3) there appear to have been two different kinds of explosions: Those associated with major ash-fall and high vertical eruption columns (greater than 10 km) and ash-poor explosions with short vertical eruption columns (less than 5-6 km). The former were preceeded by short bursts of deep seismicity, the latter were not (J. Kienle, personal communication, 1977). Although the latter appear to be phreatic, the former may be primarily or exclusively magmatic.

ZONING OF VOLATILES IN THE MAGMA CHAMBER

Kennedy's (1955) suggestion that magma chambers should be more volatile-rich at their cooler tops and sides has been refuted by Burnham (1967), who argued that osmotic pressure gradients, proposed by Kennedy to generate the zoning, would be relatively insignificant. As noted above, zoning with respect to major and minor element composition and mode has been recognized in many deposits, where it is believed to reflect comparable zoning within pre-eruption chambers. In such cases, the activity of water is likely to vary with major element composition and mode. Because temperature is not uniform within chambers, there may be unequal degrees of crystallization that lead to variable states of saturation or undersaturation. Furthermore, zoning with respect to volatiles may develop due to influx of water into the chamber via methods discussed by Lipman and Friedman (1975).

Glass inclusions contained in Augustine phenocrysts erupted in explosive eruptions during January and during the less explosive block-and-ash flow eruptions of February (Table IX) show no apparent differences in volatile-element concentration. Unfortunately, this evidence is not conclusive, since:

(1) The glass inclusions may have been trapped during crystal growth within another portion of the magma chamber (i.e., the host phenocrysts may have settled into their present enclosing magmas).

(2) At deeper levels not currently exposed, the volatile content of the magma may have decreased. It may be in part the cumulative effect of all deeper magmas that creates the explosivity of a given eruption, rather than the specific volatile content of the magma that is erupted.

VOLATILE LOSS FROM THE CHAMBER DURING THE ERUPTION

Heiken and others (1976) observed that many major caldera-forming ash-flow eruptions were preceeded by weeks or months of smaller ash-producing Plinian eruptions. They hypothesized that the initial eruptions partially drained the magma reservoir, causing some of the remaining melt to vesiculate as the internal hydrostatic pressure dropped. As a consequence of this pressure drop, large volumes of melt could become vapor-saturated relatively rapidly, and erupt explosively in the climactic stage of the eruption. Later eruptions would be less explosive, because magma would be

partly degassed during prior eruptions.

This mechanisms readily explains the initial increase in intensity that the Augustine eruption exhibited during January. It is difficult, however, to demonstrate this mechanism through direct evidence, such as shart morphology (Heiken and others, 1976).

SUMMARY

In summary, the evidence concerning the mechanism of the 1976 eruption is ambiguous. Although there is some indication from the deposits that two ash-producing eruptions were phreatic or phreatomagmatic, there is a clear difference between steam explosions (small eruption columns containing little or no ash) and magmatic eruptions (preceeded by deep seismicity, accompanied by high eruption columns containing abundant ash). The evidence from glass inclusions indicates that there was an abundant supply of water within the magma at depth. Furthermore, magma mixing may provide a mechanism (by heating and post-mixing crystallization) for magma to rapidly and suddenly exsolve substantial volumes of water. In light of this information, it seems unnecessary to postulate a major role for groundwater in controlling the explosivity of the eruption (e.g., McBirney, 1973).

There is no evidence that the magma within the pre-eruption chamber was zoned with respect to volatiles, although the evidence is not conclusive. The available

evidence, furthermore, does not preclude that free vapor could have been concentrated within portions of the chamber where it may have accumulated due to migration of vapor bubbles. Zoning of this type, if it did exist, would not, however, be likely to produce eruptions that increase in intensity, as was observed.

The only mechanism that adequately explains the increase observed in the intensity of the eruption (an extremely common characteristic of eruptions of andesitic volcanoes) is one that permits a rapid increase in the vapor or magmatic pressure within the chamber following the onset of the eruption. As suggested by Heiken and others (1976) this may result from vesiculation of the melt consequent to partial draining of the chamber. It may also result if magma mixing is stimulated by early eruptions, producing more thorough heating of cooler, vapor-saturated magmas.

CHAPTER 3: THE ABUNDANCE AND EVOLUTION OF VOLATILES IN THE MAGMAS

INTRODUCTION

In chapter 2 evidence was presented that the 1976 eruption of Augustine volcano was preceeded by a magma mixing event in which basalt from a deep source was injected into a dacite which resided within a shallow subvolcanic magma chamber. The basalt appears to have been a high-alumina basalt, with phenocrysts of chrome-rich spinel, olivine ($Fo_{86.7-80.5}$), hornblende (with inclusions of titaniferous magnetite), and aluminous augite. The dacite contained plagioclase, hypersthene, augite, and Fe-Ti oxides, as well as minor apatite. Tiny sulfide-globules, consisting primarily of intergrown chalcopyrite and pyrrhotite are contained inside olivine, hornblende, and plagioclase crystals.

Banded pumices and disequilibrium mineral assemblages, indicative of similar magma mixing events, are present in the deposits of each of the last four historic eruptions of Augustine, and in numerous prehistoric deposits. This common association of basalt with dacite strongly suggests a genetic relationship between these magmas.

In this chapter I will examine with electron probe analyses the abundance and distribution of the volatile components water, chlorine, sulfur, and fluorine in the two magmas, and the manner in which these volatile components may have evolved if the dacite magma developed by fractional crystallization of a parent similar to the 1976 basalt. I will also briefly discuss the implications of the high observed concentrations of water and chlorine for the manner

in which basalts may fractionate to form andesitic and more silicic differentiates.

DETERMINATION OF THE PRE-ERUPTION VOLATILE CONTENT OF MAGMAS

Rapid degassing during and after subaerial eruption generally prohibits direct determination of the pre-eruption volatile content of magma by analysis of eruptive rocks. Two approaches have been employed, however, to directly examine the volatile content of pre-eruption magma. Moore and his coworkers (1965, 1970, 1971, 1973, 1977), Mathez (1976), and Delaney and Meunow (1976) have examined the volatile content of glassy lavas erupted onto the seafloor, where degassing is limited by higher pressures due to the overlying water. Even the deepest samples (from 5100 m depth) contain approximately 0.1 percent vesicles, indicative of some vapor separation (primarily CO_2, Moore and others, 1977), but sulfur, water, and chlorine contents of compositionally equivalent lavas appear to be roughly constant below a critical depth (Moore, 1965).

Anderson (1973, 1974) determined pre-eruption volatile contents of subaerial lavas by examining glass inclusions within phenocrysts. Glass (formerly melt) inclusions, nearly ubiquitous features of volcanic phenocrysts, are sealed at depth by incorporation within the host crystal. Subsequent degassing can only occr by diffusion of the volatiles through the host crystal, an extremely slow process (Hofmann and Magaritz, 1976) likely to be important over

geologic time intervals only for hydrogen.

Two approaches have been used to study glass inclusions: Anderson (1973, 1974) and Sommers (1977) analyzed trapped glasses with the electron probe. Unfortunately, the electron probe cannot directly measure water, hydrogen, oxygen, or ordinarily carbon; these components must be estimated by stoichiometry (for oxygen) or by difference in an analysis that sums to less than 100%. Anderson (1973) determined water by difference in hydrous glasses of known composition and found the technique to be accurate to within $\pm$ 1.4 wt.% absolute. This accuracy is sufficient to provide meaningful results for relatively hydrous glasses.

Another approach was used by Delaney and Meunow (1976) and Sommers (1977), who thermally degassed glass-inclusion-bearing phenocrysts within a mass spectrometer. This technique permits direct detection of water, hydrogen, oxygen, and carbon species, but is not a precise quantitative technique for determining the absolute concentration of volatiles in the inclusions, in part because it requires an estimate of the inclusion-to-host ratio.

Volatile element determinations of sea floor basalts and melt inclusions in subaerial ejecta (summarized in Table XIII) have disclosed an important difference between oceanic basalts and basaltic to rhyolitic rocks of island arcs and continental margins: The latter are apparently more water- and chlorine-rich than the former. Furthermore, intermed-

TABLE XIII: Summary of determinations of volatile content of relatively non-degassed seafloor basalts and subaerial glass inclusions. Data are from Moore (1965), Moore & Fabbi (1971), Moore & Schilling (1973), Anderson (1974), Sommer (1977), and this paper. All analyses are wt.% or ppm by weight.

	OCEAN RIDGE THOLEIITE	OCEAN ISLAND		CONTINENTAL AND ISLAND ARC			AUGUSTINE	
		THOLEIITE	ALKALIC	BASALT	ANDESITE	RHYOLITE	BASALT	DACITE
H_2O	mean = 0.25-0.35 wt.%	0.45 ± .15 wt.%		1-5 wt.%	same	ca.5.4 wt.%	ca.3.5 wt.%	6.6 wt.%
Cl		100-400 ppm		100-2200 ppm	same		ca.0.25 wt.%	.3-.6 wt.%
S	800 ± 150 ppm juvenile	same	same	50-2800 ppm	same		sulfide saturated	
F		300 ppm					100 ppm	100-200 ppm
OTHER GASEOUS COMPONENTS						CO_2: 2.7% of total volatiles CO: 4.8% of total volatiles		

iate and silicic magmas of the calc-alkaline suite may be sufficiently volatile-rich that they may be saturated with an aqueous fluid phase at moderate to shallow depths within the crust. This study further supports this interpretation.

DISTRIBUTION OF VOLATILES WITHIN MAGMAS

The volatile components in magmas may be contained within crystals and immiscible sulfide liquids, dissolved within the melt phase, or disseminated as a free fluid phase. The volatile content of crystalline phases and sulfide globules can generally be measured directly, and that of the melt phase may be deduced from the composition of glass inclusions. The composition of the free fluid phase, however, cannot usually be measured and its behavior is generally unknown. Does it accumulate near the top of a chamber? Does it remain dispersed through the melt? Does it escape through the walls of the chamber? I will present the results of microprobe analyses of the volatile content of crystalline phases and of glass inclusions in olivine, plagioclase, and pyroxene phenocrysts. This information can be used to predict the composition of the fluid phase, more accurately, perhaps, than we could hope to measure it. The composition of the fluid phase will not be considered further here, but will be discussed in a future paper dealing with the composition of Augustine fumarole emissions.

VOLATILE ELEMENTS IN CRYSTALLINE PHASES

Volatile element-rich primary minerals recognized in

the 1976 Augustine ejecta include hornblende, apatite, and Fe- and Cu-rich sulfides which occur in globular intergrowths. Hornblende and sulfide-globules were present within the basalt prior to magma mixing; apatite and sulfide globules are present within the dacite.

HORNBLENDE

Hornblende occurs as phenocrysts and as inclusions within olivine, but probably did not constitute more than 2-3 modal percent of the basalt that mixed with the dacite. It appears to have crystallized relatively near the liquidus in the basalt, but is invariably resorbed in the andesitic pumices. Crystal aggregates of pyroxene, plagioclase, and Fe-Ti oxide pseudomorphing hornblende are also present within dacite pumices. These may have resulted from hornblende breakdown during an earlier magma mixing event or from hornblende that may have broken down during crystallization of a melt parental to the dacite.

Representative hornblende analyses have been reported in Table VII. According to the classification scheme of Leake (1968), these are tschermakitic hornblendes. They appear to be very uniform in composition.

The abundance of volatile elements in hornblende is summarized in Table XIV. No fluorine was detected, and chlorine varies from 0.01 to 0.12 wt.%, but is ordinarily less than 0.03 wt.%. Water presumably constitutes the remaining volatile constituent. There is no indication from

TABLE XIV: Volatile element concentrations in apatite and hornblende (Wt.%).

APATITE

Sample no.:	P1-9	J-1-5
Analysis no.:	(1)	(2)
Cl	2.10	1.75
S	0.12	0.16
F	1.39	1.29
Summation Deficiency	----	----

HORNBLENDE

Sample no.:	J-1-3B	J-1-3B	J-1-3B
Analysis no.:	(1)	(2)	(3)
Cl	0.02	0.02	0.03
S	0.01	0.01	0.01
F	0.00	0.00	n.d.
Summation Deficiency	3.03	2.04	3.15

the optical properties of the hornblende that it is a water-deficient "basaltic hornblende", hence water probably constitutes between 1½ and 2 wt.%. This is consistent with the summation deficiencies in the hornblende analyses (3.15 to 1.32 wt.%).

APATITE

Apatite occurs as tiny euhedral inclusions in pyroxenes, plagioclase, and Fe-Ti oxides, as well as discrete crystallites within the dacites. It is a trace component, and constitutes much less than one volume percent of the dacite. Apatite has not yet been recognized in phenocrysts inherited from the basalt, and almost certainly had not begun to crystallize in that magma prior to magma mixing.

Fluorine, chlorine, and sulfur analyses of apatite are summarized in Table XIV. Because of the high chlorine- and fluorine-content, there is probably very little hydroxyl in the apatite. Furthermore, there appears to be no summation deficiency in the analyses, which might correspond to water.

SULFIDES

Two tiny globules of intergrown Cu- and Fe-sulfide minerals were observed within two plagioclase phenocrysts in dacite (one erupted in January, one in February). Many more such globules (all less than 30 microns maximum width) were observed in olivine and particularly hornblende phenocrysts, but none were observed within the groundmass of the pumices.

Electron probe X-ray intensity images for sulfur, cop-

per, and nickel, and a reverse-image sample current display of one of the globules in plagioclase is shown in Figure 16. The plagioclase (An_{57}) is contained in a dacite block erupted in February. The block itself has a rhyolitic groundmass (analysis 5, Table III) and shows no evidence of having been mixed with more basic magma during the mixing event that preceeded the 1976 eruption. The globule, then, appears to have been in equilibrium with the andesitic to dacitic magma in which its host phenocryst was growing at the time of enclosure.

The globule consists of two discrete sulfide phases, one copper-rich (probably chalcopyrite), the other copper-poor (probably pyrrhotite or its more nickel- and copper-rich equivalent, monosulfide solid solution). The globule is roughly circular in cross-section, but appears to be flattened where plagioclase is adjacent to chalcopyrite. The pyrrhotite, on the other hand, does not appear to have adjusted shape in response to the enclosing plagioclase, and was probably solid at the time of entrapment.

Globules in olivine and hornblende vary from subspherical to irregular rod-like or ellipsoidal shapes. They may have been, in apparent contrast to the spherule in Figure 16, entirely molten at the time of entrapment.

The sulfide globules are generally too small to permit accurate microprobe analyses of their constituent phases. One globule, however, contains approximately 42 wt.% sulfur.

Figure 16: Electron probe X-ray intensity images for sulfur, nickel, and copper, and a reverse-image sample current display of a sulfide globule in plagioclase. Bright areas in X-ray intensity images are richer in the element sought. Sample current display illustrates the surface configuration of the sample--dark patches are holes in the globule surface. These photographs illustrate that the globule consists of a copper-poor sulfide mineral (pyrrhotite or monosulfide solid solution) and a copper-rich sulfide mineral (probably chalcopyrite). The pyrrhotite shows no adjustment to the enclosing plagioclase, and was probably solid before entrapment. Chalcopyrite is flattened on one surface adjacent to plagioclase, and may have been molten at the time of entrapment.

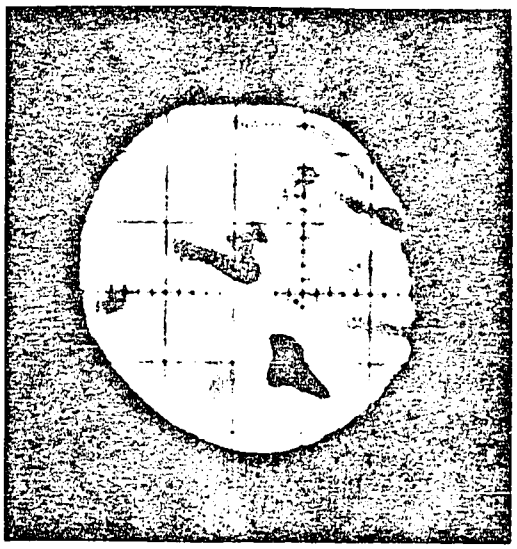

SAMPLE CURRENT

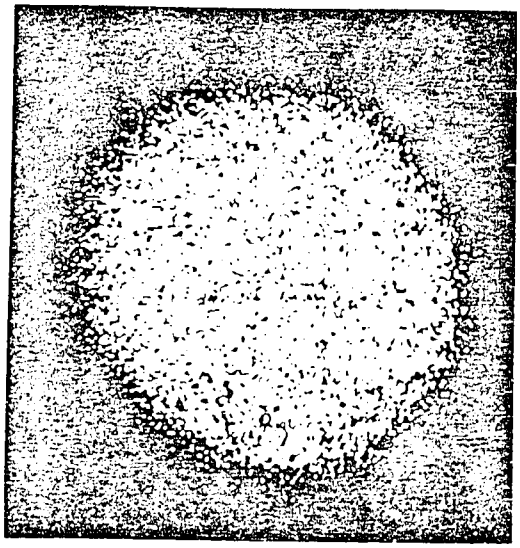

SULFUR

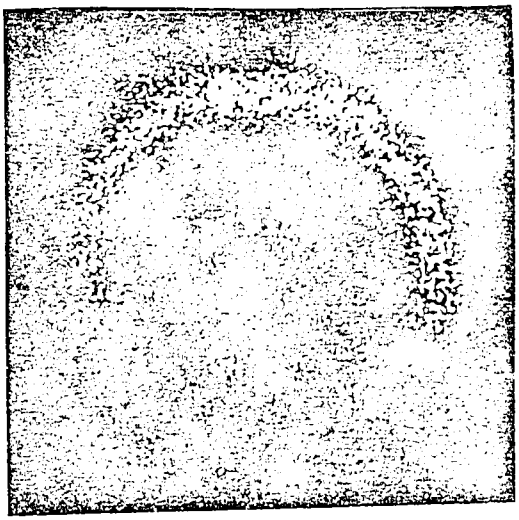

COPPER

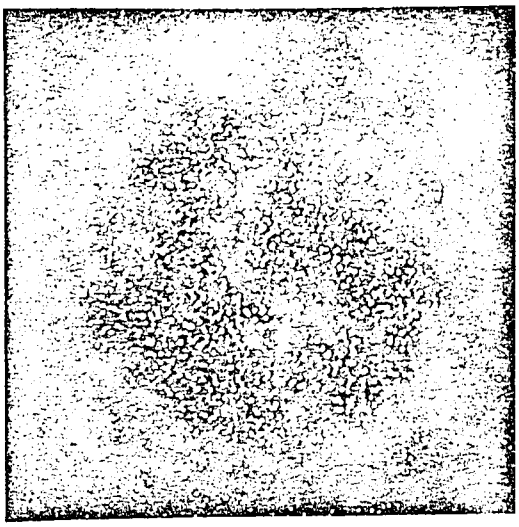

NICKEL

Comparison of X-ray intensity images, like those shown in Figure 16, disclose no notable compositional differences between sulfide globules inherited from the basalt and those from the dacite. Both appear to contain approximately 10-20 volume % chalcopyrite.

VOLATILE ELEMENTS IN THE MELT

THE OCCURRENCE OF GLASS INCLUSIONS IN PHENOCRYSTS IN THE 1976 EJECTA

Glass inclusions are rare in hornblende and olivine phenocrysts in the 1976 ejecta, but are very common in pyroxene and plagioclase phenocrysts.

GLASS INCLUSIONS IN PLAGIOCLASE

In plagioclase, glass inclusions may be sparse (a few inclusions per crystal) or extremely abundant (to several hundred inclusions per crystal), and occur in two texturally distinct forms: (1) generally small (less than 20 microns maximum diameter) spherical or slightly flattened ellipsoidal inclusions that occur along crystal growth zones and along twin composition planes, or (2) irregular-shaped inclusions of up to approximately 300 microns maximum diameter, that occur within areas with patchy zoning (Vance, 1965). The composition of the plagioclase host within these patchy zones is variable, but is generally more calcic than the plagioclase immediately surrounding these zones.

One or more vapor bubbles are invariably present within the glass inclusions (except where they have been truncated

during thin sectioning). The volume of the bubble, or total volume of all bubbles, is usually between 3 and 8% of the volume of the entire inclusion. Rare inclusions are also present that contain bubbles which appear to make up 20-30% of the total inclusion volume. Unfortunately, due to optical interference, the fluid and/or solid phases within the bubbles could not usually be seen. The vapor phase within the bubbles was examined by crushing numerous crystals in glycerine with the aid of a crushing stage (Roedder, 1972). Unfortunately, most inclusions exploded during crushing, and the disruption obscured the vapor bubbles that were released. One inclusion, however, yielded a bubble that immediately expanded to many times the volume it had occupied within the inclusion. Within less than a second, the volume of this bubble decreased, leaving a smaller bubble, roughly one-seventh of the volume of the original large bubble, which gradually dissolved within two to three minutes.

Some glass inclusions contain small crystals of one or more different types: (1) Some small crystallites of pyroxene and opaque oxides, which are commonly present within plagioclase phenocrysts, border against or extend into glass inclusions. These crystals apparently started to grow before the glass inclusion was formed. (2) Tiny needles of pyroxene (?) are rarely enclosed entirely within glass inclusions. These may have grown before or after entrapment of the melt. (3) Minute reddish or brown dust, too small to

identify optically, is present near the glass-host interface in some inclusions. This may be a sulfide phase. (4) The walls of bubbles within some glass inclusions are lined by equal spaced submicron-size "spherules" which occur and appear much like sulfide-spherules that line vesicles in submarine basalts (Moore and Calk, 1971; Mathez and Yeats, 1976). (5) Within the relatively few vapor bubbles in glass inclusions whose interior could be seen (because they were truncated and filled with epoxy during sectioning) two types of inclusions were observed: Many contain tiny opaque granules, which may be contaminants introduced during sectioning. Two bubbles, of roughly 100 examined that were filled with epoxy, contain colorless cubic daughter crystals, possibly halite or fluorite, both of which have been reported in similar occurrences in plutonic or volcanic rocks (Roedder and Coombs, 1972; Macdonald and Katsura, 1965).

Cracks extend from some glass inclusions into the adjacent host crystal.

GLASS INCLUSIONS IN PYROXENE

Glass inclusions are less abundant in pyroxene than in plagioclase. They are usually of moderate size (20-50 microns) and rarely larger or smaller, and are commonly adjacent to Fe-Ti oxide crystals also enclosed by the pyroxene. Zoning is not as clearly visible in pyroxene as it is in plagioclase, hence, the relationship of the glass inclusions to zoning or resorption features within the pyroxene hosts

are not known.

Secondary crystals and vapor bubbles within the glass inclusions in pyroxene resemble those in plagioclase, except that crystallites of pyroxene are uncommon.

GLASS INCLUSIONS IN OLIVINE AND HORNBLENDE

Glass inclusions in hornblende and olivine differ from those in plagioclase and pyroxene primarily in that they are extensively crystallized. Individual inclusions in olivine appear to contain some or all of the following minerals: Hornblende, augite, spinel, pyrrhotite, and possibly other sulfides. While the mode of individual inclusions is difficult to evaluate, it appears to vary significantly, and individual inclusions enclose from approximately 25% to more than 75% crystals, of which hornblende appears to be the most abundant.

Vapor bubbles or cavities are usually visible within glass inclusions in olivine and hornblende. They appear to be of variable size and shape, and some appear to be confined to interstices between crystals and the inclusion wall. Because of the dark crystals within inclusions, and the irregular shape of the vapor bubbles or cavities, relative bubble and inclusion volumes cannot be reliably estimated.

ANALYTICAL METHODS

All analyses were obtained using an ARL-EMX five-channel electron probe. Analyses were made in two or three

separate runs, and attempts were made to analyze, wherever possible, spots adjacent to, but not coincidental with earlier analyzed spots. The operating conditions, and the sequence in which various elements were analyzed, varied somewhat during the runs. Accelerating potential was 10 or 15 KeV, sample current 0.05 to 0.08 microamps, beam size 5-20 microns, and integration time 10-20 seconds.

Mineral standards were used and corrections for all elements except F were made for drift, background, deadtime, and ZAF using EMPADR (Rucklidge and Gasparini, 1969). Counts on F were corrected by hand for drift and background and compared to the counts in an apatite or CaF_2 standard. An apatite with 0.91 wt.% Cl was used to standardize Cl. Cross-determinations with several other chloropatites and a natural obsidian gave results that agreed to within 10%.

Because water or hydrogen cannot be determined directly with the electron probe, the water content has been estimated by assuming that it is the "missing component" in an analysis that sums to less than 100%. Anderson (1973) used this method to analyze synthetic hydrous glasses containing 3 to 11 wt.% H_2O, and obtained results accurate to within $\pm$ 1.4 wt.% absolute. I have not performed similar tests, but to check for systematic errors, anhydrous or slightly hydrous glasses were analyzed frequently during runs. Totals for these glasses range from 98 to 101%. Results were not normalized.

Error in the water content can be introduced by the presence of any minor or trace element other than those sought in the analysis. It is unlikely that such elements, including oxygen (which may be underestimated in the analysis if all Fe is reported as FeO), exceed 0.2 to 0.3 wt.%. A more serious difficulty is presented by Na-loss apparent in many analyses, particularly those of glass inclusions in basalt, which were analyzed with a 5 micron beam. Some of these inclusions appear to be 1½ to 2 wt.% (absolute) lower in Na than other inclusions. It is not clear that this amount can simply be added to the analytical total to give a better estimate of water content, in as much as the relative abundances of other components must have increased as Na-decreased. Furthermore, the behavior of water during electron bombardment is unknown, and it is possible that water has also been lost during the analysis.

In view of the high water content apparent in glass inclusions in plagioclase and pyroxene (6½ wt.%$\pm$1½ wt.% 2σ), these results appear to be meaningful, in spite of the analytical uncertainty in determining water by difference. Confidence in these analyses is also justified by their consistency. Estimates of the water content of glass inclusions in olivine are much less reliable, however, in view of the significant Na-loss, the small number of samples that have been analyzed, and the analytical difficulties posed by the presence of crystalline material within the glasses.

COMPOSITION OF GLASS INCLUSIONS

The compositions of glass inclusions are reported in Table XV. Those in plagioclase and pyroxene are relatively uniform rhyolite or high-silica dacite. Those in olivine are much more variable and range from "andesite" to "dacite", but may have originally been basaltic.

Several features of the analyses of glass within plagioclase and pyroxene are noteworthy and some are illustrated by variation diagrams in Figure 17. These features include: (1) The summation deficiency in all the analyses only varies from 5.33 to 7.67 wt.%. This is within the analytical uncertainty of the mean (6.58 wt.%), and implies that the water content is relatively constant. (2) The FeO contents of the glasses in plagioclase vary from .90 to 2.54 wt.%, and the MgO contents vary from .25 to .57 wt.%. In comparison, the FeO-and MgO-contents of the groundmass of dacite pumices are 1.86 to 2.00 and 0.36 to 0.39 wt.% respectively. (3) The abundances of the following elements appear to increase as FeO increases: MgO, Cl, S; SiO_2 decreases with increasing FeO. Other elements show no clear pattern, or appear to remain constant as FeO increases (e.g., CaO, Na_2O, K_2O). MgO/FeO and Cl/FeO decrease as FeO increases.

The composition of glass included in olivine is extremely variable, due primarily to the variable state of crystallization of the inclusions. This variability prob-

TABLE XV: Glass inclusion analyses (Wt.%).

Sample:	P1-7A	P1-7B	J-2-6A	J-1-5	J-1-5	J-1-5	J-1-3B	J-1-1	J-1-5
Analysis:	(1)	(2)	(3)	(4)	(5)	(6)	(7)	(8)	(9)
SiO_2	54.83	67.81	60.78	66.16	60.55	64.00	66.93	69.76	72.10
Al_2O_3	23.60	14.78	17.74	17.11	20.15	18.23	16.45	13.11	12.29
TiO_2	.52	.41	1.41	.01	.06	.03	.02	.37	.36
FeO*	2.47	3.95	3.63	1.80	1.88	2.65	2.29	2.30	2.71
MgO	.63	1.52	1.46	1.06	1.05	1.51	.86	.32	.40
MnO	n.d.	n.d.	n.d.	n.d.	n.d.	.08	.04	.06	.04
CaO	9.30	2.94	6.69	3.10	4.27	3.81	2.99	1.93	1.91
Na_2O[a]	1.31	1.58	3.22	1.65	1.31	3.40	.93	3.53	2.80
K_2O	.51	2.44	1.82	1.09	.95	.60	.84	1.72	1.50
P_2O_5	.18	.30	.30	.16	.15	.38	.24	.10	.06
Cl	.34	.97	.44	.39	.35	.81	.45	.33	.36
S	.24	.02	.02	.06	.07	.05	.01	.01	.02
F	n.d.	n.d.	n.d.	n.d.	n.d.	.00	n.d.	.02	.00
TOTAL	93.93	96.72	97.51	92.59	90.79	95.56	92.05	93.55	94.54
H_2O[b]	6.07	3.28	2.49	7.41	9.21	4.44	7.95	6.45	5.46
HOST	$Fo_{85.4}$	$Fo_{84.3}$	OLIVINE	$Fo_{83.6}$	$Fo_{83.2}$	Fo_{86}	$Fo_{81.2}$	OPX	OPX
ROCK TYPE	Andesite	Andesite	Andesite	Andesite	Andesite	Andesite	Andesite	Andesite	Andesite
	JANUARY	JANUARY	JANUARY	JANUARY	JANUARY	JANUARY	JANUARY	JANUARY	JANUARY

[a] Na_2O-analyses are unreliable due to possible volatilization during electron probe analysis.

[b] H_2O-content estimated by difference (see text).

TABLE XV: Glass inclusion analyses (Wt.%). (Continued)

Sample:	J-1-3	J-1-1	J-1-3	J-1-3	J-1-4	J-1-4	J-1-4	J-1-4	J-1-5
Analysis:	(10)	(11)	(12)	(13)	(14)	(15)	(16)	(17)	(18)
SiO_2	71.24	71.52	70.25	70.74	68.70	71.48	70.14	70.77	71.67
Al_2O_3	13.15	12.49	13.09	13.15	12.77	12.76	12.58	12.02	12.37
TiO_2	.28	.18	.16	.15	.53	.34	.64	.42	.22
FeO*	1.83	1.34	1.54	1.49	2.54	2.14	2.60	1.97	1.57
MgO	.31	.34	.44	.40	.48	.44	.57	.46	.43
MnO	.09	.06	.05	.03	.08	.04	.05	.08	.06
CaO	2.10	1.44	1.96	1.96	2.09	1.64	1.77	2.16	1.43
Na_2O[a]	2.72	3.80	3.44	2.78	2.49	2.68	2.76	2.82	3.06
K_2O	1.81	2.09	1.95	2.01	1.86	2.00	1.84	1.80	1.73
P_2O_5	.07	.05	.06	.05	.11	.04	.04	.10	.03
Cl	.32	.32	.35	.37	.55	.52	.58	.40	.40
S	.02	.00	.01	.01	.05	.01	.04	.02	.01
F	.00	.00	.00	.00	.00	.07	.11	.02	.05
TOTAL	93.94	93.64	93.30	93.13	92.25	94.16	93.73	93.02	93.02
H_2O[b]	6.06	6.36	6.70	6.87	7.75	5.84	6.27	6.98	6.98
HOST	CPX	An_{48}	An_{52}	An_{52}	An_{58}	An_{76}	An_{67}	An_{52}	An_{54}
ROCK TYPE	Andesite	Dacite	Andesite	Andesite	Dacite	Dacite	Dacite	Dacite	Andesite
	JANUARY	JANUARY	JANUARY	JANUARY	JANUARY	JANUARY	JANUARY	JANUARY	JANUARY

TABLE XV: Glass inclusion analyses (Wt.%). (Continued)

Sample:	J-1-5	J-1-5	J-1-5	P1-8	P1-8	P1-8	P1-8	P1-9	P1-9
Analysis:	(19)	(20)	(21)	(22)	(23)	(24)	(25)	(26)	(27)
SiO_2	72.09	71.47	72.40	72.01	69.84	69.34	69.15	69.10	72.73
Al_2O_3	12.17	11.77	12.34	12.50	12.63	12.69	12.41	13.33	13.08
TiO_2	.24	.25	.25	.33	.40	.44	.36	.28	.11
FeO*	1.62	1.57	2.17	1.48	2.05	2.42	1.96	2.41	1.06
MgO	.42	.42	.48	.32	.31	.38	.30	.53	.27
MnO	.05	.05	.07	.07	.09	.08	.08	.09	.05
CaO	1.44	1.56	1.77	1.77	2.10	1.49	1.89	2.20	2.26
Na_2O[a]	3.02	3.16	2.86	3.57	3.07	3.48	3.17	1.71	2.15
K_2O	1.76	1.90	1.83	2.06	2.19	2.34	2.10	1.98	1.86
P_2O_5	.05	.06	.04	.10	.07	.02	.06	.06	.04
Cl	.39	.39	.42	.34	n.d.	n.d.	.59	.63	.24
S	.00	.00	.02	.02	n.d.	n.d.	.03	.03	.03
F	.01	.00	.04	.00	n.d.	n.d.	.27	.00	.05
TOTAL	93.25	92.60	94.67	94.59	92.75	92.66	92.37	92.34	93.93
H_2O[b]	6.75	7.40	5.33	5.41	7.25	7.34	7.63	7.66	6.07
HOST	An_{52}	An_{52}	An_{52}	PLAG	PLAG	PLAG	PLAG	PLAG	PLAG
ROCK TYPE	Andesite	Andesite	Andesite	Andesite	Andesite	Andesite	Andesite	Andesite	Andesite
	JANUARY	JANUARY	JANUARY	JANUARY	JANUARY	JANUARY	JANUARY	JANUARY	JANUARY

TABLE XV: Glass inclusion analyses (Wt.%). (Continued)

Sample:	P2-5	P2-5	AUG-4	AUG-4	AUG-4	AUG-4
Analysis:	(28)	(29)	(30)	(31)	(32)	(33)
SiO_2	71.57	71.36	73.60	70.00	74.40	73.25
Al_2O_3	12.56	12.65	11.77	11.61	11.69	11.82
TiO_2	.22	.24	.35	.24	.19	.16
FeO*	1.52	1.57	1.80	2.22	.90	1.68
MgO	.42	.40	.37	.55	.25	.38
MnO	.09	.06	.06	.05	.02	.04
CaO	1.82	2.20	1.43	1.32	1.40	1.35
Na_2O[a]	2.71	2.88	2.82	2.91	3.26	2.87
K_2O	1.54	1.59	1.95	1.96	1.87	1.91
P_2O_5	.04	.02	.07	.05	.05	.04
Cl	.32	.37	.35	.40	.23	.38
S	.03	.02	.00	.00	.01	.01
F	.02	.12	.03	.00	.00	.00
TOTAL	92.87	93.49	94.58	92.33	94.26	93.86
H_2O[b]	7.13	6.51	5.42	7.67	5.74	6.14
HOST	PLAG	PLAG	An_{57}	An_{53}	An_{54}	An_{47}
ROCK TYPE	Dacite	Dacite	Dacite	Dacite	Dacite	Dacite
	JANUARY	JANUARY	FEBRUARY	FEBRUARY	FEBRUARY	FEBRUARY

TABLE XV: Glass inclusion analyses (Wt.%). (Continued)

Sample:	P2-5	P2-5	AUG-4	AUG-4	AUG-4	AUG-4
Analysis:	(28)	(29)	(30)	(31)	(32)	(33)
SiO_2	71.57	71.36	73.60	70.00	74.40	73.25
Al_2O_3	12.56	12.65	11.77	11.61	11.69	11.82
TiO_2	.22	.24	.35	.24	.19	.16
FeO*	1.52	1.57	1.80	2.22	.90	1.68
MgO	.42	.40	.37	.55	.25	.38
MnO	.09	.06	.06	.05	.02	.04
CaO	1.82	2.20	1.43	1.32	1.40	1.35
Na_2O^a	2.71	2.88	2.82	2.91	3.26	2.87
K_2O	1.54	1.59	1.95	1.96	1.87	1.91
P_2O_5	.04	.02	.07	.05	.05	.04
Cl	.32	.37	.35	.40	.23	.38
S	.03	.02	.00	.00	.01	.01
F	.02	.12	.03	.00	.00	.00
TOTAL	92.87	93.49	94.58	92.33	94.26	93.86
H_2O^b	7.13	6.51	5.42	7.67	5.74	6.14
HOST	PLAG	PLAG	An_{57}	An_{53}	An_{54}	An_{47}
ROCK TYPE	Dacite	Dacite	Dacite	Dacite	Dacite	Dacite
	JANUARY	JANUARY	FEBRUARY	FEBRUARY	FEBRUARY	FEBRUARY

Figure 17: Variation of MgO/FeO*, Cl/FeO*, MgO, CaO, Na_2O, and K_2O with FeO* in glass inclusions in plagioclase. Vertical and horizontal lines correspond to the concentration or ratio of concentrations of these elements in the rhyolite mesostasis of dacite pumices. (The value of Cl in the rhyolite is not shown because Cl was lost from the magma during ascent.)

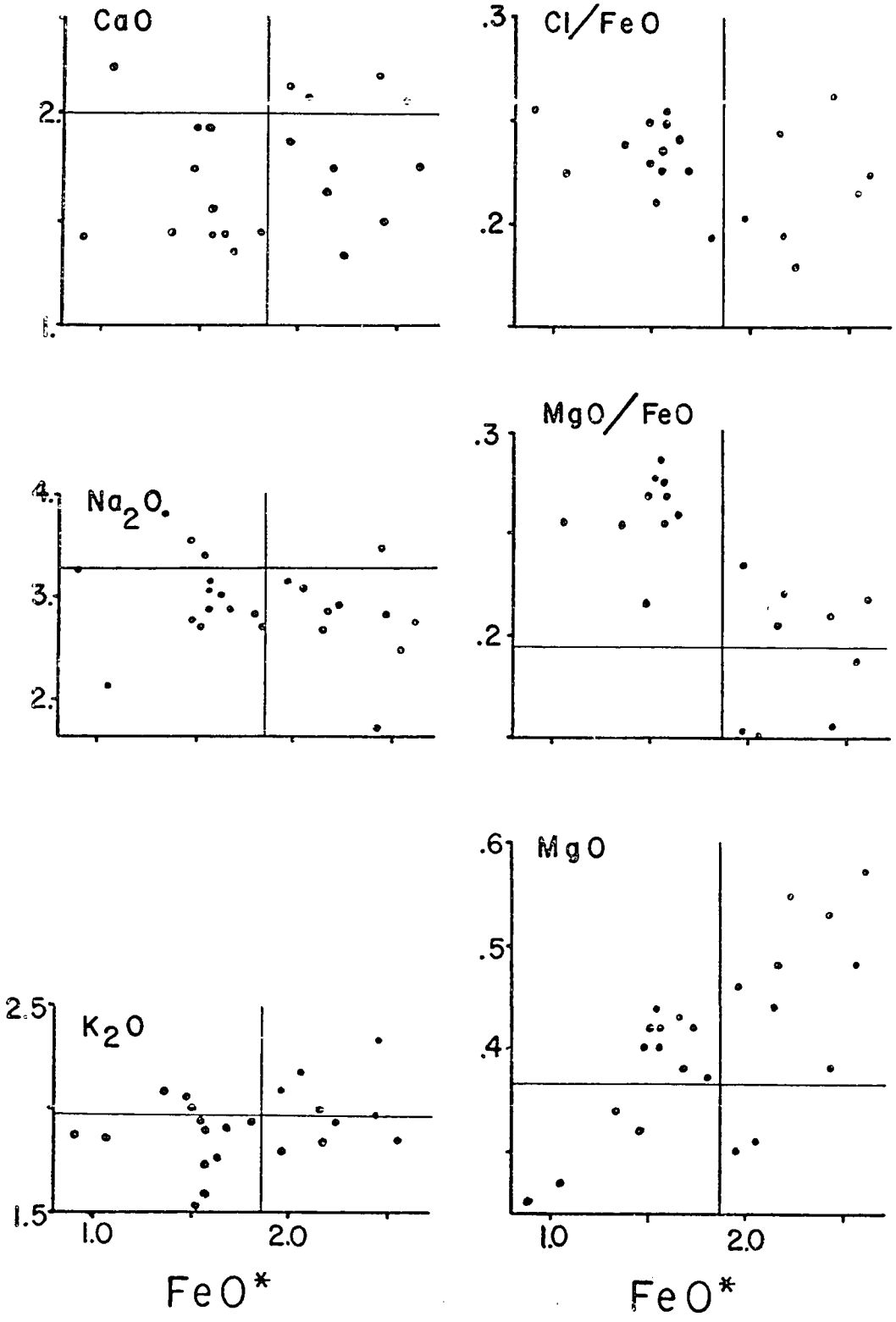
CaO
2.
Cl/FeO
.3
.2
MgO/FeO
.3
.2
4.
Na_2O
3.
2.
MgO
.6
.5
.4
2.5
K_2O
1.5
1.0
2.0
FeO*
1.0
2.0
FeO*

ably reflects the different quenching history experienced by different crystals during the magma mixing event. The presence of crystallites in the inclusions causes analytical problems, because it is difficult to precisely reoccupy spots during separate runs, and small changes in beam location may result in significant changes in composition. For this reason, many more partial analyses of glass inside inclusions were also obtained, but are not reported because in one or two of the runs the same glass was not analyzed (Al was monitored in all runs to check this.). The analyses reported appeared to be the most reliable, in that they yielded similar Al_2O_3 contents on each run. Several more partial analyses yielded SiO_2-contents of 54 $\pm$ 1 wt.%, in agreement with analysis 1.

In light of the analytical difficulties involved, the composition of glass in olivine should be interpreted with caution.

The following features of the analyses of glass inclusions in olivine are notable: (1) The extremely low TiO_2-content of analyses 4 to 7 is surprising. It appears that Ti was fractionated out of the melt by growth of a Ti-rich phase, possibly Fe-Ti oxide. Hornblende may also have removed a significant amount of Ti. (2) The Al_2O_3-content is high in all inclusions, but is lower in the more silicic than in the more mafic glasses. In light of the alumina contents of hornblende (14-16 wt.%) and clinopyroxene (3½-

8½ wt.%), depletion in the Al_2O_3-content of the inclusions indicates that a more aluminous phase has played a significant part in post-entrapment devitrification. This phase may be spinel, which has been seen in some inclusions, or plagioclase, which has not yet been recognized in the inclusions. (3) CaO is strongly depleted in silicic relative to basic inclusions. This may be explained by crystallization of hornblende and/or augite.

HAZARDS FOR THE INTERPRETATION OF GLASS INCLUSION COMPOSITIONS

For the following reasons, the composition of glass inclusions in Augustine phenocrysts may not directly represent the composition of the melt in which the host crystals were growing:

1. POST-ENTRAPMENT CRYSTALLIZATION OF THE INCLUSION

After entrapment, the melt within inclusions continued to precipitate the host phase and commonly other minerals as well. A fluid phase was also exsolved from the melt during post-entrapment crystallization.

Textural and geochemical methods used by Anderson (1974b) and Watson (1976) to determine the initial composition of partly crystallized inclusions have proved unsuccessful for the Augustine samples. In chapter 2, a method was presented by which the initial composition of inclusions in olivine could be estimated within a narrow range, the variability arising from uncertainty in the mode and com-

position of the devitrification minerals. This method, however, depended upon determining the initial MgO-content of the inclusions through the use of olivine-liquid distribution coefficients. Similar methods are much less reliable for glass inclusions inside plagioclase or pyroxene, because crystal-liquid distribution coefficients for these minerals depend too much upon factors which are not well known, such as composition, temperature, and water pressure. Consequently, it has not been possible to correct for post-entrapment crystallization of plagioclase and pyroxene hosts. The similarity of composition of glass included in these two minerals suggests, however, that post-entrapment crystallization has been relatively minor, and that the compositions of inclusions are not very different from those of the initial trapped melts.

Unfortunately, separation of a fluid phase from the trapped melt poses a greater problem, because the composition of the fluid phase cannot be readily determined. It will become apparent later in this discussion that the volatile composition of the trapped melt in plagioclase and pyroxene crystals changed very little during crystallization. Separation of a fluid from the melt trapped in olivine may have had a greater effect, which cannot be evaluated without knowledge of the abundance of CO_2 in the melt. Because this cannot be evaluated, it merely adds to the uncertainty in the estimate of the volatile content of

the basalt.

2. THE EFFECT OF CRYSTAL-LIQUID INTERFACE DIFFUSION GRADIENTS

Fenn and Luth (1973) observed fluid inclusions in feldspar crystals experimentally grown in a fluid-undersaturated melt. These non-representative inclusions formed, they suggested, because water accumulated at the crystal-liquid interface as it was rejected from the anhydrous feldspar. Diffusion, this interpretation presumes, was too slow to permit the melt to homogenize near the interface.

Concentration gradients have been observed in glasses surrounding plagioclase (Bottinga and others, 1966) and olivine (Anderson, 1967; Donaldson, 1975). Elements that enter the crystal are ordinarily depleted in the melt within 10-25 microns of the crystal margin; rejected elements are usually enriched. The percentage of increase or decrease of each element, as well as the width of the affected zone, depends upon the composition of the crystal and the melt, the diffusion rate for each element, and the crystal-face growth or melting rate, as well as secondary effects such as the rate at which the crystal moves with respect to its enclosing melt, and the cooling history of the melt. The apparent absence of concentration gradients from around phenocrysts in the Augustine ejecta is not sufficient evidence that they did not exist when melt inclusions were forming, since gradients are likely to form only when the crystal growth rate

is diffusion-controlled (Kirkpatrick, 1976). It is under this condition (relatively rapid crystal growth) that melt inclusions are most likely to form (Lofgren, 1974).

Precise quantification of the effect of interface diffusion gradients upon the composition of glass inclusions is not possible, due to uncertainties in most of the above mentioned factors. Observations of Bottinga and others (1966) and Donaldson (1975), summarized in Table XVI, demonstrate that the increase or depeltion of an element near the interface may be significant, commonly amounting to more than 20%. Unfortunately, some elements diffuse more rapidly than others, so that the composition within the interface cannot be described by crystal addition or subtraction alone.

Clearly, the size of a glass inclusion is a critical factor in judging the importance of the interface effect. For a rectangular inclusion (length:width:width = 3:1:1), assuming a 10 micron wide diffusion gradient, the volume of non-representative melt is 100% for widths less than or equal to 20 microns, but is only 12.5% for w = 40 microns. Because most glass in crystals is contained in small inclusions less than 20 microns in diameter, an analytical technique that averages the compositions of all inclusions (i.e., degassing in a mass spectrometer) will be examining primarily non-representative compositions.

Glass inclusions examined in this study are primarily

TABLE XVI: Width of diffusion aureoles around plagioclase and olivine phenocrysts reported by Bottinga and others (1966) and Donaldson (1975), and maximum observed values of depletion or enrichment of the aureole relative to the parent melt.

	OLIVINE (Donaldson, 1975)		PLAGIOCLASE (Bottinga & others, 1966)	
Element	Gradient width (microns)	Relative enrichment or depletion	Gradient width (microns)	Relative enrichment or depletion
SiO_2	1.6-5.6	+ 4.0 %	ca. 7	+ 3 %
Al_2O_3	4.8-16.0	+ 11.9 %	ca. 7	- 12 %
TiO_2	no gradient	no change	n.d.	n.d.
FeO*	4.5-16.0	- 6.2 %	ca. 12	+ 31 %
MgO	6.0-20.0	- 36.3 %	ca. 10	+ 28 %
CaO	4.0-14.4	+ 4.0 %	no gradient	no change
Na_2O	4.8-25.6	+ 21.5 %	no gradient	no change
K_2O	no gradient	no change	n.d.	n.d.

Diffusion coefficients of selected ions relative to the diffusion coefficient of iron. All diffusion coefficients are calculated from the relationship reported by Magaritz & Hofmann (1976):

$$\log D_{1300} = -1.47 \log (Z^2R) - 5.55$$

where Z is the charge of the ion and R is its radius. This equation was determined for basaltic compositions at 1300° C, and while its diffusion coefficients do not necessarily reflect those in the rhyolite, the relative differences between the diffusion coefficients of various elements may be comparable.

$D^{Mg}/D^{Fe} = 1.10$

$D^{Na}/D^{Fe} = 1.61$

$D^{Ca}/D^{Fe} = 1.68$

$D^{K}/D^{Fe} = 2.25$

$D^{Cl}/D^{Fe} = 3.07$

large (greater than 80 microns diameter), although some of those examined within olivine were smaller (to a minimum of 40-50 microns diameter). Anderson (1973) examined some inclusions even smaller, and recognized no systematic compositional variation with size of the inclusions. I have uncovered no apparent correlations between composition and size in several inclusions that occur within a single plagioclase phenocryst, and therefore conclude, as did Anderson (1973) and Donaldson (1975), that for large inclusions, the interface diffusion gradient effect is insignificant.

3. CONTAMINATION OF THE INTERFACE MELT BY RESORPTION PRIOR TO MELT ENTRAPMENT

In as much as most glass inclusions in plagioclase occur within patchy zoned portions of the crystal, it appears that most were trapped following an eipsode of crystal resorption (Vance, 1965). Resorption may be a sign that the melt surrounding the crystal was rapidly changing, by magma mixing or crystal settling, for example. Moreover, it is possible that the melt immediately surrounding the resorbed crystal may have been "contaminated" by the partial melting products of that crystal, at the time the inclusions were trapped. This process may have been responsible for the formation of melt inclusions whose MgO- and FeO-contents are less than that of the rhyolitic groundmass of dacitic pumices, which presumably represents more differentiated melt than that which contained the phenocrysts when the

inclusions were trapped.

The rate of rehomogenization of crystal/liquid interface composition gradient is a function of chemical potential gradients and the diffusion coefficient of the element in question. Although it is not possible to precisely quantify either of these factors, a qualitative judgment of the relative efficacy of homogenization of different elements can be obtained by examining the diffusion coefficients determined for other melts (e.g., Magaritz and Hofmann, 1976). The relative diffusion coefficients of several important ions are shown in Table XIV, and imply that:

1. If Mg and Cl diffuse more rapidly than Fe (as is suggested by their diffusion coefficients), then MgO/FeO and Cl/FeO may be greater within the contaminated aureole than within the initial parent melt, as Mg and Cl diffuse more rapidly into the "diluted" melt.

2. Some rapidly diffusing cations (e.g., K^+ and H^+) may homogenize quickly and thereafter remain unchanged as FeO increases.

The behavior of Ca, Na, and Al during the development of the inclusions is more complex, since, following entrapment, these elements may be removed by crystallization of the host. During resorption the aureole will become strongly enriched in CaO and Al_2O_3, only slightly enriched in Na_2O (since the Na_2O content of the plagioclase is only slightly greater than that in the magma), and depleted in SiO_2. If,

after melting has ceased, a more calcic plagioclase begins to grow, crystallization of only part of the volume of plagioclase contributed by melting may reverse this trend. The final results may be quite complex, depending as well upon the stage at which the melt inclusion is sealed from the parent magma.

THE ABUNDANCE OF VOLATILE ELEMENTS IN THE MELT PHASE OF THE BASALT

Unfortunately, glass inclusions in olivine can provide only a rough estimate of the volatile element concentration in basalt. In particular, the water content is difficult to estimate due to: (1) Analytical difficulties, especially sodium-loss and possible interference with fine devitrification minerals. (2) Variable modes of devitrification minerals including, in part, hydrous hornblende. Sulfur content of the initial trapped melt is difficult to evaluate as well, due to the crystallization of sulfides from the trapped melt. The variability that characterizes the sulfur-content of the trapped glasses may be due to sulfide-supersaturation of some glasses (Mathez, 1977, personal communication). The chlorine content of the glasses is also extremely variable, and does not appear to vary strictly in response to changes in the amount of residual glass in partly devitrified inclusions. It may be due in part to variations in the chlorine content of hornblende within inclusions (in some analyses it is as high as 0.12 wt.%). For

various reasons, the initial trapped melt compositions may have been variable, as well.

The estimated pre-eruption volatile contents of the basalt and dacite are summarized in Table XIII, and are discussed below.

WATER CONTENT OF THE BASALT

A moderate to high water content during crystallization of the basalt can be inferred from: (1) The presence of hornblende; Eggler and Burnham (1973) found hornblende to be stable in andesitic magmas only when a_{H_2O} exceeds 0.3. (2) Early crystallization of clinopyroxene and absence (or later appearance) of plagioclase, matching the crystallization sequence of hydrous olivine tholeiites (Yoder and Tilley, 1962; Holloway and Burnham, 1972), but contrasting with the sequence observed in anhydrous tholeiites, in which plagioclase crystallizes before clinopyroxene (Yoder and Tilley, 1962; Green and Ringwood, 1967).

Summation deficiencies in analyses of glass inclusions in olivine range from 9.21 to 2.49 wt.%. Because of the variable degree of crystallization within different inclusions, variable water contents can be expected in the residual glasses. However, because summation deficiencies do not increase with the concentration of K_2O, or another element that indicates the degree of post-entrapment crystallization, it is difficult to evaluate the original parent melt compositions, and to judge the analytical error, which

profoundly effects the estimated water content. For this reason, I have estimated initial water contents (3.6 to 5.5 wt.%) calculated assuming various modes of devitrification from analysis 1, Table XV, the composition of the glass inclusion which appears to have undergone the least devitrification (see Table XI).

CHLORINE CONTENT OF THE BASALT

Chlorine contents range from 0.34 wt.% in the least differentiated glass (analysis 1, Table XV) to 0.97 wt.% in the most differentiated glass (analysis 2). The variability in other analyses does not, however, follow a predictable trend, and it is, therefore, difficult to interpret the meaning of each analysis. I have, therefore, estimated the chlorine content of the initial trapped melt, from the reconstruction of analysis 1, Table XV (Table XI), to be roughly 0.13-0.28 wt.%.

SULFUR CONTENT OF THE BASALT

The measured sulfur content of the glass inclusions varies from 100 to 700 ppm (0.01-0.07 wt.%) plus one analysis of 0.24 wt.%, which may be "contaminated" by the presence of a sulfide phase within the X-ray generating volume. Because sulfide phases separated from the trapped melt, it is difficult to evaluate the sulfur content of the initial trapped melt. On the other hand, the presence of sulfide globules within phenocrysts and inclusions indicates that the melt was therefore controlled by the equilibrium between

the sulfide and silicate melts. This might be used to evaluate the pre-eruption sulfur content of the melt.

The sulfur and FeO*-contents of glass inclusions in olivine, plagioclase, and pyroxene are illustrated in Figure 19. The data do not define a trend. If the trend observed by Mathez (1976) in ocean floor basalts is approximately equivalent to that in the Augustine magmas during their crystallization at depth, then the pre-eruption sulfur content of the basalt magma (assuming FeO = 8.31 to 10.76 wt.%) was roughly 1400 to 2200 ppm (0.14 - 0.22 wt.%).

FLUORINE CONTENT OF THE MELT PHASE OF THE BASALT

Fluorine was sought in one glass inclusion in olivine (analysis 6, Table XV). Despite the relatively devitrified state of this inclusion, which would lead to concentration of fluorine in the melt phase, fluorine was not detected in the analysis, and hence probably does not exceed 50-100 ppm.

THE ABUNDANCE OF VOLATILE ELEMENTS IN THE MELT PHASE OF THE DACITE

Glass inclusions in plagioclase and pyroxene are relatively easy to analyze, due to their larger size and the absence or scarcity of daughter crystals. The analyses may, therefore, be viewed with much greater confidence than those determined of inclusions in olivine. As discussed earlier, however, many of the glass inclusions within plagioclase appear to have trapped non-representative melt "diluted" by partly melted plagioclase. Because the effect of this

"dilution" on the measured concentration of volatile elements cannot be quantified, I will consider the composition of glass inclusions in plagioclase only with more than 1.85 wt.% FeO* (the concentration of FeO* in the groundmass of dacite pumices). This selection procedure eliminates the inclusions with the lowest Cl-content (covering the range 0.23 to 0.40 wt.%), but does not otherwise alter the estimates of the pre-eruption volatile content of the dacite.

WATER CONTENT OF THE MELT PHASE OF THE DACITE

The summation deficiencies in analyses of glass inclusions in plagioclase and pyroxene vary from 5.33 to 7.67 wt.%, and average 6.58 wt.%. This variation is relatively minor, and is probably less than the uncertainty in the analysis.

The following features of glass inclusions in plagioclase and pyroxene indicate that the dacite melt was saturated with respect to an aqueous fluid phase prior to entrapment of the inclusions: (1) Despite the variable K_2O content of the inclusions (1.50 to 2.34 wt.%) and the variable composition of the host crystals, the water contents of the inclusions (by difference) are relatively uniform. Fractional crystallization producing a 75% increase in K_2O would be accompanied by a similar change in water content. The absence of such an increase implies that the water concentration was held nearly constant by effervescence when the abundance exceeded the solubility limit. (2) The water

content of glass inclusionsin plagioclase and pyroxene is approximately one-half to one-third the content that would be expected had that magma been derived from a basalt parent with 3½ wt.% water. (3) The chlorine concentration in glass inclusions in plagioclase and pyroxene should also be much greater than that in the basalt (assuming that the dacite formed from the basalt by fractional crystallization). The similar concentrations in glass inclusions derived from the two separate magmas implies that chlorine was removed during fractionation. Crystalline phases sufficiently Cl-rich to remove the chlorine have not been recognized; rather it appears that chlorine may have been partitioned into an aqueous fluid phase (Kilinc and Burnham, 1972; Anderson, 1974) and migrated out of the system in free vapor bubbles. (4) Rare, large relative volume bubbles (20-30% of the inclusion volume) inside some glass inclusions probably formed in part as free vapor bubbles trapped with the melt. In contrast, Anderson (1973) argued that the uniformity of relative bubble sizes in many samples he examined oppose entrapment of a fluid-saturated melt. Several factors, however, make both Anderson's and my own interpretation of our respective observations tenuous: (a.) relative bubble and inclusion volumes are difficult to measure with accuracy; (b.) the relative size of bubbles may vary due to differences in the amount and/or mode of post-entrapment crystallization or resorption; (c.) inclusions may trap

different melt compositions with different volatile element compositions; (d.) in a fluid-saturated melt entrapment of a bubble may be an infrequent and fortuitous event.

The pre-eruption dissolved-water content of the rhyolitic mesostasis of the dacite, then, was roughly equivalent to the water content of the inclusions, because during post-entrapment crystallization, the water content was maintained at the pre-entrapment concentration by the pressure-dependent solubility limit.

CHLORINE CONTENT OF THE MELT PHASE OF THE DACITE

The chlorine content of the glass inclusions in plagioclase and pyroxene ranges from 0.23 to 0.63 wt.%. If "diluted" low FeO* inclusions are eliminated, then Cl ranges from 0.35 to 0.63 wt.%.

Post-entrapment crystallization and separation of a fluid phase changes the chlorine content of the melt phase only slightly, because the increase in the residual melt during crystallization of chlorine-poor phases was nearly balanced by the loss of chlorine into the fluid phase (illustrated in Figure 18, and discussed in greater detail in the following section). The concentration of chlorine in the rhyolitic mesostasis of the dacite, then, was within the approximate range 0.35 to 0.63 wt.%.

SULFUR CONTENT OF THE MELT PHASE OF THE DACITE

Sulfur varies from less than 50 to approximately 550 ppm in glasses included in plagioclase and pyroxene. Some

of these inclusions contain various types of secondary sulfide minerals, however, and the content within inclusions is not necessarily equivalent to the initial trapped melt composition.

The presence of distinct sulfide globules within plagioclase phenocrysts indicates that the dacite, like the basalt, was sulfide-saturated. The sulfur content of the melt phase, then, was controlled by the sulfide liquid-silicate liquid equilibrium. Unfortunately, the scatter in the data precludes recognition of the form of the S-FeO relationship, and extrapolation of the relationship observed by Mathez (1976) to the FeO-poor compositions represented by the inclusions is not advisable.

The sulfur-content, then, of the melt phase of the dacite can only be roughly estimated to be within the range from approximately 50 to 550 ppm (0.005-0.055 wt.%).

FLUORINE CONTENT OF THE MELT PHASE OF THE DACITE

Fluorine analyses reported in Table XV are extremely variable. Most melt inclusions contain little F (less than 100-200 ppm), but some contain substantially high amounts (200-2700 ppm). The erratic values may reflect the presence of an unknown F-rich crystalline phase in some inclusions. The absence of a correlation between P and F or Cl and F argues against apatite as that phase. Fluorite has been recognized in Mt. Lassen dacites by Macdonald and Katsura (1965), but has not been identified in the Augustine ejecta.

Figure 18: The relationship between the H_2O, Cl, and K_2O contents of Augustine magmas. The diagonal line labelled "Fractional crystallization" illustrates the expected change in H_2O- and Cl-content of the residual melt during fractional crystallization of a basalt that initially contains 3½ wt.% H_2O, 0.25 wt.% Cl, and 0.5 wt.% K_2O, assuming equal bulk crystal/liquid distribution coefficients for all three elements ($D^{xl/liq}=0$). The dashed portion of this line is above the solubility limit for the Augustine magma at its pre-eruption depth, but would describe the change in a similar magma fractionating at greater depth. The solid horizontal line at 6½ wt.% H_2O (labelled "H_2O") illustrates the uniformity of water-content with fractionation, expected for crystallization of the Augustine water-saturated magma at constant depth. The stippled area encloses the analyses of glasses included in plagioclase and pyroxene phenocrysts. The change in Cl-content of the melt during crystallization of the magma after it becomes fluid-saturated is shown by the curved lines (labelled "Cl"), each based on a different value for $K = Cl_{vapor}/Cl_{melt}$ (values taken from Kilinc and Burnham, 1972). Curves labelled with the value of a particular vapor/melt distribution coefficient illustrate the path of composition change of the melt assuming that the melt experiences perfect fractional vaporization; that is, the aqueous fluid phase is immediately isolated from the remaining melt. The data points shown (analyses of "undi-

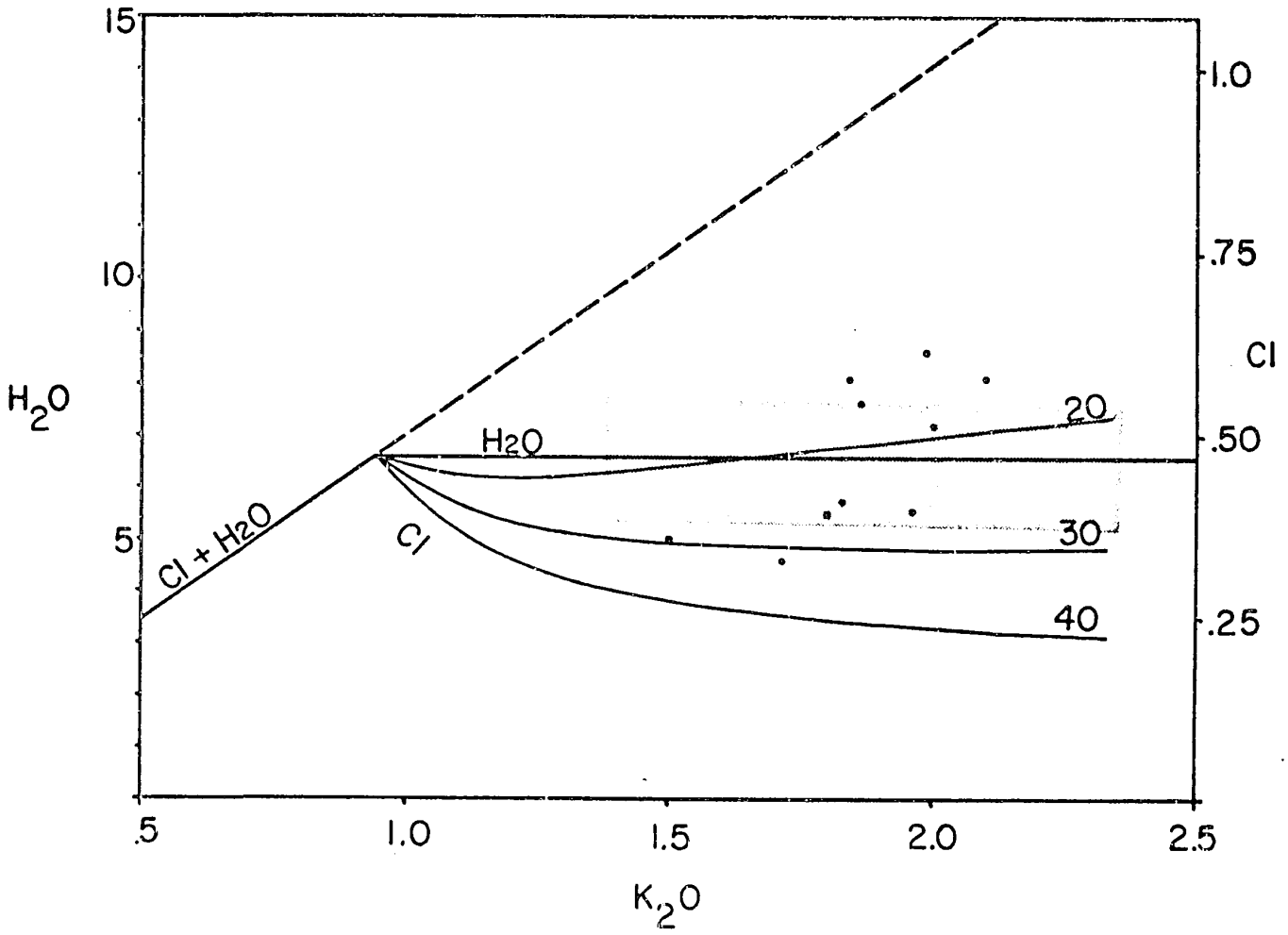
15
10
5
H_2O
1.0
.75
Cl
.50
.25
20
H_2O
30
40
Cl + H_2O
Cl
.5
1.0
1.5
2.0
2.5
K_2O

luted" glass inclusions in plagioclase and pyroxene) are consistent with a constant value for K of approximately 10. It is likely, however, that the distribution coefficients did not remain constant, and the actual path may therefore be very different from those shown. This diagram illustrates the profound effect on the abundance of chlorine in the magma resulting from exsolution of an aqueous vapor phase.

The distribution of F, then, remains an unsolved problem, but it seems to be extremely low in abundance in the melt phase (less than 200 ppm).

EVOLUTION OF VOLATILES WITHIN THE MAGMA

Volatiles in the Augustine magmas appear to have evolved primarily through four processes: (1) Fractional crystallization, involving primarily volatile-poor phases, but also hornblende and apatite; (2) Separation of an immissible sulfide liquid; (3) Separation of a fluid phase; (4) Magma mixing.

Addition of volatile elements through assimilation of country rock or introduction of groundwater may also occur (Lipman and Friedman, 1975), and isotopic studies are planned to test for these processes. It will remain to be seen whether either process had any effect upon the composition of the dacite, but it is unlikely that the volatiles within glass inclusions could have been introduced in this manner, since, as discussed in chapter 2, (1) the basalt apparently arrived at the level of the shallow crustal reservoir only months before the eruption, and (2) the glass inclusions within olivine were trapped within the stability field of hornblende, at depths of roughly 25-75 km, probably below the region of groundwater penetration.

In the following section I will discuss how each volatile component may have evolved in the melt, if the dacite originated by fractional crystallization of a basalt similar

to that which participated in the 1976 eruption.

WATER

The evolution of water in the Augustine magmas was controlled primarily by fractional crystallization during the early stages of differentiation of the parent basalt, and effervescence of an aqueous fluid after attainment of water saturation.

Crystallization of hornblende with roughly 2 wt.% water during the early stages of crystallization of the basalt probably had only a moderate effect on the evolution of water. In view of its absence from the dacite, and the presence instead of pyroxene-plagioclase-magnetite clusters pseudomorphing hornblende, it appears that relatively minor amounts of hornblende may have been removed during crystallization, and that some of the water initially tied up within the hornblende may have later been released to the melt as hornblende broke down.

In Figure 18 I have illustrated the calculated evolution of water during fractional crystallization of a basalt containing 3.5 wt.% H_2O, assuming that $\bar{D}_{H_2O}=\bar{D}_{K_2O}\cong 0$. Enrichment of water in the resitual melt ceases when water saturation is achieved with 6.58 wt.% H_2O. This diagram illustrates two other points: (1) Andesitic magmas with approximately 1 wt.% K_2O may also have been water-saturated; (2) Fractional crystallization of such a basalt at greater depths could have produced dacites with as much as 10-15

wt.% H_2O.

CHLORINE

Relatively little information is available from which to judge the solubility of chlorine in magmas. Iwasaki and Katsura (1967) determined that at 1 atm, temperature = 1030° to 1290° C, in the absence of water, the solubility of HCl decreased with decreasing f_{HCl}, with increasing temperature, and with increasing SiO_2 in the melt (from about 1.5 wt.% for basalt to 0.1 wt.% for rhyolite at 1030° C). Like water, it is probable that Cl-solubility increases profoundly with pressure, hence, on the basis of the 1 atm data, little can be said of the solubility at depth. Despite the relatively high Cl-content of the Augustine magmas, it is unlikely that they could have achieved saturation with respect to chlorine during crystallization.

Apatite, with 1.75 to 2.10 wt.% Cl, is the only Cl-rich mineral recognized in the 1976 ejecta. However, chlorine loss by crystallization of apatite cannot have been very significant, since the P_2O_5-contents of the melt phase of the basaltic and dacitic magmas preclude crystallization of more than 1% apatite, containing 0.02 wt.% Cl.

Cl may, however, be strongly partitioned into an aqueous fluid phase coexisting with a melt (Kilinc and Burnham, 1972). Distribution coefficients ($m_{Cl_{vapor}}/m_{Cl_{melt}}$) determined by Kilinc and Burnham (1972) range from 13 to 167 at temperatures of 700-750° C, P=2-8 kb, in melts of quartz

monzonite, granodiorite, granite, and trondhjemite. Under the approximate pressures of the Augustine magma chamber (1-3 kb) the distribution coefficients determined are in the range of 40-60. Based on two determinations only, the effect of increasing temperature appears to be to increase the distribution coefficient.

In Figure 18, I have illustrated the behavior of chlorine during fractional crystallization of the basalt parent with 3.5 wt.% H_2O and 0.25 wt.% Cl. The assumtions inherent in the diagram are stated in its caption. Until water-saturation was achieved, the chlorine content of the residual melt increased. Subsequent to the attainment of water-saturation, the chlorine content of the melt may have immediately declined as chlorine entered the aqueous fluid phase. During subsequent crystallization the concentration of chlorine in the residual melt may remain relatively constant over a moderately wide crystallization interval, if the distribution coefficients illustrated in Figure 18 approximately match those in the natural system. The concentration may continue to decline in the residual melt for higher values of K, or it may increase if K is smaller.

SULFUR

The presence of immiscible sulfide globules in plagioclase, olivine, and hornblende implies that the Augustine magmas were sulfide-saturated at the time that the globules were incorporated into their hosts.

The solubility of sulfides in mafic melts is a function of f_{S_2}, f_{O_2}, a_{FeO}, temperature, pressure, and melt composition (Haughton and others, 1974; Mathez, 1976). Haughton and others (1974) and Mathez (1976) recognized covariance between the FeO and S content of experimental and natural sulfide-saturated melts (Figure 19). Mathez (1976) attributed this covariance to dissolution of sulfur in the melt via an exchange reaction of the type:

$$FeO + \tfrac{1}{2}S_2 = FeS + \tfrac{1}{2}O_2 \qquad \text{Eqn 3}$$

From the equilibrium expression for this reaction:

$$K = (a_{FeS})(f_{O_2})^{\frac{1}{2}}/(a_{FeO})(f_{S_2})^{\frac{1}{2}} \qquad \text{Eqn 4}$$

it can be seen that the sulfur concentration of the silicate melt at constant K will depend upon f_{S_2}, f_{O_2}, and a_{FeO}. K, in turn, will vary with temperature and pressure.

The covariances determined by Haughton and others (1974) and Mathez (1976) are shown in Figure 19, along with the analyses of Augustine melt inclusions. The difference between the curves may reflect differences in K (from Eqn 4) that result from temperature or, more likely, pressure differences; or different oxygen and/or sulfur fugacities at constant K.

Although the stability of sulfides is controlled by factors that in our present state of knowledge cannot be fully evaluated, Figure 19 can be used in the same manner as a chemical potential diagram to predict the behavior of sulfides in a silicate melt during fractional crystallization

Figure 19: FeO*- and S-contents of glass inclusions in plagioclase (solid dots), compared to experimental data of Haughton and others (1974) (shown as "X"'s, and curve defined by all their data), and curve fitting compositions determined by Mathez (1976) in sulfide-saturated seafloor basalts. The covariance defined by the curves can be used in the sense of a chemical potential diagram (sulfides are stable in the upper left of the diagram). Scatter of the Augustine data is too great to define a reliable curve, but the data are consistent with a slope subparallel to that of Mathez (1976). The direction of change produced by crystallization of plagioclase, olivine (Fo_{84}), and magnetite (modified from Mathez, 1976) is illustrated in the upper left, and suggests that crystallization of the phases observed in the Augustine magmas would have led to and maintained sulfide-saturation of the Augustine magmas.

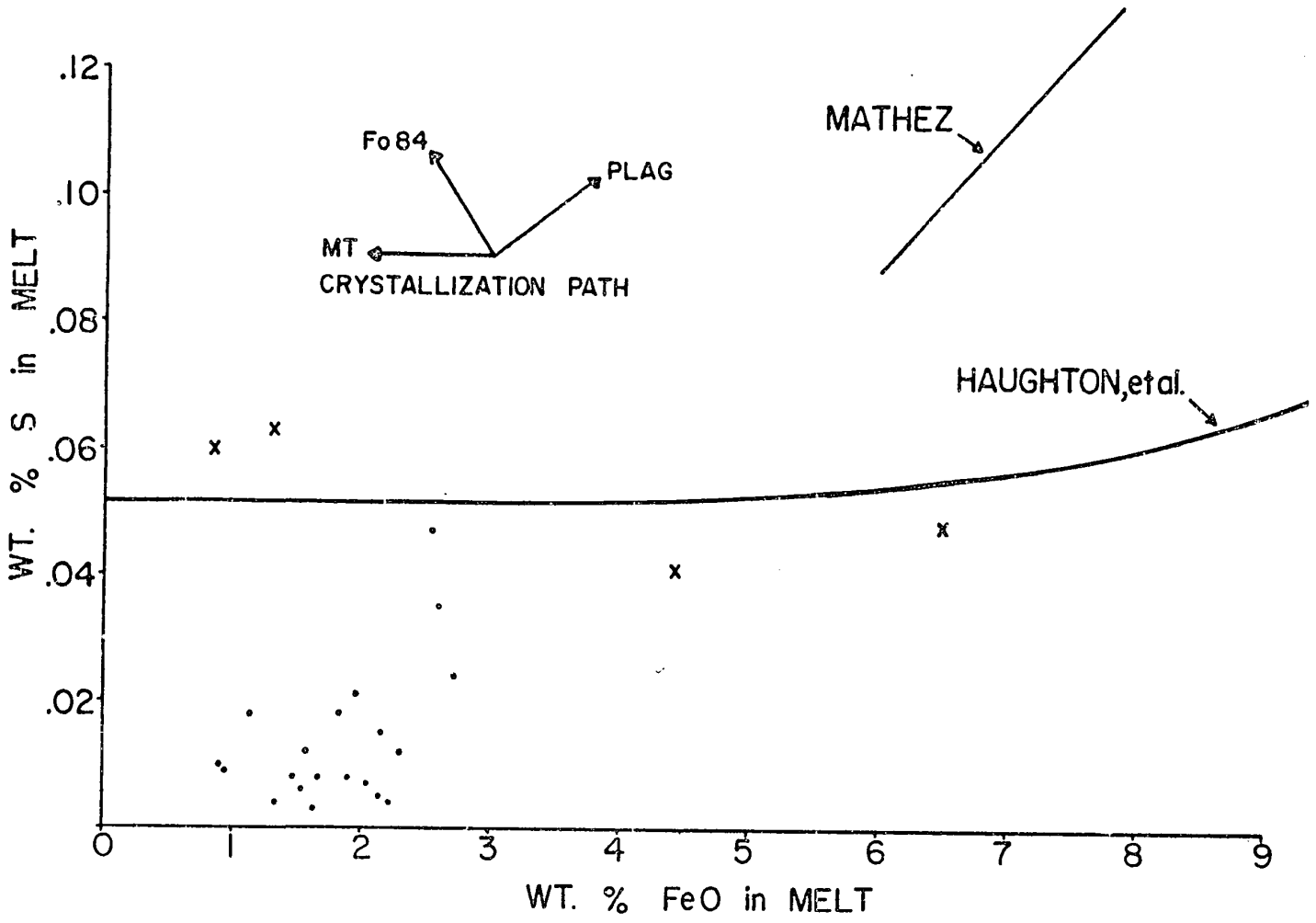
.12
.10
.08
.06
.04
.02
WT. % S in MELT
Fo 84
PLAG
MT
CRYSTALLIZATION PATH
MATHEZ
HAUGHTON, et al.
0
1
2
3
4
5
6
7
8
9
WT. % FeO in MELT

(see Mathez, 1976, Figure 6). The FeO-S Covariance curve separates the field of sulfide-saturation (upper left on Figure 19) from the field of sulfide-undersaturation. In reality, this covariance transgresses a number of variables that contribute to its form, most importantly oxygen and sulfur fugacities, but the consistency observed by Mathez as well as Czamanske and Moore (1977) suggests that the effects of the variation in these factors in the natural systems observed combine to yield roughly equivalent FeO-S covariance. However, because the Augustine magmas represent an appreciably different composition range than those examined by Mathez (1976) and Czamanske and Moore (1977), there is no reason to expect the covariance to persist in the Augustine magmas in the form exhibited by the seafloor basalts. The composition of sulfide-saturated melt inclusions could be used to empirically define the form of the covariance in the Augustine magmas, (see Figure 19), but scatter in the analyses yields a poorly defined trend.

The effects of fractional crystallization upon the parental basalt are as follows: During the initial crystallization, when olivine, Cr-rich spinel, augite, hornblende, and magnetite were crystallizing from the magma, the dissolved sulfur content of the residual melt would have increased as FeO decreased, moving the magma into the sulfide-saturation field. Mathez suggested that crystallization of plagioclase alone would drive a melt away from

saturation, and crystallization of a combination of feldspar and ferromagnesian phases could drive a melt along a path parallel to the saturation boundary (see Figure 19). Interpretation of the effect of crystallization from Figure 19 depends a great deal upon the slope of the FeO-S covariance, and it can be seen that a more gradual slope than that observed by Mathez, such as that reported by Haughton and others (1974) would imply a trend towards sulfide-saturation even for crystallization of plagioclase alone. Over the entire range of crystallization represented by the Augustine magmas, it appears that crystallization would have maintained the sulfide-saturation state of the magma.

If the conditions that led to and maintained sulfide-saturation of the Augustine magmas are typical of magmas elsewhere, then sulfide-saturation may be a relatively common, possibly uniform feature of andesitic and silicic melts at depth, as appears to be the case for basaltic rocks (Mathez, 1976; Anderson 1974b, 1975). Sulfide globules, evidence of sulfide-saturation, are common in basaltic lavas, but have not been reported previously in silicic rocks, except for the late stage silicic residue of a Hawaiian tholeiitic lava lake (Skinner and Peck, 1969). R.L. Smith (reported by Moore and Calk, 1971) has, in addition, observed sulfide-decorated vesicles in a dacite. In the Augustine dacites the globules are extremely rare, and can only be distinguished from the much more common Fe-Ti oxides

in polished sections. Hence, they are likely to be overlooked in silicic rocks, as they were until recently in basic rocks.

OTHER PETROLOGIC IMPLICATIONS

1. THE RATE OF MAGMA SUPPLY

Banded pumices and disequilibrium mineral assemblages similar to those of the 1976 ejecta are found in the deposits of the 1883, 1935, and 1963-64 eruptions of Augustine, and in the deposits of several prehistoric eruptions. These observations, and their interpretation as set forth in chapter 2, imply that new basaltic magma is being supplied on the order of every 10-100 years.

2. ORIGIN OF THE DACITES BY FRACTIONAL CRYSTALLIZATION OF BASALT

The apparent intimate association of andesite and dacite with basalt at Augustine is strong evidence for a genetic relationship. The part played by magma mixing in that genesis is important, but appears to have been a second order effect. The abundance of crystals in the magmas and the extensive normal zoning that characterizes these crystals argues for the significance of fractional crystallization during the genesis of the magmas.

Cawthorn and O'Hara (1976) demonstrated that fractionation of a hydrous basalt employing the phases Olivine + Calcic clinopyroxene + Amphibole could produce andesitic and subsequently more silicic magmas. These minerals appear to

be near-liquidus phases in the Augustine basalt and thus provide a mechanism by which andesitic and more silicic rocks may have been derived from the basalt.

3. THE CALC-ALKALINE NON-Fe-ENRICHMENT TREND IS DUE TO MAGNETITE, NOT HORNBLENDE CRYSTALLIZATION

Calc-alkaline rock suites are characterized by the absence of Fe-enrichment on an AFM diagram over most of their crystallization range. The extremely basic members of the suite may show Fe-enrichment, but that trend (typical of tholeiitic rock suites and the Skaergaard) is terminated and Fe/Mg remains nearly constant throughout the intermediate to silicic members. Osborne (1959) argued that this trend is the result of magnetite fractionation under conditions of high oxygen fugacity. He called upon high water contents to generate the required oxygen fugacity.

Osborne's mechanism was opposed by those who believed the oxygen fugacities required were unreasonably high (e.g., Eggler, 1972; Boettcher, 1973; Fudali, 1965; Cawthorn and O'Hara, 1976). Holloway and Burnham (1972) suggested, instead, that crystallization of hornblende could keep Fe/Mg from increasing, and based their argument upon the observation that amphibole produced in their experimental runs is characterized by relatively high Fe/Mg. Allen and others (1975), in contrast, found that amphibole produced during their experiments was sufficiently magnesian to increase the Fe/Mg of the residual melt. This apparent contradiction

probably resulted because the amphibole observed in Holloway and Burnham's experiments was in equilibrium with a more fractionated residual melt.

The mineralogy of the Augustine ejecta has some bearing upon these arguments:

(1) Crystallization of hornblende (Mg/Mg + Fe = 0.72) will continue to increase Fe/Mg in the residual melt. Hornblende, it appears, is unsuitable for producing the non-Fe-enrichment trend in calc-alkaline suites.

(2) Magnetite began to crystallize relatively near the liquidus in the Augustine basalt, as indicated by its presence within hornblende phenocrysts. Holloway and Burnham (1972) also found magnetite to be a near-liquidus phase in olivine tholeiite magma at less than 10 kb, with $a_{H_2O}=0.6$, and f_{O_2} maintained by the Ni-NiO buffer. These results support Osborne's (1959) hypothesis.

4. TRACE ELEMENT EVOLUTION -- OBSCURED BY MAGMA MIXING

Several studies of basaltic and andesitic calc-alkaline rocks from other parts of the Aleutian chain have concluded that basalts were not parental to the andesites and dacites within the same province (e.g., Delong, 1973; Marsh and Carmichael, 1974; Arculus and others, 1977). They have come to this conclusion despite the sometimes close spatial and temporal association of basaltic and andesitic magmas (e.g., Arculus and others, 1977).

These conclusions are generally based upon two argu-

ments: (1) Trace element abundances in the andesitic and more silicic magmas cannot be explained through simple fractionation of the basalt employing observed phases; and (2) radiogenic isotope ratios in the basic and silicic magmas are not the same.

The role of magma resupply and mixing in the trace element evolution of a magma chamber has been discussed recently by O'Hara (1977). He showed that this process can produce a very different trace element evolution than simple fractional crystallization.

The combined effects of magma mixing and fractional crystallization are illustrated in Figure 20, for a trace element strongly partitioned into early crystallizing phases. Mixing of a new batch of mafic magma with a silicic magma differentiated from a parent similar to that mafic magma will yield abundances for the trace element which are greater than expected from fractional crystallization alone. In light of the evidence at Augustine that magma resupply may be a very frequent process, the conclusions of many trace element modelling studies of andesitic rock suites should be reexamined.

Different radioisotope abundance ratios do not necessarily argue against cogenesis of two or more rocks if one has been contaminated. In view of the high water contents determined for the Augustine dacites, it is quite likely that minor melting will occur around the borders of silicic

ments: (1) Trace element abundances in the andesitic and more silicic magmas cannot be explained through simple fractionation of the basalt employing observed phases; and (2) radiogenic isotope ratios in the basic and silicic magmas are not the same.

The role of magma resupply and mixing in the trace element evolution of a magma chamber has been discussed recently by O'Hara (1977). He showed that this process can produce a very different trace element evolution than simple fractional crystallization.

The combined effects of magma mixing and fractional crystallization are illustrated in Figure 20, for a trace element strongly partitioned into early crystallizing phases. Mixing of a new batch of mafic magma with a silicic magma differentiated from a parent similar to that mafic magma will yield abundances for the trace element which are greater than expected from fractional crystallization alone. In light of the evidence at Augustine that magma resupply may be a very frequent process, the conclusions of many trace element modelling studies of andesitic rock suites should be reexamined.

Different radioisotope abundance ratios do not necessarily argue against cogenesis of two or more rocks if one has been contaminated. In view of the high water contents determined for the Augustine dacites, it is quite likely that minor melting will occur around the borders of silicic

chambers, and that contamination will occur. Due to the low Sr content of silicic relative to basic melts, the increase in the Sr-isotopic ratio by addition of a small amount of radiogenic Sr would be greater than in a basalt that assimilates the same amount of radiogenic Sr. Furthermore, because of their apparently longer residence times at shallow crustal levels, silicic melts are likely to incorporate more radiogenic Sr. In view of these factors, the small Sr-isotope ratio contrast between many basic and intermediate to silicic rocks (generally .001-.002) does not preclude derivation of the latter from the former.

Figure 20: Contrasting path of fractional crystallization (curve labelled F.C.) and a non-unique magma mixing line (involving two magmas at different stages of fractional crystallization). The distribution coefficient used (10) is not necessarily realistic for the full range of crystallization of a magma, but was chosen to illustrate the effect of mixing of primitive and differentiated magmas on the abundance of magmaphile elements, such as V, Cr, Ni, or Co, which ordinarily enter early formed crystalline phases. See O'Hara (1977) for a more rigorous discussion of this effect.

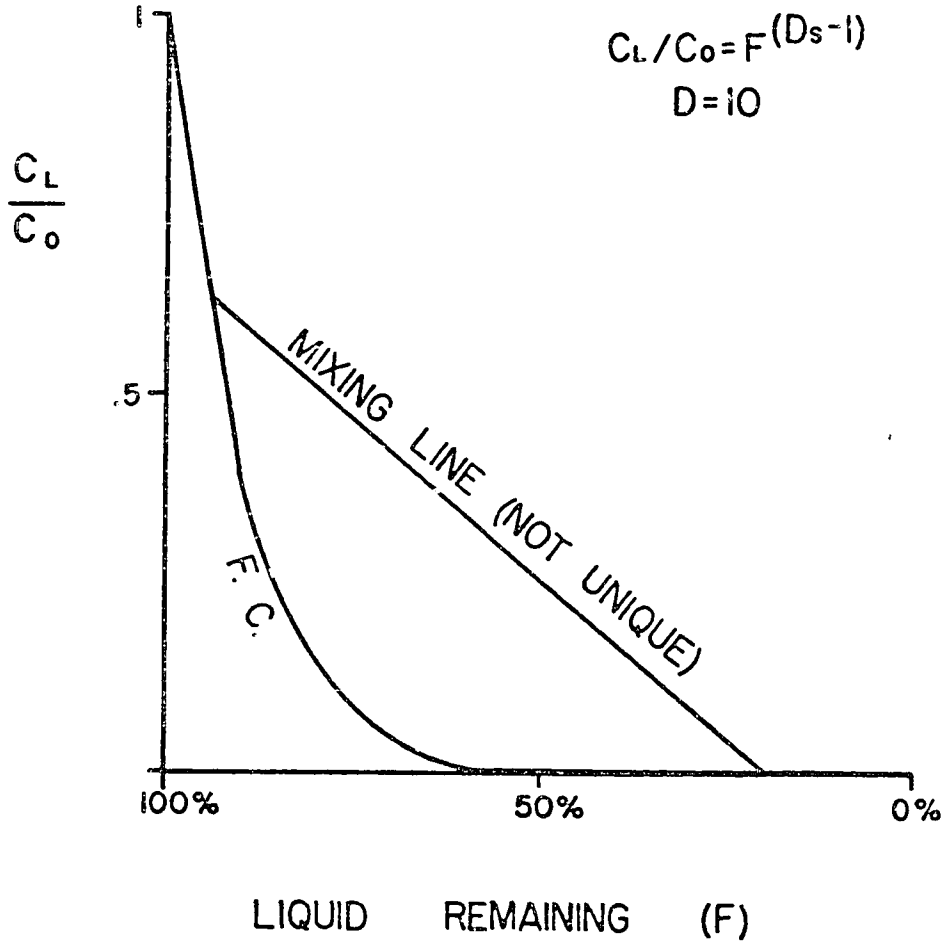
$C_L / C_o = F^{(D_s-1)}$
D=10
$\frac{C_L}{C_o}$
1
.5
MIXING LINE (NOT UNIQUE)
F. C.
100%
50%
0%
LIQUID REMAINING (F)

REFERENCES

Allen, J.C., A.L. Boettcher, and G. Marland (1975) "Amphiboles in andesite and basalt: I. Stability as a function of P-T-fo_2" AM. MINERAL. 60 (1069-1085).

Anderson, A.T. (1967) "Possible consequence of composition gradients in basalt glass adjacent to olivine phenocrysts (abstract)" AGU TRANS. 48 (227).

_____ (1973) "The before-eruption water contents of some high-alumina magmas" BULL. VOLC. 37 (530-552).

_____ (1974a) "Chlorine, sulfur and water in magmas and oceans" GSA BULL. 85 (1485-1492).

_____ (1974b) "Evidence for a picritic, volatile-rich magma beneath Mt. Shasta, California" JOUR. PETROL. 15 (243-267).

_____ (1975) "Some basaltic and andesitic gases" REV. GEOPH. SPACE PHYSICS 13 (37-55).

_____ (1976) "Magma mixing: petrologic process and volcanological tool" JOUR. VOLC. GEOTH. RES. 1 (3-33).

_____ and T.L. Wright (1972) "Phenocrysts and glass inclusions and their bearing on oxidation and mixing of basaltic magmas, Kilauea Volcano, Hawaii" AM. MINERAL 57 (188-216).

Arculus, R.J., S.E. Delong, R.W. Kay, C. Brooks, and S.S. Sun (1977) "The alkalic rock suite of Bogoslof Island, Eastern Aleutian arc, Alaska" JOUR. GEOL. 85 (177-186).

Aspinall, W.P., H. Sigurdsson, and J.B. Shepherd (1973) "Eruption of Soufriere Volcano on St. Vincent Island,

1971-1972" SCIENCE 181 (117-124).

Baker, Ian (1968) "Compositional variation of minor intrusions and the form of a volcano magma chamber" Q. JL. GEOL. SOC. LONDON 124 (67-79).

Barrett, S.A., D.B. Stone, and J. Kienle (1977) "A three-dimensional magnetic model of Augustine Volcano" TRANS. AGU 58 (169-179).

Becker, G.F. (1898) "Reconnaissance of the goldfields of southern Alaska, with some notes on general geology" USGS 18th ANN. REPT., PART III (28-30).

Bennett, F.D. (1971) "Vaporization waves in explosive volcanism" NATURE 234 (538-539).

Boettcher, A.L. (1973) "Volcanism and orogenic belts - the origin of andesites" TECTONOPHYSICS 17 (223-240).

Bottinga, Y., A. Kudo, and D. Weill (1966) "Some observations on oscillatory zoning and crystallization of magmatic plagioclase" AMER. MINERAL 51 (792-806).

_____ and D.R. Weill (1970) "Densities of liquid silicate systems calculated from partial molar volumes of oxide components" AMER. JOUR. SCI. 269 (169-182).

Bowman, H.R., F. Asaro, and I. Perlman (1973) "On the uniformity of composition in obsidians and evidence for magmatic mixing" J. GEOL. 81 (312-327).

Burnham, C.W. (1967) "Hydrothermal fluids at the magmatic stage" in Barnes, H.L. (editor) GEOCHEMISTRY OF HYDROTHERMAL ORE DEPOSITS, Holt, Rinehart and Winston, Inc.,

New York (34-76).

_____ (1975) "Water and magmas; a mixing model" GEOCHIM. COSMOCHIM. ACTA 39 (1077-1084).

_____ and N.F. Davis (1974) "The role of H_2O in silicate melts: II. Thermodynamic and phase relations in the system $NaAlSi_3O_8$-H_2O to 10 kilobars and 1000° C" AMER. JOUR. SCI. 270 (902-940).

_____, J.R. Holloway, and N.F. Davis (1969) "Thermodynamic properties of water to 1000° C and 10,000 bars" GSA SPEC. PAPER 132 (96 pp).

_____ and R.H. Jahns (1962) "A method for determining the solubility of water in silicate melts" AMER. JOUR. SCI. 260 (721-745).

Buffler, R. (1975) Geology of the south side of Augustine Island, Alaska STATE OF ALASKA DIV. OF GEOLOGY & GEOPHYSICS REPORT OF INVESTIGATION.

Byers, F.M., Jr. (1959) "Geology of Umnak and Bogoslof Islands Aleutian Islands Alaska" USGS BULL. 1028-L (267-369).

Carr, M.J. and R.E. Stoiber (1973) "Intermediate depth earthquakes and volcanic eruptions in Central America, 1961-1972" BULL. VOLCAN. 37 (326-337).

Cawthorn, R.G. and M.J. O'Hara (1976) "Amphibole fractionation in calc-alkaline magma genesis" A. J. SCI. 276 (309-329).

Coats, R.R. (1950) "Volcanic activity in the Aleutian Arc"

USGS BULL. 974-B (35-49).

Craig, H. (1961) "Isotopic variations in meteoric waters" SCIENCE 133 (1702-1703).

Czamanske, G.K. and J.G. Moore (1977) "Composition and phase chemistry of sulfide globules in basalt from the Mid-Atlantic Ridge rift valley near 37° N. latitude" GSA BULL. 88 (587-599).

Davis, P.M., D.B. Jackson, J. Field, and F.D. Stacey (1973) "Kilauea volcano, Hawaii: a search for the volcano-magnetic effect" SCIENCE 180 (73-74).

Delaney, J.R. (1977) "Distribution of volatiles in the glassy rims of submarine pillow basalts" Unpublished PhD Dissertation, University of Arizona, Tucson, Arizona.

_____ and D. Meunow (1976) "Volatile content of glassy pillow basalts from the Mid-Atlantic Ridge" GSA ABSTRACTS WITH PROGRAMS 8 (832-833).

Delong, S.E. (1974) "Distribution of Rb, Sr and Ni in igneous rocks, central and western Aleutian Islands, Alaska" GEOCHIM. COSMOCHIM. ACTA 38 (245-266).

Detterman, R.L. (1973) "Geologic map of the Iliamna B-2 quadrangle, Augustine Island, Alaska" USGS MAP GQ-1068.

Dibble, R.R. (1974) in PHYSICAL VOLCANOLOGY edited by Civetta, Gasparini, Luongo, and Rapolla; Elsevier, Amsterdam.

Donaldson, C.H. (1975) "Calculated diffusion coefficients

and the growth rate of olivine in a basalt magma" LITHOS 8 (163-174).

Doroshin, P.P. (1879) "O niektorykh valkanakh" (in Russian) RUSS. K. MIN. GESELL. VERH., 2nd Series 25 (44).

Dungan, M.A., J.M. Rhodes, P.E. Long, and D.P. Blanchard (1977) "Magma mixing at mid-ocean ridges. evidence from DSDP legs 45 and 46" GSA ABST. W/PROG. 9 (958-959).

Eaton, J.P. and K.J. Murata (1960) "How volcanoes grow" SCIENCE 132 (925-938).

Eggler, D.H. (1972) "Amphibole stability in H_2O-undersaturated calc-alkaline melts" EPSL 15 (28-34).

_____ and C.W. Burnham (1973) "Crystallization and fractionation trends in the system andesite-H_2O-CO_2-O_2 at pressures to 10 kb" GSA BULL. 84 (2517-2532).

Eichelberger, J.C. (1975) "Origin of andesite and dacite: evidence of mixing at Glass Mountain in California and at other circum-Pacific volcanoes" GSA BULL. 86 (1381-1391).

_____ and R. Gooley (1976) "Interaction of basalt and rhyolite magmas" GSA ABST W/PROG. 8 (851-852).

Einstein, A. (1906) "Eine neue Bestimmung der Molekuldimensionen" ANN. PHYS. (Leipzig) 19 (289-306).

Elder, J.W. (1977) "Thermal convection" JL. GEOL. SOC. LONDON 133 (293-309).

Evans, B.W. and B.R. Frost (1975) "Chrome-spinel in progressive metamorphism--a preliminary analysis" GEOCHIM.

COSMOCHIM. ACTA 39 (959-972).

Fenn, P.M. and W.C. Luth (1973) "Hazards in the interpretation of primary fluid inclusions in magmatic minerals" (abstract) GSA ANNUAL MEETING, DALLAS, 1973, PROGRAM (617).

Fenner, C.N. (1926) "The Katmai magmatic province" J. GEOL. 34 (673-772).

Fiske, R.S. and W.T. Kinoshita (1969) "Inflation of Kilauea volcano prior to its 1967-1968 eruption" SCIENCE 165 341-349).

Fudali, R.F. (1965) "Oxygen fugacities of basaltic and andesitic magma" GEOCHIM. COSMOCHIM ACTA 29 (1063-1075).

Green, D.H. and A.E. Ringwood (1967) "The genesis of basaltic magmas" CONTR. MIN. PET. 15 (103-190).

Grout, F.F. (1918) "Two-phase convection in igneous magmas" J. GEOL. 26 (481-499).

Hamilton, D.L., C.W. Burnham, and E.F. Osborn (1964) "The solubility of water and effects of oxygen fugacity and water content on crystallization in mafic magmas" JOUR. PETROL. 5 (21-39).

Haughton, D.R., P.L. Roeder, and B.J. Skinner (1974) "Solubility of sulfur in mafic magmas" ECON. GEOL. 69 (451-467).

Heiken, G. (1972) "Morphology and petrography of volcanic ashes" GSA BULL. 83 (1961-1988).

_____, P. Halleck, and T. McGetchin (1976) "Tephra

formation in ash-flow eruptions" GSA ABST. W/PROG. 8 (912).

Hildreth, W. (1976) "The Bishop Tuff: compositional zonation in a silicic magma chamber without crystal settling" GSA ABST. W/PROG. 8 (918).

Hobbs, P.V., L.F. Radke, and J.L. Stith (1976) "Eruptions of the St. Augustine volcano: airborne measurements and observations" SCIENCE 195 (871-873).

Hofmann, A.W. and M. Magaritz (1976) "Range of chemical equilibrium in partially molten rocks" ABST. CHAPMAN CONFERENCE ON PARTIAL MELTING IN THE EARTH'S UPPER MANTLE, Brookings, Oregon (21-22).

Holloway, J.R. and C.W. Burnham (1972) "Melting relations of basalt with equilibrium pressure less than total pressure" J. PETROL. 13 (1-29).

Hopson, C.A., J.S. Pallister, R.G. Coleman, and E.H. Bailey (1977) "Geologic section of the Semail ophiolite near Ibra, southeastern Oman Mountains, Sultanate of Oman" GSA ABST. W/PROG. 9 (1024-1025).

Irvine, T.N. (1977) "Origin of chromitite layers in the Muskox intrusion and other stratiform intrusions: a new interpretation" GEOLOGY 5 (273-277).

Iwasaki, B. and T. Katsura (1967) "The solubility of hydrogen chloride in volcanic rock melts at a total pressure of one atmosphere and at temperatures of 1200° C and 1290° C under anhydrous conditions" BULL. CHEM. SOC.

JAPAN 40 (554-561).

Jaeger, J.C. (1968) "Cooling and solidification of igneous rocks" in THE POLDERVAART TREATISE ON ROCKS OF BASALTIC COMPOSITION, vol. 2, H.H. Hess and A. Poldervaart, eds., Interscience, New York (503-536).

Johnston, D.A., H.-U. Schmincke, and J. Kienle (1977) "The 1976 eruption of Augustine Volcano, Alaska, and evaluation of hazards for future eruptions" GSA ABST. W/ PROG. 9 (442-443).

Johnston, M.J.S. and F.D. Stacey (1969) "Volcano-magnetic effect observed on Mt. Ruapehu, New Zealand" JGR 74 (6541-6544).

Kennedy, G.C. (1955) "Some aspects of the role of water in rock melts" GSA SPEC. PAPER 62 (489-503).

Kienle, J. and R.B. Forbes (1976) "Augustine-evolution of a volcano" ANNUAL REPORT 1975/76, Geophys. Inst., Univ. of Alaska, Fairbanks (26-48).

Kilinc, I.A. and C.W. Burnham (1972) "Partitioning of chloride between a silicate melt and coexisting aqueous phase from 2 to 8 kilobars" ECON. GEOL. 67 (231-235).

Kirkpatrick, R.J. (1975) "Crustal growth from the melt - a review" AM. MINERAL. 60 (798-814).

_____ (1977a) "Nucleation and growth of plagioclase, Makaopuhi and Alae lava lakes, Kilauea volcano, Hawaii" GSA BULL. 88 (78-84).

_____ (1977b) "Measurement and calculation of crystal

growth rates in silicate systems" CAN. MINERAL. 15 (195).

Kullerud, G., R.A. Yund, and G.H. Moh (1969) "Phase relations in the Cu-Fe-S, Cu-Ni-S, and Fe-Ni-S systems" ECON. GEOL. MONOGR. 4 (323-343).

Kuno, H. (1936) "Petrological notes on some pyroxene-andesites from Hakone volcano, with special reference to some types with pigeonite phenocrysts" JAP. J. GEOL. GEOGR. 13 (107-140).

Koster van Groos, A.F. and P.J. Wyllie (1969) "Melting relationships in the system $NaAlSi_3O_8$-NaCl-H_2O at one kilobar pressure, with petrological applications" JOUR. GEOLOGY 77 (581-605).

Lalla, D.J. and J. Kienle (1978) "Evolution of seismicity at Augustine Volcano, 1970 to 1976 eruption" GSA ABST. W/ PROG. in press.

Leake, B.E. (1968) "A catalogue of analyzed calciferous and subcalciferous amphiboles together with their nomenclature and associated minerals" GSA SPEC. PAP. 98 (210).

Lipman, P.W. (1967) "Mineral and chemical variations within an ash-flow sheet from Aso caldera, southwestern Japan" CONTR. MIN. PET. 16 (300-327).

_____ (1971) "Iron-titanium oxide phenocrysts in compositional zoned ash-flow sheets from southern Nevada" JOUR. GEOL. 79 (438-456).

_____ (1976) "Evolution of the Platorc Caldera complex and related volcanic rocks, southeastern San Juan Mountains, Colorado" USGS PROF. PAPER 852 (128 pp).

_____, R.L. Christiansen, and J.T. O'Connor (1966) "A compositionally zoned ash-flow sheet in southern Nevada" USGS PROF. PAPER 524-F (47 pp).

_____ and I. Friedman (1975) "Interaction of meteoric water with magma: an oxygen isotope study of ash-flow sheets from southern Nevada" GSA BULL. 86 (695-702).

Lofgren, G. (1974) "An experimental study of plagioclase crystal morphology: isothermal crystallization" AMER. JOUR. SCI. 274 (243-273).

Macdonald, G.A. and T. Katsura (1965) "Eruption of Lassen Peak, Cascade Range, California, in 1915" GSA BULL. 76 (475-482).

Magaritz, M. and A.W. Hofmann (1977) "REE diffusion in basalt and obsidian" GSA ABST. W/PROG. 9 (1082-1083).

March, B.D. (1976) "Some Aleutian andesites: their nature and source" JOUR. GEOL. 84 (27-45).

Mathez, E.A. (1976) "Sulfur solubility and magmatic sulfides in submarine basalt glass" JOUR. GEOPHYS RES. 81 (4269-4276).

_____ and R.S. Yeats (1976) "Magmatic sulfides in basalt glass from DSDP sites 319A and 320" INITIAL REPORTS DSDP 34 U.S. Gov't P.O., Washington, D.C.

Mauk, F.J. and J. Kienle (1973) "Microearthquakes at St.

Augustine Volcano, Alaska, triggered by earthtides" SCIENCE 193 (420-422).

McBirney, A.R. (1973) "Factors governing the intensity of explosive eruptions" BULL. VOLCANOL. 37 (443-453).

McCallum, I.S., I.D. Raedeke, and E.A. Mathez (1977) "Stratigraphy and petrology of the banded zone of the Stillwater Complex, Montana" TRANS. A.G.U. 58 (1245).

Meinel, A.B., M.P. Meinel, and G.E. Shaw (1976) "Trajectory of the Mt. St. Augustine 1976 eruption ash cloud" SCIENCE 193 (420-422).

Millhollen, G.L. (1975) "Magma contamination within the volcanic pile: Origin of andesite and dacite: Comment" GEOLOGY 3 (164-168).

Minikami, T. (1974) "Seismology of volcanoes in Japan" in PHYSICAL VOLCANOLOGY edited by Civetta, Gasparini, Luongo, and Rapolla, Elsevier, Amsterdam (chapter 1).

Moore, J.G. (1965) "Petrology of deep-sea basalt near Hawaii" A. J. SCI. 263 (40-52).

_____ (1967) "Base surge in recent volcanic eruptions" BULL VOLCANOL. 30 (337-363).

_____ (1970) "Water content of basalt erupted on the ocean floor" CONTR. MIN. PET. 28 (272-279).

_____ and L. Calk (1971) "Sulfide spherules in vesicles of dredged pillow basalt" AM. MINERAL. 56 (476-488).

_____ and B.P. Fabbi (1971) "An estimate of the juvenile sulfur content of basalt" CONTR. MIN. PET. 33

(118-127).

_____ and J.-G. Schilling (1973) "Vesicles, water, and sulfur in Reykjanes Ridge basalts" CONTR. MIN. PET. 41 (105-118).

_____, J.N. Batchelder, and C.G. Cunningham (1977) "Carbon dioxide in vesicles of mid-ocean ridge basalt" GSA ABST. W/PROG. 9 (1100-1101).

Murase, T. and A.R. McBirney (1973) "Properties of some common igneous rocks and their melts at high temperatures" GSA BULL. 84 (3563-3592).

Mysen, B.O. (1976) "The role of volatiles in silicate melts: solubility of carbon dioxide and water in feldspar, pyroxene, and feldspathoid melts to 30 kb and 1625° C" A. J. SCI. 276 (969-996).

O'Hara, M.J. (1977) "Geochemical evolution during fractional crystallization of a periodically refilled magma chamber" NATURE 266 (503-508).

Osborn, E.F. (1959) "Role of oxygen pressure in the crystallization and differentiation of basaltic magma" A. J. SCI. 257 (607-647).

Pearson, C. (1977) The internal structure of Augustine Volcano, Alaska, determined from explosion seismology; unpublished M.S. Thesis, University of Alaska, Fairbanks.

Pewe, T.L. (1975) "Quaternary geology of Alaska" USGS PROF. PAP. 835 (145 pp).

Reeder, J. and J. Lahr (1976, manuscript) "Seismometer response to air pressure waves from eruption events of Mt. St. Augustine, Alaska".

Roedder, E. (1965) "Liquid CO_2 inclusions in olivine-bearing nodules and phenocrysts from basalts" AM. MINERAL. 50 (1746-1782).

_____ (1972) "Composition of fluid inclusions" USGS PROF. PAP. 440-JJ.

_____ and D.S. Coombs (1967) "Immiscibility in granitic melts, indicated by fluid inclusions in ejected granitic blocks from Ascension Island" JOUR. PET. 8 (417-451).

Roeder, P.L. and R.F. Emslie (1970) "Olivine-liquid equilibrium" CONTR. MIN. PET. 29 (275-289).

Roobol, M.J. and A.L. Smith (1976) "Mt. Pelee, Martinique: a pattern of alternating eruptive styles" GEOLOGY 4 (521-524).

Rucklidge, J. and F.L. Gasparrini (1968) "Specifications for a computer program for processing electron microprobe analytical data" Univ. of Toronto, Toronto, Ont., Canada.

Schmincke, H.-U. (1967) "Cone sheet swarm, resurgence of Tejeda caldera, and the early geologic history of Gran Canaria" BULL. VOLCAN. 31 (153-162).

_____ and D.A. Johnston (1977) "Contrasting pyroclastic flow deposits of the 1976 eruption of Augustine volcano,

Alaska" GSA ABST. W/PROG. 9 (1161).

Shaw, H.R. (1965) "Comments on viscosity, crystal settling, and convection in granitic magmas" A. J. SCI. 263 (120-152).

_____ (1972) "Viscosities of magmatic silicate liquids: an empirical method of prediction" A. J. SCI. 272 (870-893).

_____ (1974) "Diffusion of H_2O in granitic liquids" in Hofmann, A.W. (editor) GEOCHEMICAL TRANSPORT AND KINETICS, Carnegie Inst. of Washington (231-241).

_____, T.L. Wright, D.L. Peck, and R. Okamura (1968) "The viscosity of basaltic magma: an analysis of field measurements in Makaopuhi Lava Lake, Hawaii" A. J. SCI. 266 (225-264).

Skinner, B.J. and D.L. Peck (1969) "An immiscible sulfide melt from Hawaii" ECON. GEOL. MONOGR. 4 (310-322).

Smith, R.L. (1976) "Ash-flow magmatism" GSA ABST. W/PROG. 8 (633-634).

_____ and R.A. Bailey (1966) "The Bandelier Tuff: a study of ash-flow eruption cycles from zoned magma chambers" BULL. VOLCANOL. 29 (83-104).

Sommer (1977) "Volatiles H_2O, CO_2, and CO in silicate melt inclusions in quartz phenocrysts from the rhyolitic Bandelier air-fall and ash-flow tuff, New Mexico" JOUR. GEOL. 85 (423-432).

Sparks, R.S.J. and G.P.L. Walker (1973) "The ground surge

deposit: a third type of pyroclastic rock" NATURE PHYSICAL SCIENCE 241 (62-64).

_____ and L. Wilson (1976) "A model for the formation of ignimbrite by gravitational column collapse" JL. GEOL. SOC. LONDON 132 (441-451).

_____, H. Sigurdsson, and L. Wilson (1977) "Magma mixing: a mechanism for triggering acid explosive eruptions" NATURE 267 (315-318).

Taylor, G.A.M. (1958) "The 1951 eruption of Mt. Lamington, Papua" AUSTRALIA BUR. MINERAL. RES., GEOL. AND GEOPH. BULL. 38.

Thorarinsson, S. and G.E. Sigvaldason (1972) "The Hekla eruption of 1970" BULL. VOLCANOL. 36 (269-288).

Vance, J.A. (1965) "zoning in igneous plagioclase: patchy zoning" JOUR. GEOL. 73 (636-651).

Vlodaretz, V.I. (1959) "On the underground structure of some volcanoes in Kamchatka" BULL. VOLCAN. 20 (113-120).

Watson, E.B. (1976) "Glass inclusions as samples of early magmatic liquid: determinative method and application to a South Atlantic basalt" JOUR. VOLCAN. GEOTH. RES. 1 (73-84).

Weill, D.F. and G.A. McKay (1975) "The partitioning of Mg, Fe, Sr, Ce, Sm, Eu, and Yb in lunar igneous systems and a possible origin of KREEP by equilibrium partial melting" PROC. LUNAR SCI. CONF. 6th (1143-1158).

White, D.E., I. Barnes, and J.R. O'Neil (1973) "Thermal and

mineral waters of nonmeteoric origin, California Coast Ranges" GSA BULL. 84 (547-560).

Wilcox, R.E. (1944) "Rhyolite-basalt complex on Gardiner River, Yellowstone Park, Wyoming" GSA BULL. 55 (1047-1080).

Wood, B.J. and S. Banno (1973) "Garnet-orthopyroxene and orthopyroxene-clinopyroxene relationships in simple and complex systems" CONTR. MIN. PET. 42 (109-124).

Wright, T.L. (1973) "Magma mixing as illustrated by the 1959 eruption, Kilauea volcano, Hawaii" GSA BULL. 84 (849-858).

Yoder, H.S., Jr. and C.E. Tilley (1962) "Origin of basalt magmas: an experimental study of natural and synthetic rock systems" JOUR. PET. 3 (342-532).

VITA

David Alexander Johnston was born December 18, 1949 to Thomas C. Johnston and Alice Ward Johnston in Chicago, Illinois. He graduated from H.L. Richards High School (Oak Lawn, Illinois) in June, 1967. In 1971, he received a bachelor of science degree from the University of Illinois (Urbana), where he graduated with High Honors and Distinction in Geology.